Electronic Supplementary Information

Metallopolymers in Minutes *via* Organocatalysis at Room Temperature

*Kjersti G. Oberle,[†] Elizabeth L. Whitman,[‡] Charles S. Jolly,[‡] Katherine A. Webster,[†] Benjamin S. Marx,[‡] Christopher M. Howard,[‡] Clara A. Hanger,[‡] Erin E. Ramey,[†] Yutong Zou, [†] Jared C. Lowe,[†] Mark Turlington,[‡] and Christopher R. Turlington[†]**

[†]Hope College Department of Chemistry and Biochemistry, Holland, MI 49422, United States

[‡]Berry College Department of Chemistry and Biochemistry, Mount Berry, GA, 30149, United States

Contents

I. Experimental Section

A. Materials and Methods

All reactions were performed under an atmosphere of dry nitrogen using standard drybox and Schlenk techniques, unless noted otherwise. Dichloromethane for polymerization reactions was stirred over calcium hydride for three days under nitrogen, and then was transferred by vacuum distillation into a Chemglass air-free storage vessel with activated 3 Å molecular sieves. The dichloromethane was degassed over three cycles of freeze-pump-thaw and taken into the glovebox. Benzyl alcohol was purchased from Acros Organics and purified by flash chromatography on silica gel using ethyl acetate as the eluent. The ethyl acetate was removed on a rotary evaporator and the benzyl alcohol was transferred into a Chemglass air-free storage vessel with activated 3 Å molecular sieves. The benzyl alcohol was degassed over three cycles of freeze-pump-thaw and taken into the glovebox. 1,8-Diazabicyclo[5.4.0]undec-7-ene (DBU) was purchased from Millipore Sigma (puriss., ≥99.0%, catalog number 33482) and taken into the glovebox unopened and transferred under the nitrogen atmosphere to a Chemglass air-free storage vessel with activated 3 Å molecular sieves. 1,3-diphenylurea (DPU) is commercially available but we synthesized it according to the literature.[1] The product was recrystallized from concentrated solution of ethyl acetate by layering hexane on top. The crystalline material was isolated by filtration, washed with hexane, dried under vacuum and then taken into the glovebox and stored under nitrogen. N′-[3,5-Bis(trifluoromethyl)phenyl]-N-cyclohexylthiourea (TU) was synthesized according to the literature,[2] and the thiourea catalyst was purified by flash chromatography on a silica gel column using 50/50 mixture of hexane and ethyl acetate as an eluent. The solvent was removed using rotary evaporator and the solid was dried under high vacuum at 40 °C overnight while stirring and then taken into the glovebox and stored under nitrogen. The cyclic carbonate monomer with a pendant benzyl group (benzyl 5-methyl-2-oxo-1,3-dioxane-5-carboxylate, Bn-TMC) was synthesized according to the literature.[3,4] The product was recrystallized from a concentrated solution of ethyl acetate by layering hexane on top. The crystalline material was isolated by filtration, washed with hexane, dried under vacuum, and then taken into the glovebox and stored under nitrogen. All other reagents were purchased and used as received.

Analytical thin-layer chromatography (TLC) was performed on 200 μm silica gel plates from Millipore Sigma. Visualization was accomplished via UV light, and/or the use of potassium permanganate followed by application of heat. Chromatography was performed using Silica Gel 60 (230-400 mesh) from Sorbent Technologies.

^{1}H and ^{13}C NMR spectra were recorded on either a JEOL 400 MHz spectrometer or a Bruker Avance III 400 MHz spectrometer, and ^{1}H NMR and ^{13}C NMR chemical shifts were referenced to internal TMS standard set to 0 ppm or to residual ^{1}H or the ^{13}C of the deuterated solvents, respectively. NMR data are reported as follows: chemical shift, multiplicity (s = singlet, bs = broad singlet, d = doublet, t = triplet, q = quartet, quint = quintet, sext = sextet, m = multiplet, dd = doublet of doublets, dt = doublet of triplets, td = triplet of doublets, qd = quartet of doublets), integration, coupling constant (Hz).

All GPC samples were prepared using ~3 mg of sample per 1 mL of THF and were filtered through a 0.45 μm PTFE filter. THF was used as the mobile phase for all GPC instruments. The GPC-RI data (and the traces shown in Figure 1a of the article) were collected at Hope College on a Waters Alliance HPLC System (2695 Separation Module) equipped with Waters 5 μm Styragel columns (HR 4E, HR 3, HR 4, MW linear range 200 - 400,000 g/mol, plus a guard column, 0.300 mL/minute flow rate) equipped with a Waters 2414

RI detector. GPC-LS data were either collected externally on a Waters APC separations module outfitted with three Waters Acquity columns (XT 45, XT 200, and XT 450a, MW linear range 200 - 400,000 g/mol, 0.750 mL/minute flow rate) and a Malvern OMNISEC REVEAL detector (RI, PDA, Light scattering, and Viscometer), or were collected at UC Santa Barbra's Materials Research Laboratory on a Waters Alliance HPLC System (2695 Separation Module) equipped with an Agilent PLgel 5 µm column (MiniMIX-D, 250 x 4.6 mm, MW linear range 200 - 400,000 g/mol, plus a guard column, 0.375 mL/minute flow rate) equipped with a Wyatt DAWN HELEOS-II MALS detector (laser 663.1 nm), a Wyatt Optilab rEX (RI) detector, a Wyatt ViscoStar detector, and a Waters 2996 Photodiode Array detector (PDA).

Elemental analyses were performed by Robertson Microlit Laboratories of Ledgewood, NJ. X-Ray Diffraction was completed at Purdue University on a Bruker Quest diffractometer with a fixed chi angle, a Mo Kα wavelength (λ = 0.71073 Å) sealed tube fine focus X-ray tube, single crystal curved graphite incident beam monochromator, and a Photon II area detector. The instrument is equipped with an Oxford Cryosystems low temperature device and examination and data collection were performed at 150 K. Complete crystallographic data, in CIF format, have been deposited with the Cambridge Crystallographic Data Centre. CCDC 2157240 contain the supplementary crystallographic data for this paper. These data can be obtained free of charge from The Cambridge Crystallographic Data Centre via www.ccdc.cam.ac.uk/data_request/cif. High resolution mass spectra were obtained from Vanderbilt University and were recorded on an Agilent 6540 UHD Accurate-Mass Q-Tof with the $[M+Na]^+$ ion observed.

B. Synthesis of Monomers

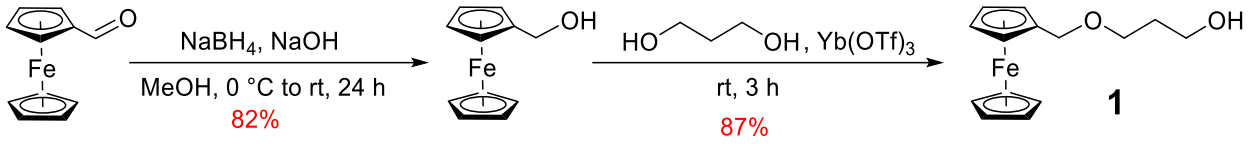

Ferrocenemethanol:[5] A solution of ferrocenecarboxaldehyde (2.00 g, 9.35 mmol, 1 equiv) in MeOH (93 mL) was cooled to 0 °C. $NaBH_4$ (1.77 g, 46.73 mmol, 5 equiv) dissolved in a 2M aqueous solution of NaOH (56 mL) was then added. The reaction mixture was allowed to slowly warm to room temperature and stirred for 24 h. MeOH was then removed from the reaction mixture via rotary evaporation. The resulting aqueous solution was extracted with Et_2O (3 x 50 mL). The organic layer was washed with H_2O (2 x 50 mL), dried over Na_2SO_4, filtered through Celite, and concentrated via rotatory evaporation to afford the product as a light orange solid in 82% yield (1.66 g). R_f = 0.55 (1:1 hexanes/EtOAc). IR (neat, cm^{-1}) 3230, 3089, 2933, 1379, 1235, 987. ^1H NMR (400 MHz, $CDCl_3$) δ 4.32 (d, 2H, J = 4.6 Hz), 4.23 (t, 2H, J = 1.8 Hz), 4.17 (m, 7H), 1.69 (t, 1H, J = 5.1 Hz). $^{13}C\{^1H\}$ NMR (100 MHz, $CDCl_3$) δ 88.4, 68.42, 68.38, 68.0, 60.9. This data is in agreement with reported literature data.[5]

3-(Ferrocenyloxy)propan-1-ol (1):[6] Ferrocenemethanol (1.66 g, 7.64 mmol, 1 equiv) was dissolved in 1,3-propanediol (31 mL) under N_2 atmosphere. Ytterbium triflate (236 mg, 0.38 mmol, 0.05 equiv) was added and the reaction was stirred at rt for 3 h at which time complete consumption of ferrocenemethanol was evident by TLC analysis. The reaction mixture was then diluted with EtOAc (70 mL), and the organic layer was then washed with H_2O (70 mL) and brine (70 mL). The organic layer was dried over Na_2SO_4, filtered and concentrated via rotary evaporation. The crude reaction mixture was purified via flash silica gel column chromatography (90:10 hexanes/EtOAc to 30:70 hexanes/EtOAc) to obtain the product as an orange solid in 87% yield (2.13 g). R_f = 0.33 (1:1 hexanes/EtOAc). IR (neat, cm^{-1}) 3413, 3082, 2957, 1356, 1231, 1059. ^1H NMR (400 MHz, $CDCl_3$) δ 4.29 (s, 2H), 4.22 (t, 2H, *J* = 1.8 Hz), 4.15 (t, 2H, J = 1.8 Hz), 4.13 (s, 5 H), 3.75 (q, 2H, J = 5.6 Hz), 3.63 (t, 2H, J = 5.6 Hz), 2.42 (t, 1H, J = 5.5 Hz), 1.81 (quint, 2H, J = 5.5 Hz). $^{13}C\{^1H\}$ NMR (100 MHz, $CDCl_3$) δ 83.4, 69.5, 69.4, 69.2, 68.6, 62.3, 32.0. This data is in agreement with reported literature data.[7]

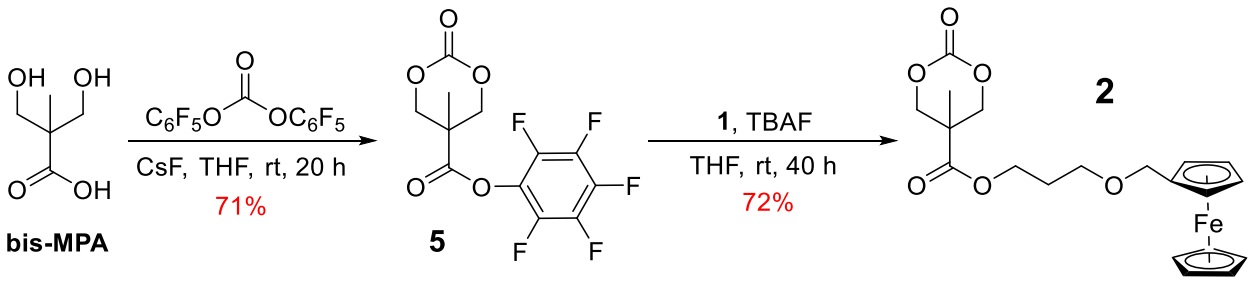

Perfluorophenyl 5-methyl-2-oxo-1,3-dioxane-5-carboxylate (5):[8] 2,2-bis(hydroxymethyl)propionic acid (bis-MPA) (1.5 g, 11.2 mmol, 1 equiv), bis(pentafluorophenyl)carbonate (11.02 g, 28.0 mmol, 2.5 equiv), and CsF (0.34 g, 2.24 mmol, 0.2 equiv) were dissolved in THF (35 mL) under N_2 atmosphere. The reaction was stirred at rt for 20 h. The solvent was removed via rotary evaporation, and the resulting white solid was suspended in CH_2Cl_2 (125 mL) and stirred for 15 min. The undissolved solid (pentafluorophenol) was removed via vacuum filtration. The filtrate was then washed with $NaHCO_3$ (sat'd aqueous, 4 x 40 mL) and

brine (40 mL), dried over Na_2SO_4, and concentrated via rotary evaporation. The crude white solid was absorbed onto silica gel and purified via flash silica gel column chromatography (100% hexanes to 20:80 hexanes/EtOAc) to obtain the product as a white solid in 71% yield (2.60 g). R_f = 0.29 (1:1 hexanes/EtOAc). IR (neat, cm^{-1}) 2979, 1782, 1735, 1518, 1082, 992. ^1H NMR (400 MHz, $CDCl_3$) δ 4.85 (d, 2H, J = 11.2 Hz), 4.37 (d, 2H, J = 11.6 Hz), 1.56 (s, 3H). $^{13}C\{^1H\}$ NMR (100 MHz, $CDCl_3$) δ 168.0, 146.9, 141.0 (m, J_{C-F} = 252.7 Hz), 140.2 (dtt, J_{C-F} = 255.1, 13.4, 3.8 Hz), 138.0 (m, J_{C-F} = 257.3 Hz), 124.4 (m), 72.5, 41.1, 17.5. This data is in agreement with reported literature data.[8]

3-(Ferrocenyloxy)propyl 5-methyl-2-oxo-1,3-dioxane-5-carboxylate (2): 3-(Ferrocenyloxy)propan-1-ol (**1**, 1.1 g, 4.01 mmol, 1 equiv) and perfluorophenyl 5-methyl-2-oxo-1,3-dioxane-5-carboxylate (**5**, 1.50 g, 4.61 mmol, 1.15 equiv) were dissolved in THF (6 mL) and stirred for 5 min to dissolve as much of the solids as possible. TBAF (1 M in THF, 0.80 mL, 0.80 mmol, 0.2 equiv) was added and the reaction was stirred at rt for 40 h. The crude reaction mixture was then absorbed onto silica gel and purified via flash silica gel column chromatography (100% hexanes to 50:50 hexanes/EtOAc) to obtain the product as an orange solid in 72% yield (1.21 g). Before use in polymerization reactions, the monomer was further purified by recrystallization. Approximately 80 mL of hexane was layered on top of a concentrated solution of 500 mg of the monomer in ethyl acetate (appx 8 mL). The mixture was filtered and washed with hexane. The non-crystalline solid was separated from the bright orange crystalline rods, and the crystalline rods were dried under high vacuum, yielding 400 mg (80% recovery). The bright orange, crystalline rods were suitable for X-ray diffraction. R_f = 0.28 (1:1 hexanes/EtOAc). IR (neat, cm^{-1}) 3084, 2960, 2854, 1753, 1730, 1465, 1337, 1237, 1180, 1089. ^1H NMR (400 MHz, $CDCl_3$) δ 4.62 (d, 2H, J = 10.8 Hz), 4.271 (t, 2H, J = 6.4 Hz), 4.266 (s, 2H), 4.22 (t, 2H, J = 1.8 Hz), 4.15 (d, 2H, J = 10.8 Hz), 4.15 (t, 2H, J = 1.8 Hz), 4.13 (s, 5H), 3.47 (t, 2H, J = 5.9 Hz), 1.90 (quint, 2H, J = 6.4 H), 1.29 (s, 3H). $^{13}C\{^1H\}$ NMR (100 MHz, $CDCl_3$) δ 171.1, 147.6, 83.2, 73.1, 69.6, 69.4, 68.7, 68.6, 65.8, 63.7, 40.2, 28.9, 17.7. Anal. Calcd (found) for $FeC_{20}H_{24}O_6$: C, 57.71 (57.61); H, 5.81 (5.79); N, 0.00 (<0.10). Crystal Data for $C_{62}H_{39}BClF_{30}IrN_2O$ (M =1636.41): monoclinic, space group P2/c (no. 13), a = 34.6729(18) Å, b = 5.8345(3) Å, c = 19.1590(10)Å, β = 106.030(2)°, V = 3725.1(3) $Å^3$, Z = 8, Z' = 2, T = 150 K, μ(MoKα) = 0.844 mm^{-1}, $Dcalc$ = 1.484 g/mm^3, 66968 reflections measured ($1.83 \leq 2\Theta \leq 37.09$), 16862 unique ($R_{int}$ = 0.0385) which were used in all calculations. The final R_1 was 0.0417 ($I > 2\sigma(I)$) and wR_2 was 0.0941 (all data), with a goodness-of-fit on F^2 = 1.098.

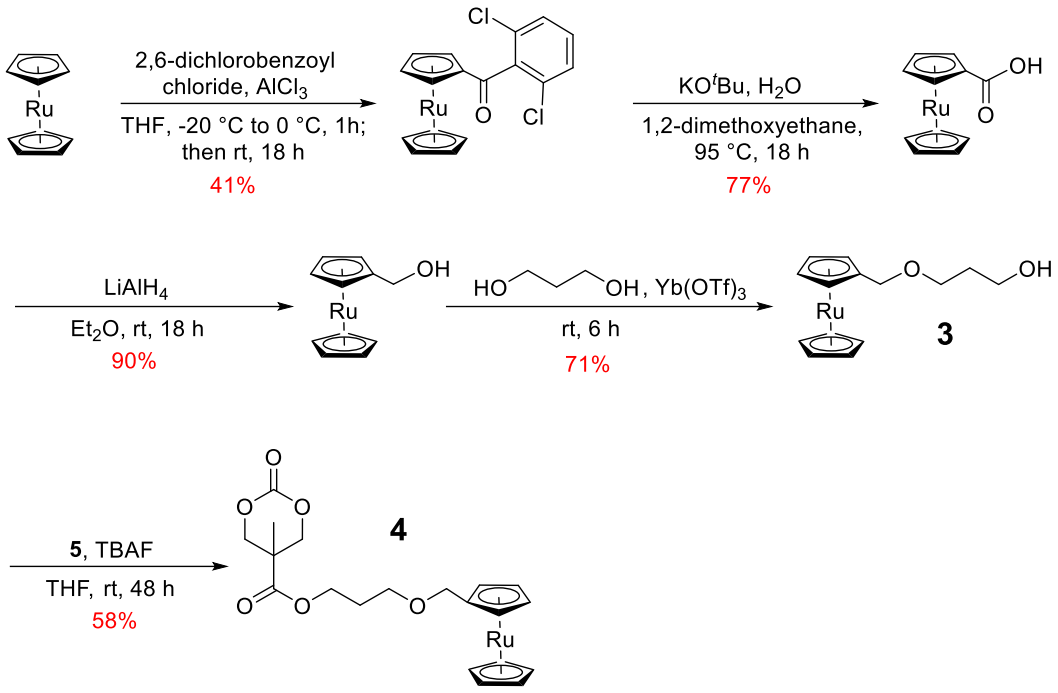

2,6-Dichlorobenzoylruthenocene:[9] Ruthenocene (1.173 g; 5.07 mmol; 1 equiv) was suspended in dry CH_2Cl_2 (47 mL) under an N_2 atmosphere, and 2,6-dichlorobenzoyl chloride (0.726 mL; 5.07 mmol; 1 equiv) was added. The mixture was cooled to -20 °C and anhydrous $AlCl_3$ (0.676 g; 5.07 mmol; 1 equiv) was added in one portion. The mixture was warmed to 0 °C over the course of 1 h, and then the cold bath was removed and the reaction was stirred at rt for 18 h. The mixture was then cooled to 0 °C, H_2O (10 mL) was added, and the organic and aqueous layers were separated. The aqueous layer was extracted with CH_2Cl_2 (3 x 15 mL). The organic layer was concentrated via rotary evaporation, redissolved in EtOAc (40 mL), and subsequently washed with H_2O (20 mL) and brine (20 mL). The organic layer was dried over Na_2SO_4, filtered, and concentrated via rotary evaporation. The crude product was purified via flash silica gel column chromatography (100% hexanes to 85:15 hexanes:EtOAc) to afford the product as a yellow solid in 41% yield (0.84 g). R_f = 0.39 (9:1 hexanes:EtOAc). FTIR (neat, cm^{-1}) 3286, 3088, 1646, 1285. ^1H NMR (400 MHz, $CDCl_3$): δ 7.33 (m, 2H), 7.27 (m, 1H), 4.98 (m, 2H), 4.82 (m, 2H), 4.67 (s, 5H). ^{13}C NMR (100 MHz, $CDCl_3$): δ 194.7, 138.3, 132.3, 130.5, 128.4, 84.1, 73.8, 72.9, 71.9. This data is in agreement with reported literature data.[9]

Ruthenocenecarboxylic Acid:[9] 2,6-Dichlorobenzoylruthenocene (0.84 g; 2.07 mmol; 1 equiv) was dissolved in 1,2-dimethoxyethane (15.6 mL) and KO^{t}Bu (2.32 g; 20.7 mmol; 10 equiv) and H_2O (134 µL; 7.45 mmol; 3.6 equiv) were added. The flask was fitted with a reflux condenser and the mixture was stirred at 95 °C for 18 h under an N_2 atmosphere. The mixture was then diluted with H_2O (15 mL), allowed to cool to rt, and then diluted with Et_2O (15 mL). The ruthenocene carboxylate was extracted into the aqueous layer using 1 M NaOH (2 x 10 mL). The combined aqueous layers were acidified with 1 M HCl, and the crude product was extracted into EtOAc (4 x 20 mL). The organic layer was dried over Na_2SO_4, filtered, and concentrated via rotary evaporation, affording the desired compound as a yellow solid in 77% yield (0.44 g) which was used without further purification. R_f = 0.24 (1:1 hexanes:EtOAc). FTIR (neat, cm^{-1}) 3100, 2971, 2561, 1656, 1477, 1288. ^1H NMR (DMSO-D_6): δ 12.08 (brs, 1H), 5.02 (t, 2H, J = 1.7 Hz), 4.74

(t, 2H, J = 1.7 Hz), 4.61 (s, 5H). ^{13}C NMR (DMSO-D_6): δ 170.7, 76.3, 72.8, 71.6. This data is in agreement with reported literature data.[9]

Hydroxymethylruthenocene: The procedure was adapted from that reported by Ciampi and coworkers.[10] To a rapidly stirring suspension of $LiAlH_4$ (0.42 g, 11.1 mmol) in dry Et_2O (17 mL) at rt was added a solution of ruthenocenecarboxylic acid (0.44 g, 1.6 mmol) in dry Et_2O (19 mL). Stirring was continued for 18 hours at rt under an N_2 atmosphere. To the crude reaction mixture was added a 1:1 EtOH:H_2O mixture (17 mL) in small portions to destroy excess $LiAlH_4$. Then, the reaction mixture was transferred to ice-cold 2 M NaOH (80 mL). The aqueous and organic phases were separated, and the aqueous layer was extracted with Et_2O (2 × 15 mL). The combined organic extracts were washed with 1 M NaOH solution (3 × 15 mL) and H_2O (3 × 15 mL), dried over Na_2SO_4, filtered through Celite, and concentrated via rotary evaporation. The crude reaction mixture was purified via flash silica gel column chromatography (100% hexanes to 60:40 EtOAc:hexanes) to afford the product in 90% yield (0.37 g). R_f = 0.62 (1:1 hexanes:EtOAc). FTIR (neat, cm^{-1}) 3218, 3091, 2868, 1667, 986. ^{1}H NMR (400 MHz, $CDCl_3$) δ 4.67 (m, 2H), 4.62 (s, 5H), 4.56 (m, 2H), 4.01 (d, 2H, J = 5.5 Hz), 1.13 (t, 2H, J = 5.5 Hz); ^{13}C NMR (100 MHz, $CDCl_3$) δ 95.5, 70.8, 70.5, 58.7. This data is in agreement with reported literature data.[11]

3-(Ruthenocenyloxy)propan-1-ol (3): Hydroxymethylruthenocene (0.37 g, 1.42 mmol, 1 equiv) was dissolved in 1,3-propanediol (5.77 mL) and then ytterbium triflate (44 mg, 0.07 mmol, 0.05 equiv) was added. The reaction was stirred at rt for 6 h under an N_2 atmosphere. The reaction mixture was then diluted with EtOAc (20 mL) and the organic layer was washed with H_2O (20 mL) and brine (20 mL). The organic layer was dried over Na_2SO_4, filtered and concentrated via rotary evaporation. The crude product was purified via flash silica gel column chromatography (100% hexanes to 70:30 EtOAc:hexanes) to afford the product in 71% yield (0.32 g). R_f = 0.46 (1:1 hexanes:EtOAc). FTIR (neat, cm^{-1}) 3360, 3094, 2856, 1655, 1232, 1073. ^{1}H NMR (400 MHz, $CDCl_3$) δ:4.63 (m, 2H), 4.53 (s, 5H), 4.52 (m, 2H), 4.09 (s, 2H), 3.75 (t, 2H, J = 5.6 Hz), 3.64 (t, 2H, J = 6.0 Hz), 2.59 (brs, 1H), 1.82 (quintet, 2H, J = 5.6 Hz); ^{13}C NMR (100 MHz, $CDCl_3$) δ: 86.8, 71.5, 70.6, 69.00, 68.97, 61.7, 32.0. HRMS (ESI+ /Q-TOF) m/z: $[M + Na]^+$ calcd for $C_{14}H_{18}O_2Ru$, 343.0246; found, 343.0247.

3-(Ruthenocenyloxy)propyl 5-methyl-2-oxo-1,3-dioxane-5-carboxylate (4): 3-(Ruthenocenyloxy)propan-1-ol (**3**, 0.57 g, 1.78 mmol, 1 equiv) and perfluorophenyl-5-methyl-2-oxo-1,3-dioxane-5-carboxylate (**5**, 1.02 g, 3.12 mmol, 1.75 equiv) were dissolved in THF (3.2 mL) and stirred for 5 min to dissolve as much of the solids as possible. TBAF (1 M in THF, 0.53 mL, 0.53 mmol, 0.3 equiv) was added and the reaction was stirred at rt for 48 h under an N_2 atmosphere. The crude reaction mixture was then absorbed onto silica gel and purified via flash silica gel column chromatography (100% hexanes to 70:30 EtOAc:hexanes) to afford the product in 58% yield (0.47 g). Before polymerization reactions, the monomer was further purified by recrystallization. Approximately 80 mL of hexane was layered on top of a concentrated solution of 501.2 mg of the monomer in ethyl acetate (appx 8 mL). The clear crystalline material was recovered by filtration, washed with hexane, and dried under high vacuum, yielding 399.0 mg (80% recovery). R_f = 0.29 (1:1 hexanes:EtOAc). FTIR (neat, cm^{-1}) 3081, 2911, 1756, 1729, 1460, 1236, 1169, 1082. ^{1}H NMR (400 MHz, $CDCl_3$) δ: 4.64 (m, 4 H), 4.52 (s, 7 H), 4.28 (t, 2H, J = 6.4 Hz), 4.19 (d, 2 H, J = 10.4 Hz), 4.05 (s, 2 H), 3.49 (t, 2 H, J = 6.0 Hz), 1.91 (quint, 2 H, J = 6.2 Hz), 1.29 (s, 3 H). ^{13}C NMR (100 MHz, $CDCl_3$) δ: 171.0, 147.5, 86.6, 73.0, 71.9, 70.7, 70.6, 68.9, 65.7, 63.6, 40.1, 28.8, 17.5. Anal. Calcd (found) for $RuC_{20}H_{24}O_6$: C, 52.05 (52.01); H, 5.24 (5.41); N, 0.00 (<0.10).

C. Screening Reactions

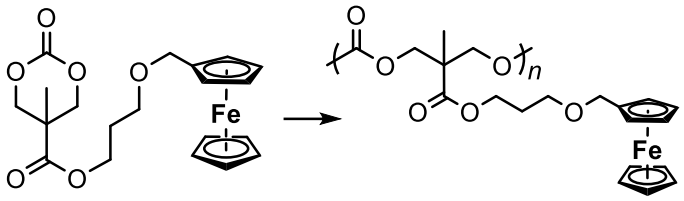

Entry	*Monomer*	*Co-Catalysts (%)*	*Monomer: Initiator*	*Time (Conv)*	*M_n (10^3) GPC-RI*	*Dispersity*
S1	**2**	TU(5%)/NHC(2%)	100:1	3 h (9%)	4	1.08
S2	**2**	TU(5%)/KH(2%)	100:1	6 h (64%)	13	1.24
S3	**2**	DPU(15%)/NHC(5%)	100:1	1 m (70%)	3 & 49	1.48 & 1.22

Table S1. Homopolymerization screening reactions with ferrocene monomer **2** in dichloromethane, using benzyl alcohol as an initiator. Estimates for the molecular weights were determined in-house using GPC-RI calibrated to polystyrene standards. Entry S3 was a bimodal distribution. NHC = 1,3-di-*t*-butylimidazol-2-ylidene.

The GPC-RI calibrated to polystyrene standards gave less-than-expected molecular weights for the metallopolymers. For example, when the molecular weight of the polymer sample (Entry 3 in Table 1 in the communication) was analyzed by GPC-RI calibrated to polystyrene standards, it gave an M_n = 33,500 and a dispersity of 1.09. This was much lower than the value determined by GPC-LS (M_n = 82,000, dispersity of 1.22). Similar observations of GPC-RI giving lower than expected molecular weights for metallopolymers with bulky pendant groups have been reported by others.[12,13] Accordingly, GPC-LS was utilized in all future experiments to accurately determine metallopolymer molecular weights.

D. Synthesis of Polymers/Diblocks and Mechanistic Studies

Table 1 Entry 1: Homopolymerization of Ferrocene Monomer 2 (Monomer:Initiator = 300:1) with TU. In a 3 mL vial with a screw cap and PTFE septum in the glovebox, 3.0 mg (0.0081 mmol, 6 mole %) of 1-(3,5-bis(trifluoromethyl)-phenyl)-3-cyclohexyl-2-thiourea (TU) catalyst, 60.0 mg (0.14 mmol, 0.92 *M*) of ferrocene monomer **2**, 150 μL of DCM, and 6.0 μL of a benzyl alcohol initiator solution (0.080 *M* in DCM, 4.8 x10^{-4} mmol benzyl alcohol) were added respectively. Once all the reagents dissolved, 1.2 μL of 1,8-diazabicyclo[5.4.0]undec-7-ene (DBU, 0.0080 mmol, 6 mole %) was added to begin the polymerization. The reaction was stirred at room temperature for 1 hour, and then the sample was taken out of the glovebox and quenched with a drop of acetic acid. The solvent was blown off and the crude product was dried under high vacuum for 5 minutes. The sample was dissolved in *d*-chloroform and analyzed by ^{1}H NMR spectroscopy to determine the percent conversion (89%). The solvent was blown off and the residue was dissolved in a minimal amount of THF, and the solution was added dropwise to 15 mL of vigorously stirring water chilled to 0 °C in a 20 mL tared scintillation vial. After the product precipitated, stirring was stopped and the purified product settled at the bottom of the vial. The water was decanted using a pipette or needle and syringe. Because the polymer sample was stuck to the stir bar, the purified sample was dissolved in a minimal amount of chloroform, the stir bar was removed, the solvent was blown off, and the product was dried under vacuum for 3-5 hours, yielding 49.0 mg (82%). ^{1}H NMR (400 MHz, $CDCl_3$) δ 4.26-4.18 (m, 12H), 4.13 (s, 5H), 3.45 (m, 2H), 1.85 (m, 2H) ,1.22 (s, 3H). GPC-LS (expected M_n = 111,139) M_n = 85,850, M_w = 91,630, $Đ$ = 1.13.

Table 1 Entry 2: Homopolymerization of Ferrocene Monomer 2 (Monomer:Initiator = 100:1). In a 1.5 mL vial with a screw cap and PTFE septum in the glovebox, 0.6 mg (0.0028 mmol, 6 mole %) of 1,3-diphenylurea catalyst, 20.0 mg (0.048 mmol, 0.84 *M*) of ferrocene monomer **2**, 50.0 μL of dichloromethane (DCM), and 6.0 μL of a benzyl alcohol initiator solution (0.080 *M* in DCM, 4.8 x10^{-4} mmol benzyl alcohol) were added respectively. Once all the reagents dissolved, 1.0 μL of a DCM solution of catalyst DBU (1.4 *M*, 0.0014 mmol, 3 mole %) was added to begin the polymerization. The reaction was stirred at room temperature for 30 minutes, and then the sample was taken out of the glovebox and quenched with a drop of acetic acid. The solvent was blown off and the crude product was dried under high vacuum for 5 minutes. The sample was dissolved in *d*-chloroform and analyzed by ^{1}H NMR spectroscopy to determine the percent conversion (87%). The equilibrium monomer concentration of **2** was calculated to be 0.12 *M*. The solvent was blown off, and the residue was dissolved in a minimal amount of THF and dialyzed against 400 mL of water in a 3.5 kD molecular weight cutoff dialysis bag. The product solution was transferred to a tared vial, and the dialysis bag was rinsed with 2 mL of chloroform and also added to the tared vial. The combined solvents were blown off and the product was dried under vacuum overnight, yielding 15.3 mg (77%). ^{1}H NMR (400 MHz, $CDCl_3$) δ 4.26-4.18 (m, 10H), 4.13 (overlapping 2H and 5H singlets), 3.45 (m, 2H), 1.86 (m, 2H), 1.22 (s, 3H). GPC-LS (expected M_n = 36,213) M_n = 35,249, M_w =41,716, $Đ$ = 1.18.

Table 1 Entry 3: Homopolymerization of Ferrocene Monomer 2 (Monomer:Initiator = 300:1). In a 3 mL vial with a screw cap and PTFE septum in the glovebox, 1.8 mg (0.0085 mmol, 6 mole %) of 1,3-diphenylurea catalyst, 60.0 mg (0.14 mmol, 0.92 *M*) of ferrocene monomer **2**, 150 μL of DCM, and 6.0 μL of a benzyl alcohol initiator solution (0.080 *M* in DCM, 4.8 x10^{-4} mmol benzyl alcohol) were added respectively. Once all the reagents dissolved, 0.6 μL of DBU (0.0040 mmol, 3 mole %) was added to begin the polymerization. The reaction was stirred at room temperature for 30 minutes, and then the sample was

taken out of the glovebox and quenched with a drop of acetic acid. The solvent was blown off and the crude product was dried under high vacuum for 5 minutes. The sample was dissolved in *d*-chloroform and analyzed by ^{1}H NMR spectroscopy to determine the percent conversion (79%). The solvent was blown off and the residue was dissolved in a minimal amount of THF, and the solution was added dropwise to 15 mL of vigorously stirring water chilled to 0 °C in a 20 mL tared scintillation vial. After the product precipitated, stirring was stopped and the purified product settled at the bottom of the vial. The water was decanted using a pipette or needle and syringe. Because the polymer sample was stuck to the stir bar, the purified sample was dissolved in a minimal amount of chloroform, the stir bar was removed, the solvent was blown off, and the product was dried under vacuum for 3-5 hours, yielding 40.8 mg (68%). ^{1}H NMR (400 MHz, $CDCl_3$) δ 4.28-4.15 (m, 12H), 4.13 (s, 5H), 3.45 (t, 2H), 1.85 (m, 2H) ,1.22 (s, 3H). GPC-LS (expected M_n = 98,651) M_n = 81,560, M_w = 80,490, $Đ$ = 1.22.

Table 1 Entry 4: Homopolymerization of Ruthenocene Monomer 4 (Monomer:Initiator = 90:1). In a 1.5 mL vial with a screw cap and PTFE septum in the glovebox, 0.6 mg (0.0028 mmol, 7 mole %) of 1,3-diphenylurea catalyst, 20.4 mg (0.043 mmol, 0.76 *M*) of ruthenocene monomer **4**, 50 μL of DCM, and 6.0 μL of a benzyl alcohol initiator solution (0.080 *M* in DCM, 4.8 x10^{-4} mmol benzyl alcohol) were added respectively. Once all the reagents dissolved, 1 μL of a DCM solution of catalyst DBU (1.4 *M*, 0.0014 mmol, 3 mole %) was added to begin the polymerization. The reaction was stirred at room temperature for 30 minutes, and then the sample was taken out of the glovebox and quenched with a drop of acetic acid. The solvent was blown off and the crude product was dried under high vacuum for 5 minutes. The sample was dissolved in *d*-chloroform and analyzed by ^{1}H NMR spectroscopy to determine the percent conversion (84%). The equilibrium monomer concentration was calculated to be 0.14 *M*. The solvent was blown off and the residue was dissolved in a minimal amount of THF. The sample was then dialyzed against 400 mL of water overnight at a 3.5 kD molecular weight cutoff. The product was transferred to a tared vial, the dialysis bag was rinsed with 2 mL of chloroform and added to the tared vial. The combined solvents were blown off and the product was dried under vacuum overnight, yielding 16.9 mg (85%). ^{1}H NMR (400 MHz, $CDCl_3$) δ 4.64 (s, 2H), 4.52 (overlapping 2H and 5H singlets) , 4.27-4.19 (m, 6H), 4.05 (s, 2H), 3.49 (m, 2H), 1.85 (m, 2H), 1.23 (s, 3H). GPC-LS (expected M_n = 34,903) M_n = 37,980, M_w = 47,464, $Đ$ = 1.25.

Mechanistic experiments – Chain Extension with Ferrocene Monomer 2 (2:2:Initiator = 150:150:1). In a 3 mL vial with a screw cap and PTFE septum in the glovebox, 0.6 mg (0.0028 mmol, 6 mole %) of 1,3-diphenylurea, 20.0 mg (0.048 mmol, 0.84 *M*) of ferrocene monomer **2**, 50 μL of DCM, and 4.0 μL of a benzyl alcohol initiator solution (0.080 *M* in DCM, 3.2 x10^{-4} mmol benzyl alcohol) were added respectively. Once all the reagents dissolved, 1 μL of a DCM solution of catalyst DBU (1.4 *M*, 0.0014 mmol, 3 mole %) was added to begin the polymerization. The reaction was stirred at room temperature for 30 minutes, and then 50 μL of DCM was added to the solution. A 25 μL aliquot was taken out of the glovebox and quenched with a drop of acetic acid. The solvent was blown off and an ^{1}H NMR spectrum of the aliquot revealed 76% conversion of **2** to the polymer, and the aliquot was analyzed by GPC-LS (expected M_n= 47,481) M_n=50,983, M_w=54,463, $Đ$= 1.07. The remaining reaction solution was immediately added to a 3 mL vial with a screw cap and PTFE septum with 20.0 mg (0.048 mmol) of ferrocene **2** monomer and stirred for an additional 30 minutes. The reaction was then taken out of the glovebox and quenched with a drop of acetic acid. The solvent was blown off and the product was dried under high vacuum for 5 minutes. The product was dissolved in *d*-chloroform and analyzed by ^{1}H NMR spectroscopy to determine the percent conversion

(67%). ^{1}H NMR (400 MHz, $CDCl_3$) δ 4.28-4.16 (m, 12H), 4.13 (s, 5H), 3.45 (m, 2H), 1.87 (m, 2H), 1.22 (s, 3H). GPC-LS (expected M_n = 89,339) M_n = 106,972, M_w = 115,872, $Đ$ = 1.08.

Mechanistic experiments – Percent Conversions and M_n's with Ferrocene Monomer 2 (Monomer:Initiator = 300:1). In a 1.5 mL vial with a screw cap and PTFE septum in the glovebox, 2.4 mg (0.011 mmol, 6 mole %) of 1,3-diphenylurea catalyst, 80.0 mg (0.19 mmol, 0.92 *M*) of ferrocene monomer **2**, 200.0 μL of DCM, and 7.9 μL of a benzyl alcohol initiator solution (0.080 *M* in DCM, 6.3 x10^{-4} mmol benzyl alcohol) were added respectively. Once all the reagents dissolved, 3.4 μL of a DCM solution of catalyst DBU (1.4 *M*, 0.0048 mmol, 3 mole %) was added to begin the polymerization. The reaction was stirred at room temperature for 30 minutes. Aliquots (25 μL each) were taken and quenched with benzoic acid at 2, 4, 6, 8, 10, 15, 20, and 30 minutes. The solvent was blown off each aliquot and then they were dried under high vacuum for 5 minutes. The samples were dissolved in *d*-chloroform and analyzed by ^{1}H NMR spectroscopy to determine the percent conversions. The samples were also analyzed by GPC-RI to determine molecular weight and dispersity.

Table 2 Entry 5: Heterobimetallic Diblock Copolymerization of Ferrocene Monomer 2 and Ruthenocene Monomer 4 (2:4:Initiator=100:100:1). In a 1.5 mL vial with a screw cap and PTFE septum in the glovebox, 0.7 mg (0.0033 mmol, 7 mole %) of 1,3-diphenylurea, 20.0 mg (0.048 mmol, 0.84 *M*) of ferrocene monomer **2**, 50 μL of DCM, and 6.0 μL of a benzyl alcohol initiator solution (0.080 *M* in DCM, 4.8 x 10^{-4} mmol benzyl alcohol) were added respectively. Once all the reagents dissolved, 1.4 μL of a DBU solution (1.4 *M*, 0.0019 mmol, 4 mole %) was added to initiate the polymerization. The reaction was stirred at room temperature for 30 minutes. The reaction was transferred using a microliter syringe to a 1.5 mL vial containing 22.0 mg (0.048 mmol, 0.83 *M*) of ruthenocene monomer **4**. The reaction was stirred for an additional 30 minutes at room temperature. The sample was then quenched with acetic acid. The solvent was blown off and the crude product was dried under vacuum for 5 minutes. The sample was dissolved in *d*-chloroform and analyzed by ^{1}H NMR spectroscopy to determine that percent conversion of **2** and **4** to polymer was 95% combined. The solvent was blown off and the residue was dissolved in a minimal amount of THF. The sample was then dialyzed against 400 mL of water overnight at a 3.5 kD molecular weight cutoff. The product transferred into a tared vial, the dialysis bag was rinsed with 2 mL of chloroform and added to the tared vial. The combined solvents were blown off and the product was dried under high vacuum for 3-5 hours, yielding 30.4 mg (72%). ^{1}H NMR (400 MHz, $CDCl_3$) δ 4.63 (s, 2H), 4.52 (s, 7H), 4.26-4.20 (m, 12H), 4.13 (s, 5H), 4.05 (s, 2H), 3.47(m, 2H), 1.85(m, 2H), 1.23 (overlapping singlets, 3H). ^{13}C NMR (100 MHz, $CDCl_3$) δ 172.1, 154.6, 86.9, 83.5, 72.0, 70.9, 70.8, 69.6, 69.4, 69.0, 68.8, 68.6, 66.0, 62.9, 46.7, 29.1, 17.6. GPC-LS (expected M_n = 83,356) M_n = 96,401, M_w = 111,736, $Đ$= 1.16.

Table 2 Entry 6: Diblock Copolymerization of Ruthenocene Monomer 4 and Bn-TMC (4:Bn-TMC:Initiator =145:200:1). In a 1.5 mL vial with a screw cap and PTFE septum in the glovebox, 1.4 mg (0.0066 mmol, 9 mole %) of 1,3-diphenylurea catalyst, 32.1 mg (0.070 mmol, 1.2 *M*) of ruthenocene monomer **4**, 50 μL of DCM, and 6.0 μL of a benzyl alcohol initiator solution (0.080 *M* in DCM, 4.8 x10^{-4} mmol benzyl alcohol) were added respectively. Once all the reagents dissolved, 2.3 μL of a DCM solution of catalyst DBU (1.4 *M*, 0.0031 mmol, 4 mole %) was added to begin the polymerization. The reaction was stirred at room temperature for 30 minutes. An additional 50 μL of DCM were added and the reaction stirred for a minute. The reaction was measured in a microliter syringe and a quarter of the reaction was taken for an aliquot. The aliquot was taken out of the glovebox and quenched with a drop acetic of acid. The solvent

was blown off and an ^{1}H NMR spectrum of the aliquot revealed 90% conversion of **4** to polymer. The remaining three-quarters of the reaction was immediately added to a 1.5 mL vial with a screw cap and PTFE septum with 24.0 mg (0.096 mmol, 1.3 *M*) of **Bn-TMC** monomer. The reaction stirred at room temperature for an additional 30 minutes, and then the sample was taken out of the glovebox and quenched with a drop of acetic acid. The solvent was blown off and the product was dried under high vacuum for 5 minutes. The product was dissolved in *d*-chloroform and analyzed by ^{1}H NMR spectroscopy to determine the percent conversion of the **Bn-TMC** monomer (91%). The solvent was blown off and the residue was dissolved in a minimal amount of THF. The product was then dialyzed against 400 mL of water overnight at a 3.5 kD molecular weight cutoff. The product was transferred into a tared vial and the dialysis bag was rinsed with 2 mL of chloroform and added to the tared vial. The combined solvents were blown off and the product was dried under vacuum for 3-5 hours, yielding 30.7 mg (55%). ^{1}H NMR (400 MHz, $CDCl_3$) δ. 7.31 (m, 6H), 5.12 (s, 2H), 4.64 (s, 2H), 4.53 (overlapping 2H and 5H singlets), 4.27-4.19 (m, 6H), 4.06 (s, 2H), 3.48 (m, 2H), 1.87 (m, 2H), 1.22 (overlapping singlets, 3H). ^{13}C NMR (100 MHz, $CDCl_3$) δ 172.0, 154.6, 135.5, 128.7, 128.5, 128.1, 86.9, 72.0, 70.9, 70.8, 69.0, 68.7, 67.2, 66.0, 62.9, 46.7, 29.1, 17.6, 17.5. GPC-LS (expected M_n = 105,661) M_n = 92,707, M_w = 104,765, $Đ$ = 1.13.

Table 2 Entry 7: Diblock Copolymerization of Bn-TMC and Ruthenocene Monomer 4 (Bn-TMC: 4:Intiator=200:145:1). In a 1.5 mL vial with a screw cap and PTFE septum in the glovebox, 1.5 mg (0.0071 mmol, 7 mole %) of 1,3-diphenylurea catalyst, 26.0 mg (0.104 mmol, 1.9 *M*) of **Bn-TMC** monomer, 50 μL of DCM, and 6.0 μL of a benzyl alcohol initiator solution (0.080 *M* in DCM, 4.8 x10^{-4} mmol benzyl alcohol) were added respectively. Once all the reagents dissolved, 2.2 μL of a DCM solution of catalyst DBU (1.4 *M*, 0.0031 mmol, 3 mole %) was added to begin the polymerization. The reaction was stirred at room temperature for 30 minutes. An additional 50 μL of DCM were added and the reaction stirred for a minute. The reaction was measured in a microliter syringe and a quarter of the reaction was taken for an aliquot. The aliquot was taken out of the glovebox and quenched with a drop of acetic acid. The solvent was blown off and an ^{1}H NMR spectrum of the aliquot revealed 97% conversion of **Bn-TMC** to the polymer, and the aliquot was analyzed by GPC-LS (expected M_n = 48,549) M_n = 48,073, M_w = 57,065, $Đ$ = 1.19. The remaining three-quarters of the reaction was immediately added to a 1.5 mL vial with a screw cap and PTFE septum with 32.0 mg (0.069 mmol, 0.92 *M*) of ruthenocene monomer **4**. The reaction was stirred at room temperature for an additional 30 minutes, and then the sample was taken out of the glovebox and quenched with a drop of acetic acid. The solvent was blown off and the crude product was dried under high vacuum for 5 minutes. The product was dissolved in *d*-chloroform and analyzed by ^{1}H NMR spectroscopy to determine the percent conversion of **4** (88%). The solvent was blown off and the residue was dissolved in a minimal amount of THF. The sample was then dialyzed against 400 mL of water overnight at a 3.5 kD molecular weight cutoff. The product was transferred to a tared vial and the dialysis bag was rinsed with 2 mL of chloroform and added to the tared vial. The combined solvents were blown off and the product was dried under vacuum for 3-5 hours, yielding 40.2 mg (69%). ^{1}H NMR (400 MHz, $CDCl_3$) δ. 7.30 (m, 6H), 5.12 (s, 2H), 4.63 (s, 2H), 4.52 (overlapping 2H and 5H singlets), 4.30-4.19 (m, 6H), 4.05 (s, 2H), 3.48 (m, 2H), 1.87 (m, 2H), 1.22 (overlapping singlets, 3H). ^{13}C NMR (100 MHz, $CDCl_3$) δ 172.0, 154.5, 135.5, 128.7, 128.5, 128.1, 86.9, 72.0, 70.9, 70.8, 69.0, 68.7, 67.2, 66.0, 62.9, 46.7, 29.1, 17.6, 17.5. GPC-LS (expected M_n = 109,072) M_n = 115,357, M_w = 128,053, $Đ$ = 1.11.

E. References

(1) Lin, B.; Waymouth, R. M. Urea Anions: Simple, Fast, and Selective Catalysts for Ring-Opening Polymerizations. *J. Am. Chem. Soc.* **2017**, *139* (4), 1645–1652.

(2) Pratt, R. C.; Lohmeijer, B. G. G.; Long, D. A.; Lundberg, P. N. P.; Dove, A. P.; Li, H.; Wade, C. G.; Waymouth, R. M.; Hedrick, J. L. Exploration, Optimization, and Application of Supramolecular Thiourea−Amine Catalysts for the Synthesis of Lactide (Co)Polymers. *Macromolecules* **2006**, *39* (23), 7863–7871.

(3) Pratt, R. C.; Nederberg, F.; Waymouth, R. M.; Hedrick, J. L. Tagging Alcohols with Cyclic Carbonate: A Versatile Equivalent of (Meth)Acrylate for Ring-Opening Polymerization. *Chem. Commun.* **2008**, No. 1, 114–116.

(4) Tan, E. W. P.; Hedrick, J. L.; Arrechea, P. L.; Erdmann, T.; Kiyek, V.; Lottier, S.; Yang, Y. Y.; Park, N. H. Overcoming Barriers in Polycarbonate Synthesis: A Streamlined Approach for the Synthesis of Cyclic Carbonate Monomers. *Macromolecules* **2021**, *54* (4), 1767–1774.

(5) Germaneau, R.; Chavignon, R.; Tranchier, J.-P.; Rose-Munch, F.; Rose, E.; Collot, M.; Duhayon, C. (H6-Arene)Tricarbonylchromium and Ferrocene Complexes Linked to Binaphthyl Derivatives. *Organometallics* **2007**, *26* (25), 6139–6149.

(6) Marsh, B. J.; Hampton, L.; Goggins, S.; Frost, C. G. Fine-Tuning of Ferrocene Redox Potentials towards Multiplex DNA Detection. *New J Chem* **2014**, *38* (11), 5260–5263.

(7) Edzang, R. W. N.; Lejars, M.; Brisset, H.; Raimundo, J.-M.; Bressy, C. RAFT-Synthesized Polymers Based on New Ferrocenyl Methacrylates and Electrochemical Properties. *RSC Adv.* **2015**, *5* (94), 77019–77026.

(8) Sanders, D. P.; Fukushima, K.; Coady, D. J.; Nelson, A.; Fujiwara, M.; Yasumoto, M.; Hedrick, J. L. A Simple and Efficient Synthesis of Functionalized Cyclic Carbonate Monomers Using a Versatile Pentafluorophenyl Ester Intermediate. *J. Am. Chem. Soc.* **2010**, *132* (42), 14724–14726.

(9) Slootweg, J. C.; Albada, H. B.; Siegmund, D.; Metzler-Nolte, N. Efficient Reagent-Saving Method for the N-Terminal Labeling of Bioactive Peptides with Organometallic Carboxylic Acids by Solid-Phase Synthesis. *Organometallics* **2016**, *35* (18), 3192–3196.

(10) Ciampi, S.; Eggers, P. K.; Le Saux, G.; James, M.; Harper, J. B.; Gooding, J. J. Silicon (100) Electrodes Resistant to Oxidation in Aqueous Solutions: An Unexpected Benefit of Surface Acetylene Moieties. *Langmuir* **2009**, *25* (4), 2530–2539.

(11) Barlow, S.; Cowley, A.; Green, J. C.; Brunker, T. J.; Hascall, T. The Ruthenocenylmethylium Cation: Isolation and Structures of H5-Cyclopentadienyl-H6-Fulvene-Ruthenium(II) Salts. *Organometallics* **2001**, *20* (25), 5351–5359.

(12) Rüttiger, C.; Hübner, H.; Schöttner, S.; Winter, T.; Cherkashinin, G.; Kuttich, B.; Stühn, B.; Gallei, M. Metallopolymer-Based Block Copolymers for the Preparation of Porous and Redox-Responsive Materials. *ACS Appl. Mater. Interfaces* **2018**, *10* (4), 4018–4030.

(13) Alkan, A.; Gleede, T.; Wurm, F. R. Ruthenocenyl Glycidyl Ether: A Ruthenium-Containing Epoxide for Anionic Polymerization. *Organometallics* **2017**, *36* (16), 3023–3028.

II. NMR Spectra from Synthesis of Monomers

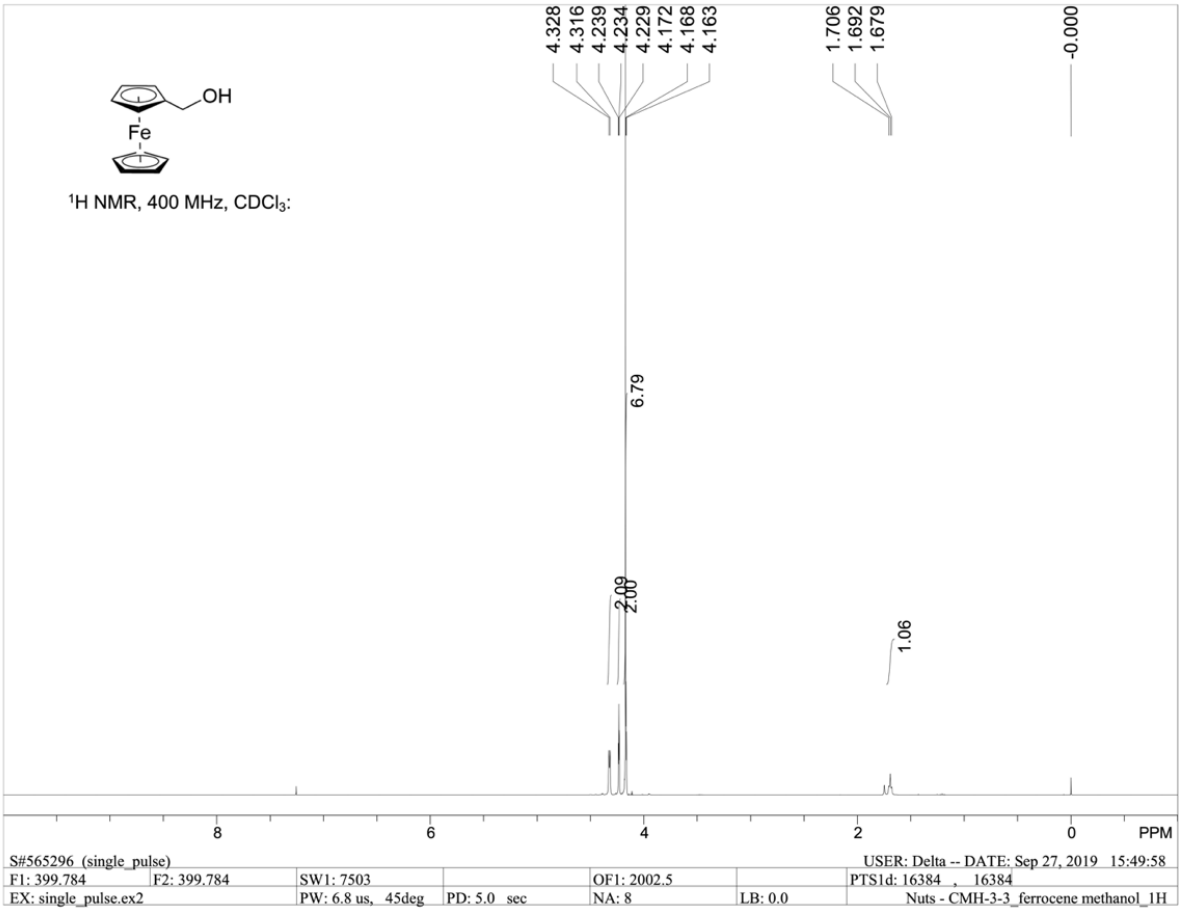

Figure S1. The ^{1}H NMR spectrum ($CDCl_3$) of Ferrocenemethanol.

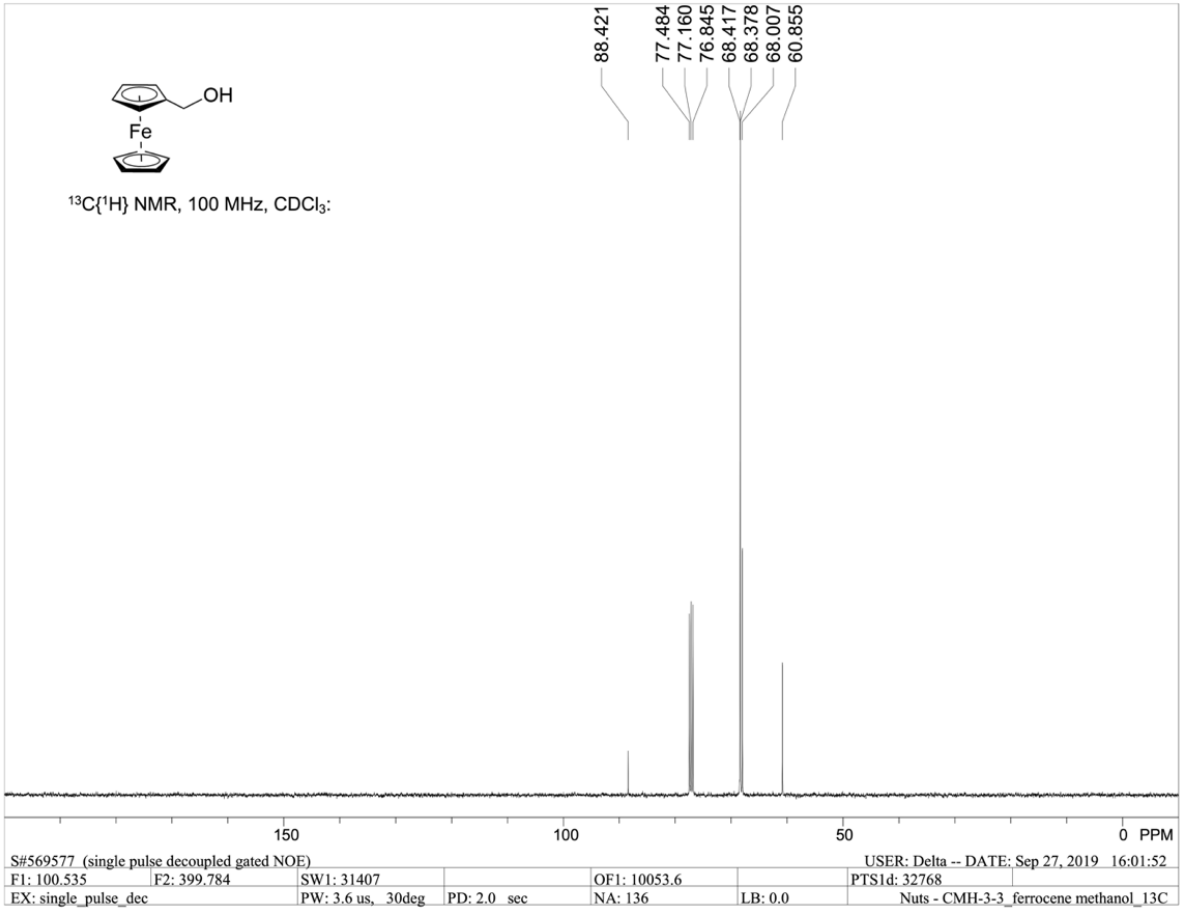

Figure S2. The ^{13}C NMR spectrum ($CDCl_3$) of Ferrocenemethanol.

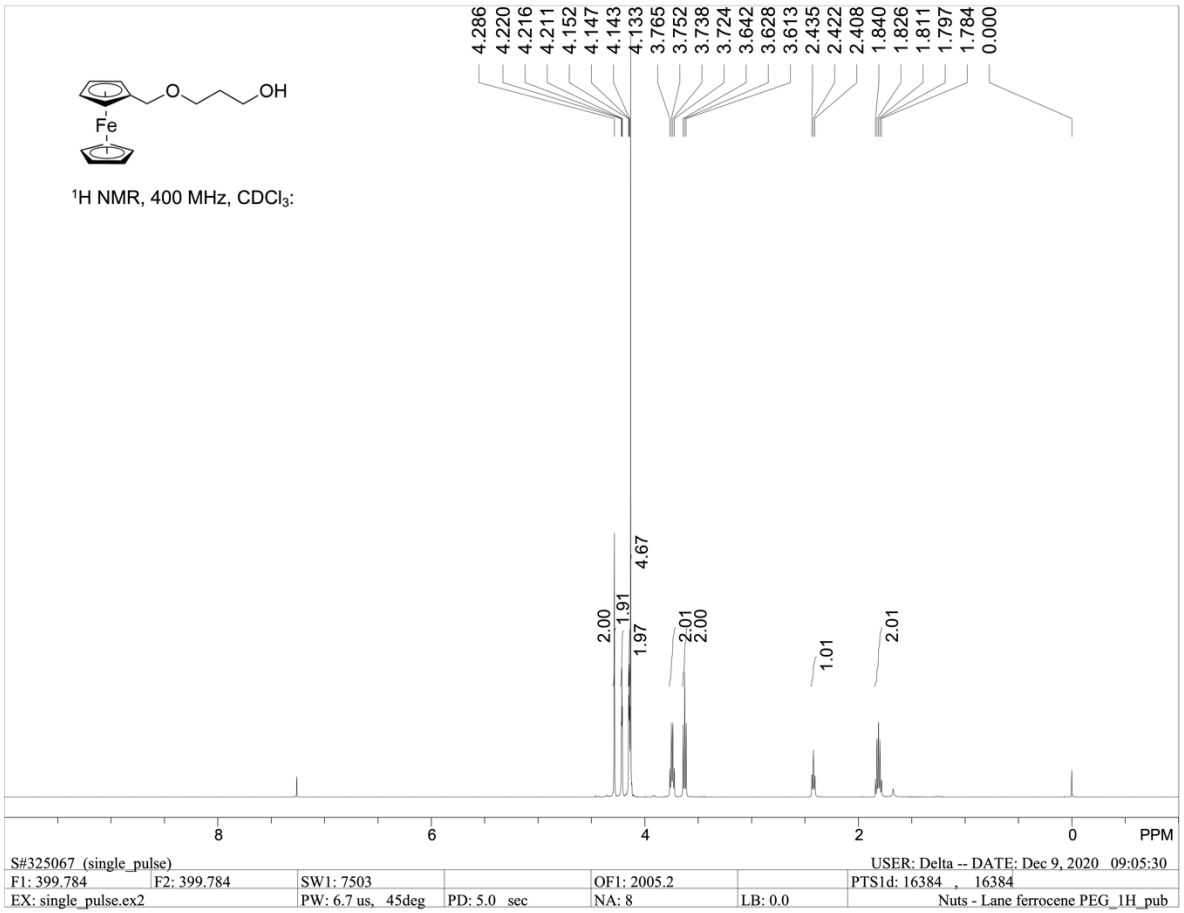

Figure S3. The ^{1}H NMR spectrum ($CDCl_3$) of 3-(Ferrocenyloxy)propan-1-ol **(1)**.

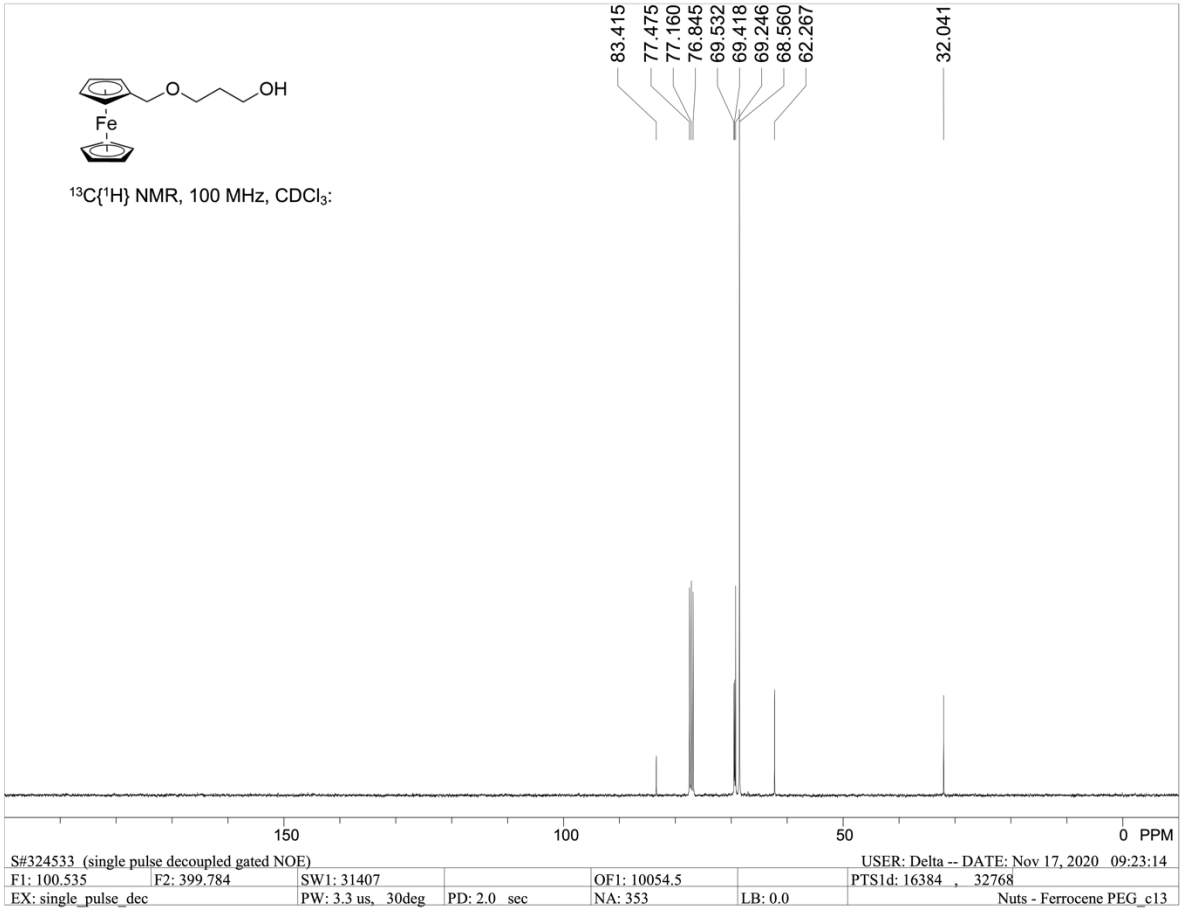

Figure S4. The ^{13}C NMR spectrum ($CDCl_3$) of 3-(Ferrocenyloxy)propan-1-ol **(1)**.

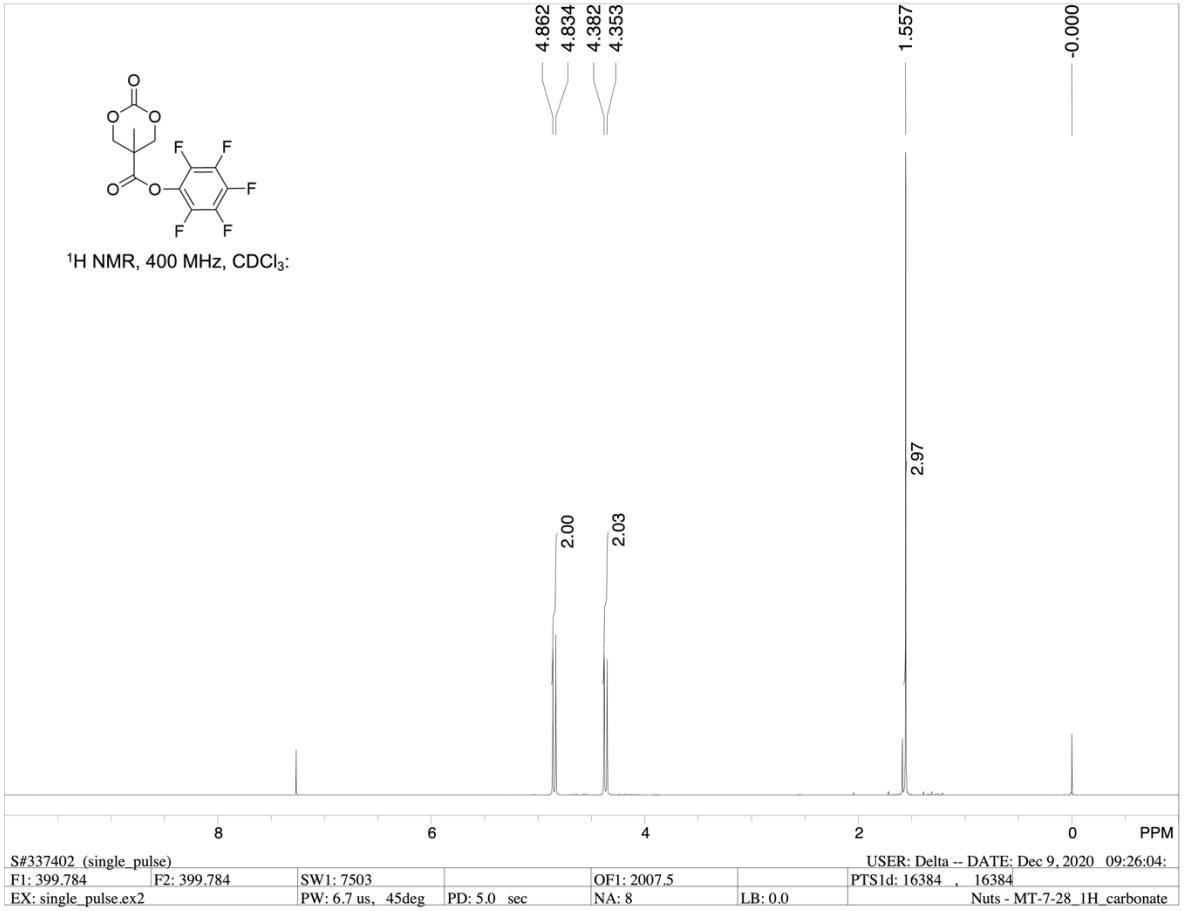

Figure S5. The ^{1}H NMR spectrum ($CDCl_3$) of Perfluorophenyl 5-methyl-2-oxo-1,3-dioxane-5-carboxylate **(5)**.

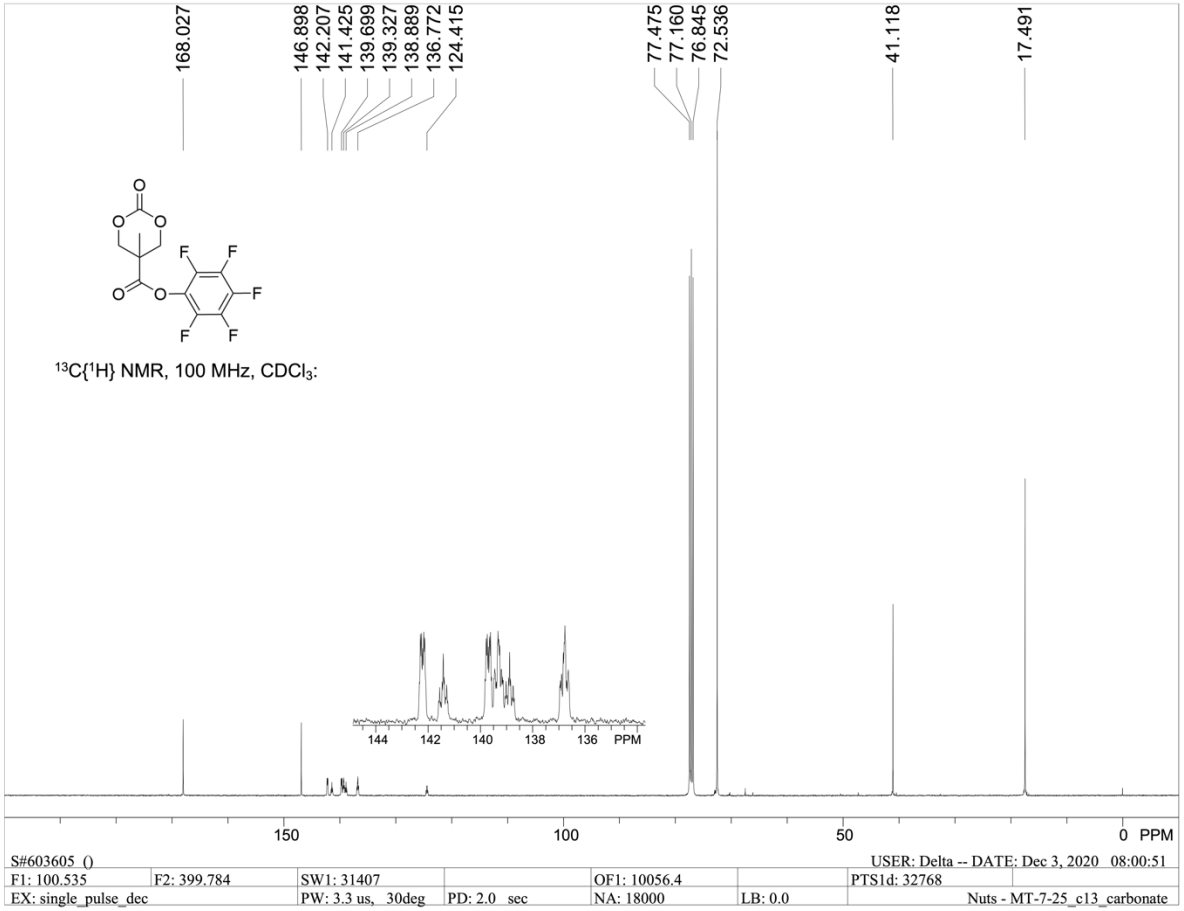

Figure S6. The ^{13}C NMR spectrum ($CDCl_3$) of Perfluorophenyl 5-methyl-2-oxo-1,3-dioxane-5-carboxylate **(5)**.

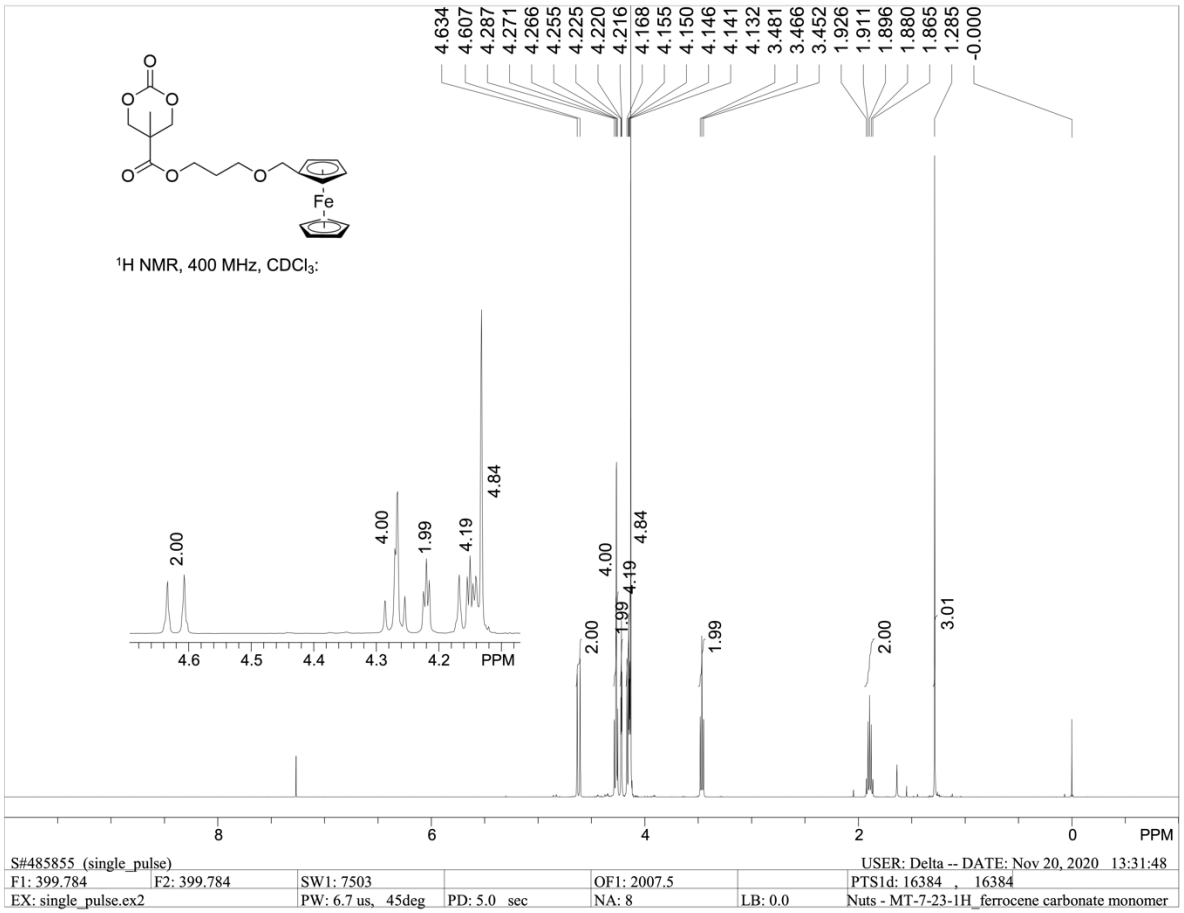

Figure S7. The ^{1}H NMR spectrum ($CDCl_3$) of 3-(Ferrocenyloxy)propyl 5-methyl-2-oxo-1,3-dioxane-5-carboxylate **(2)**.

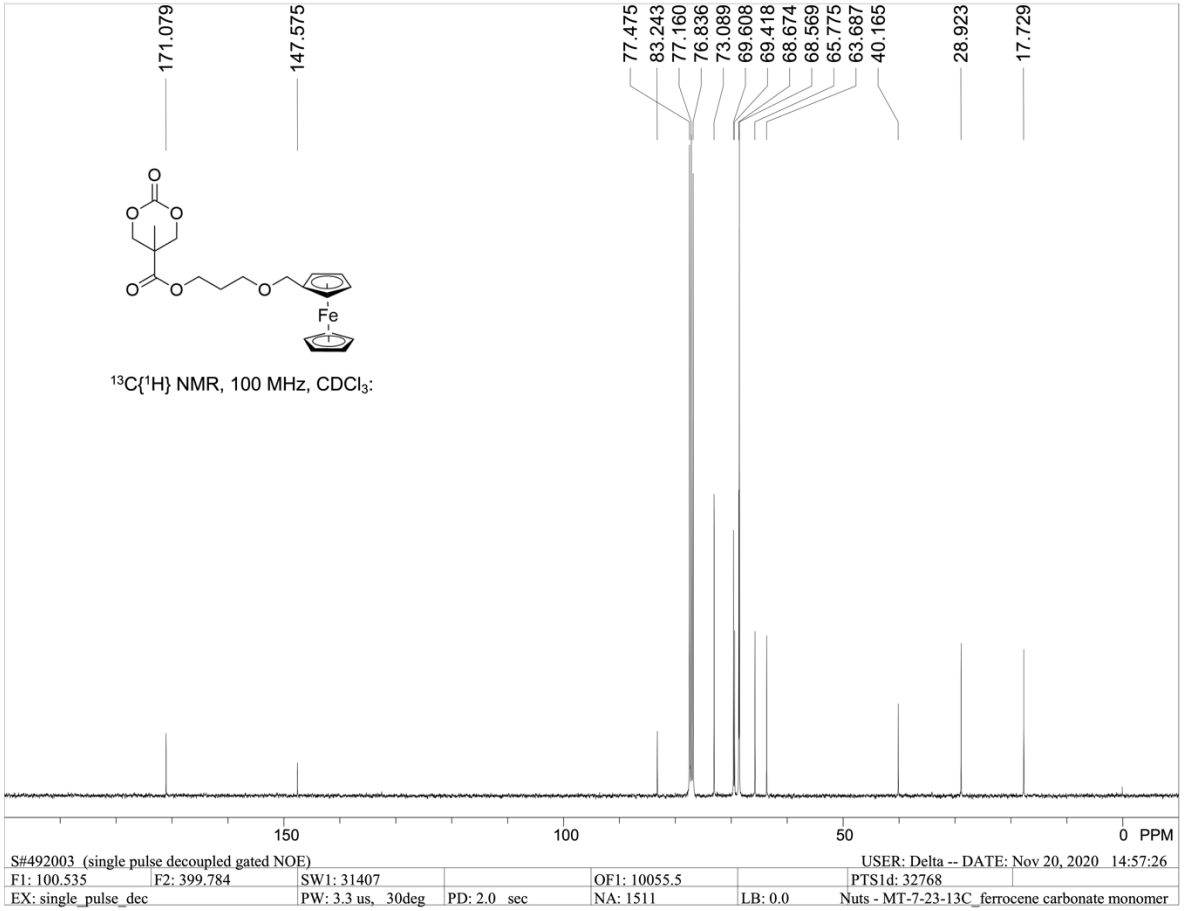

Figure S8. The ^{13}C NMR spectrum ($CDCl_3$) of 3-(Ferrocenyloxy)propyl 5-methyl-2-oxo-1,3-dioxane-5-carboxylate **(2)**.

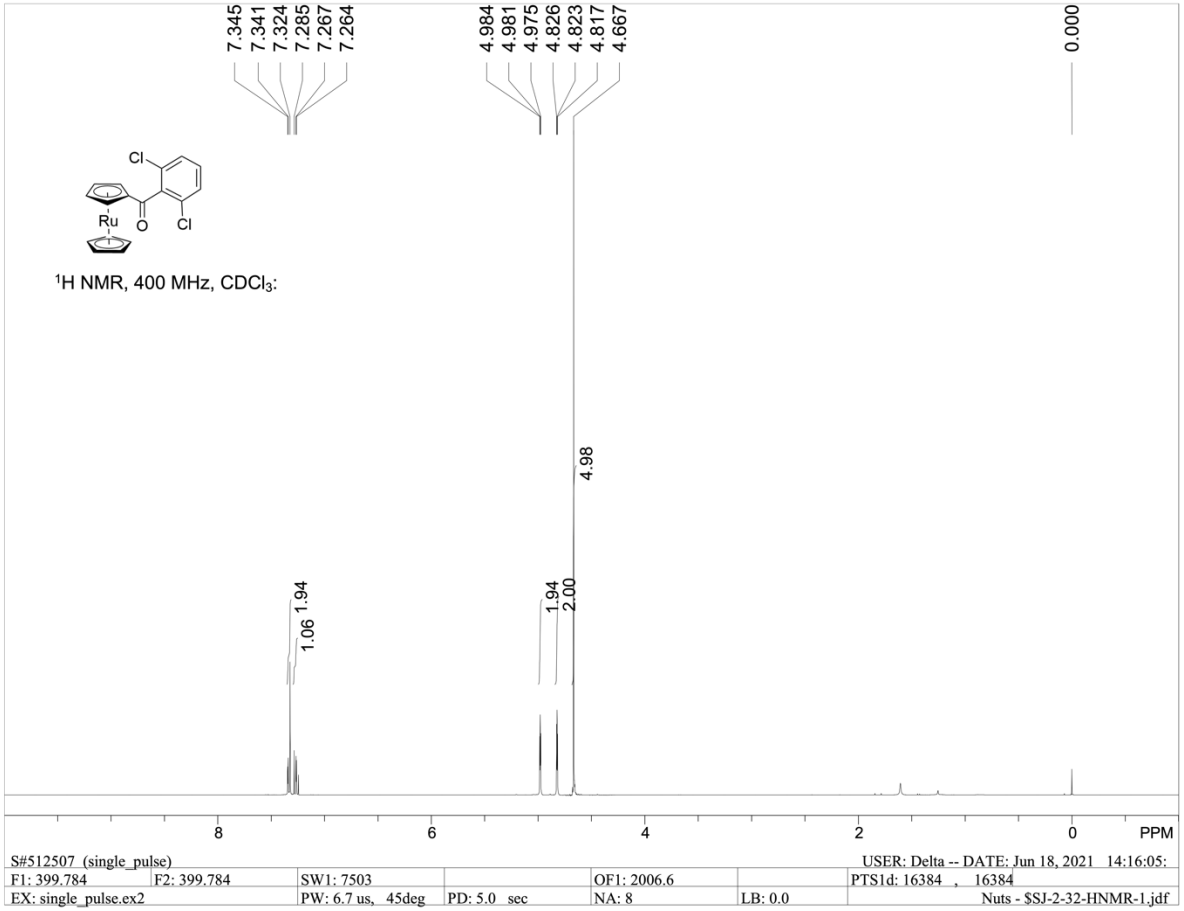

Figure S9. The ^{1}H NMR spectrum ($CDCl_3$) of 2,6-Dichlorobenzoylruthenocene.

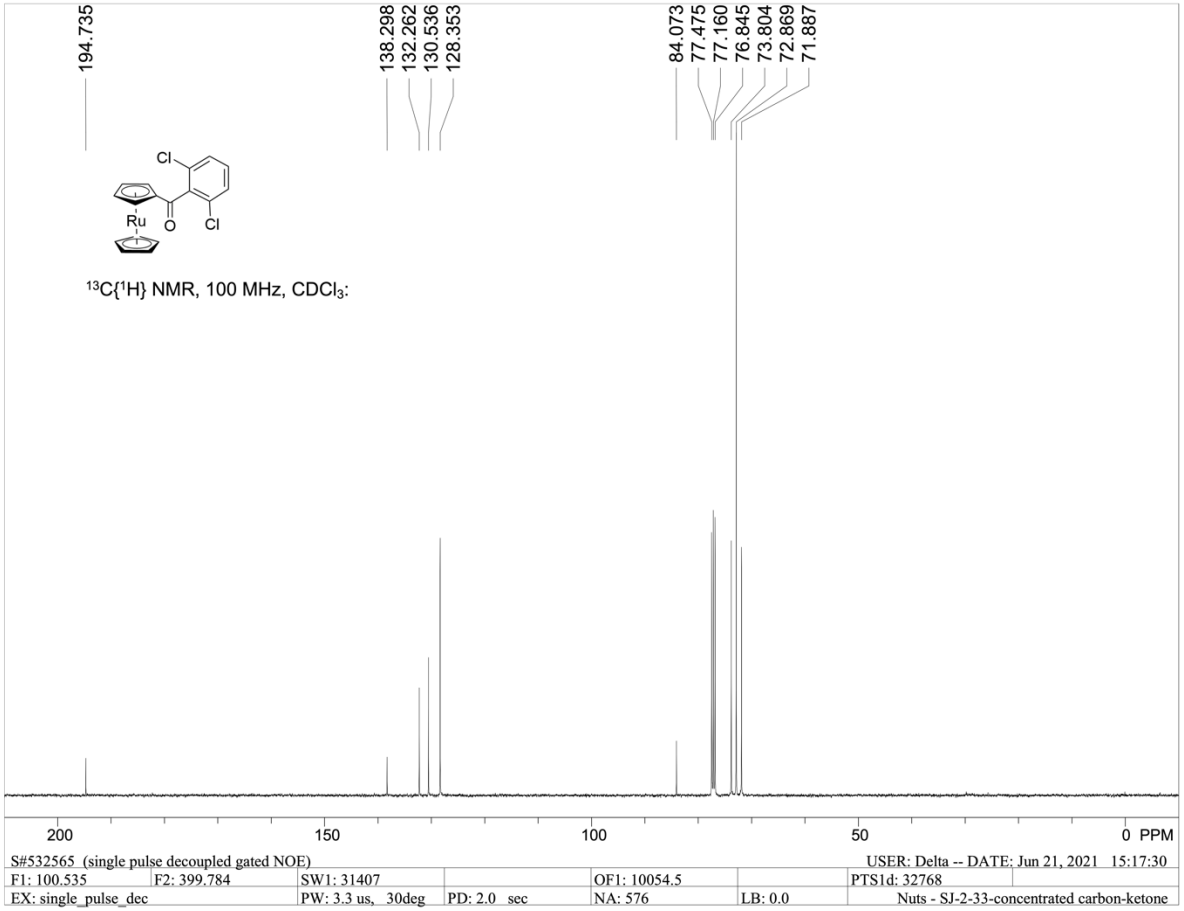

Figure S10. The ^{13}C NMR spectrum ($CDCl_3$) of 2,6-Dichlorobenzoylruthenocene.

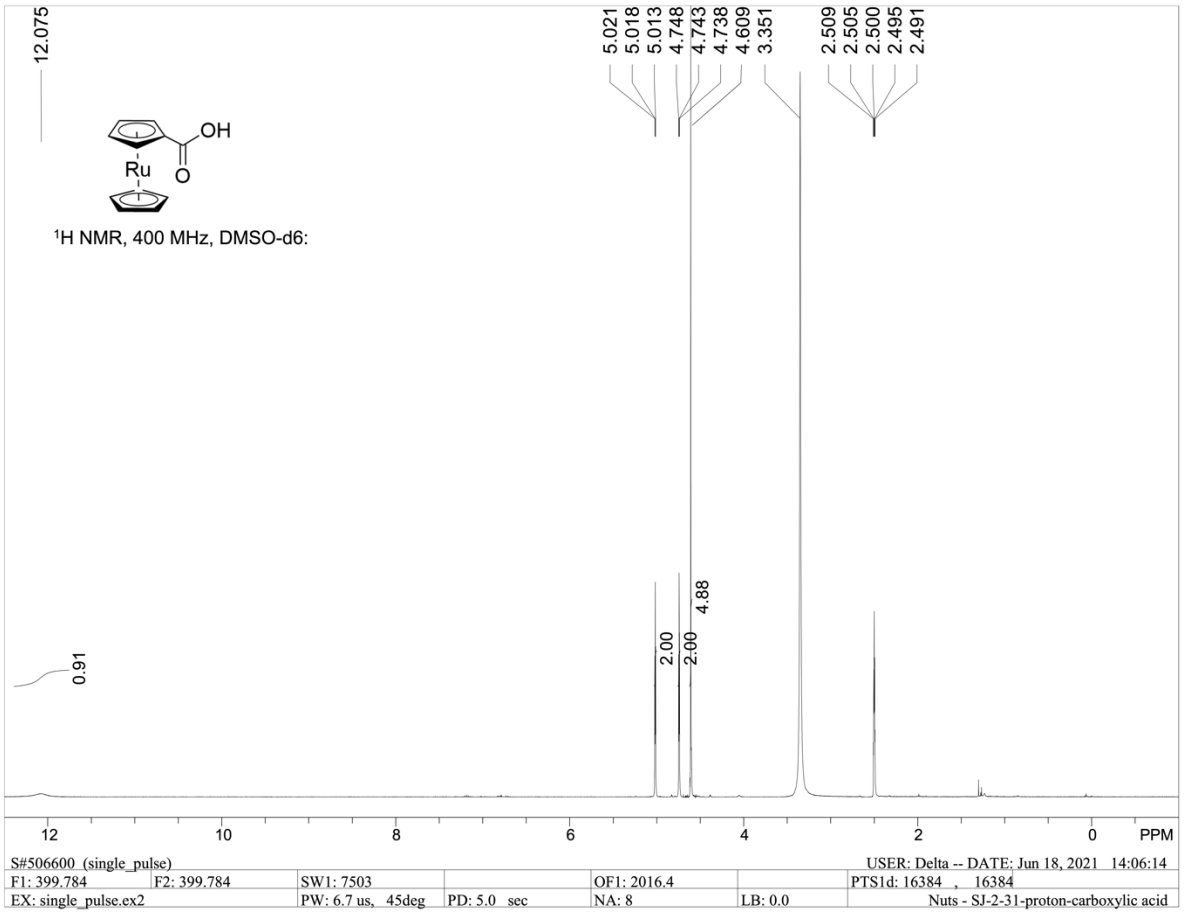

Figure S11. The ^{1}H NMR spectrum (DMSO-d_6) of Ruthenocenecarboxylic Acid.

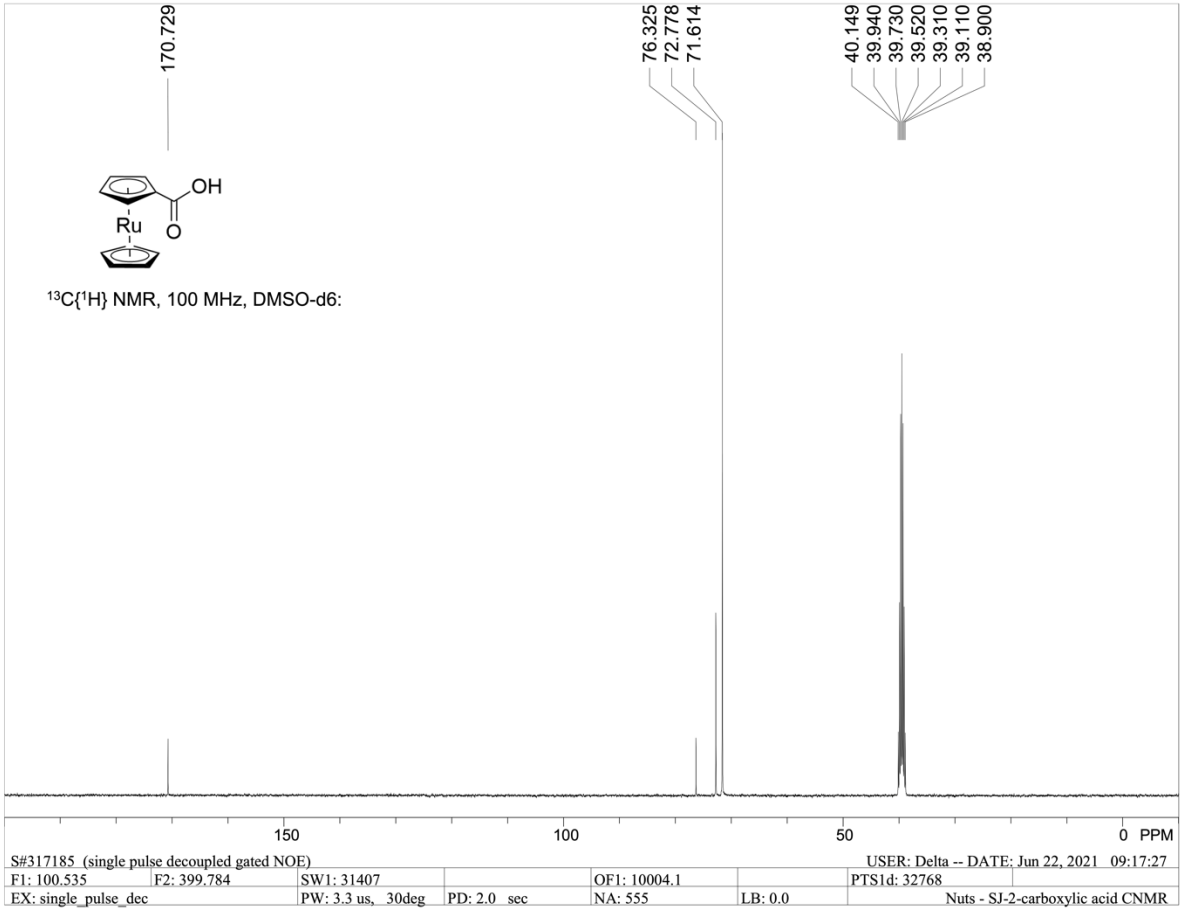

Figure S12. The ^{13}C NMR spectrum (DMSO-d_6) of Ruthenocenecarboxylic Acid.

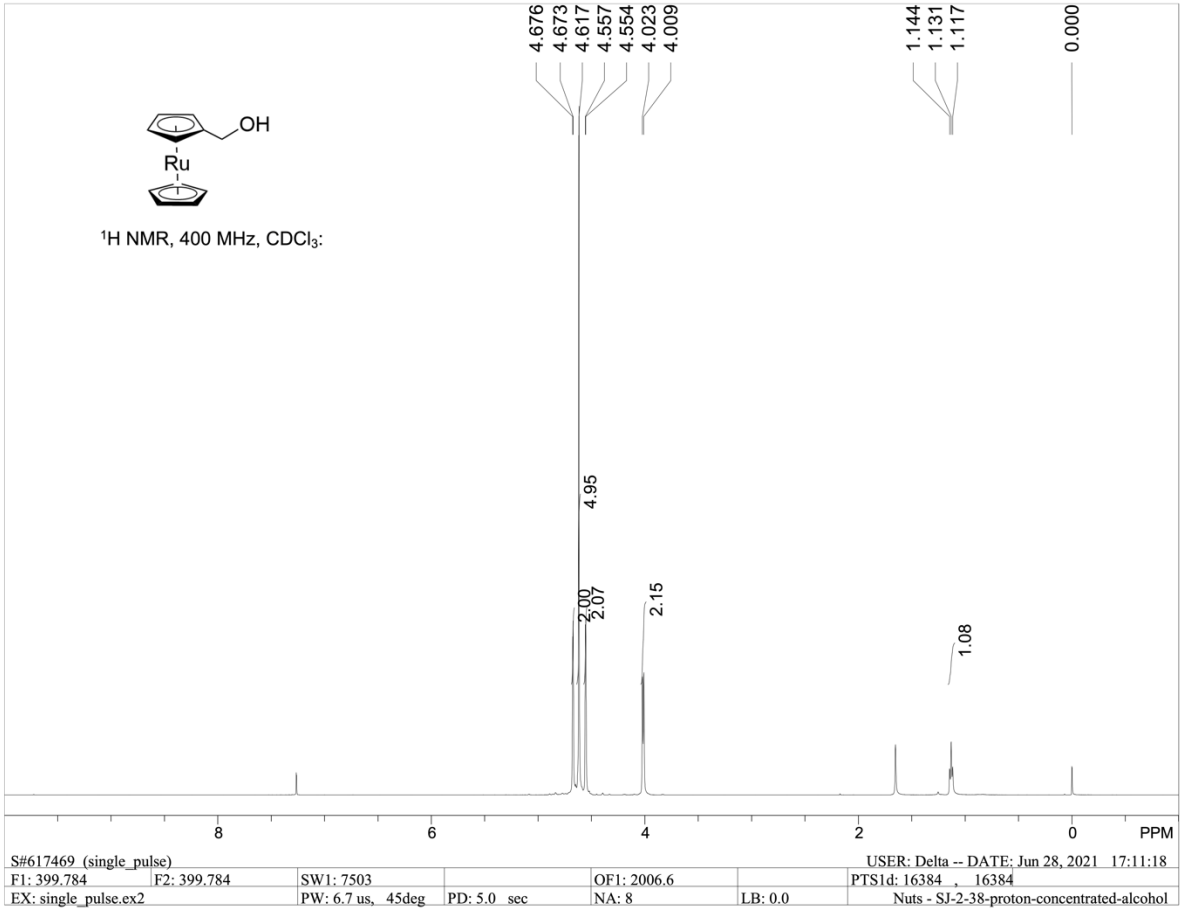

Figure S13. The ^{1}H NMR spectrum ($CDCl_3$) of Hydroxymethylruthenocene.

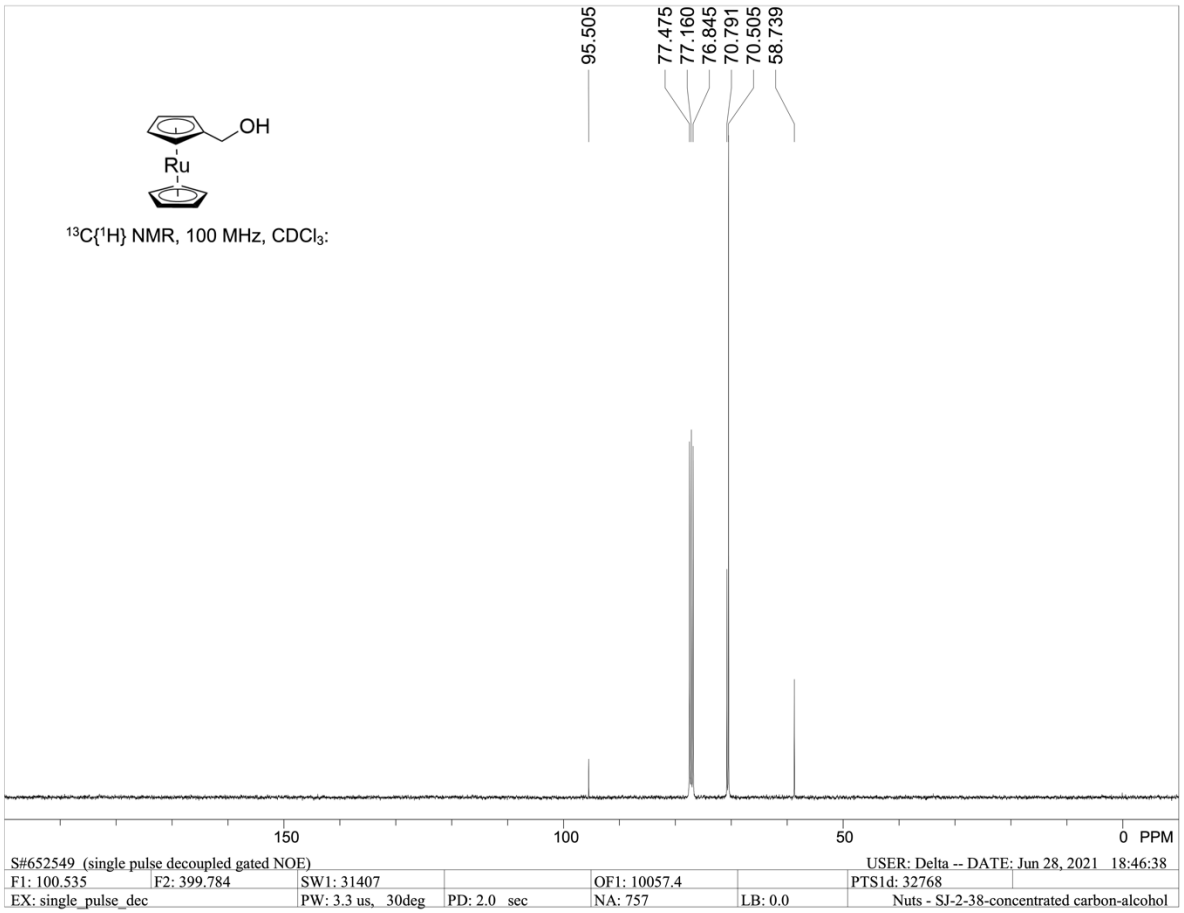

Figure S14. The ^{13}C NMR spectrum ($CDCl_3$) of Hydroxymethylruthenocene.

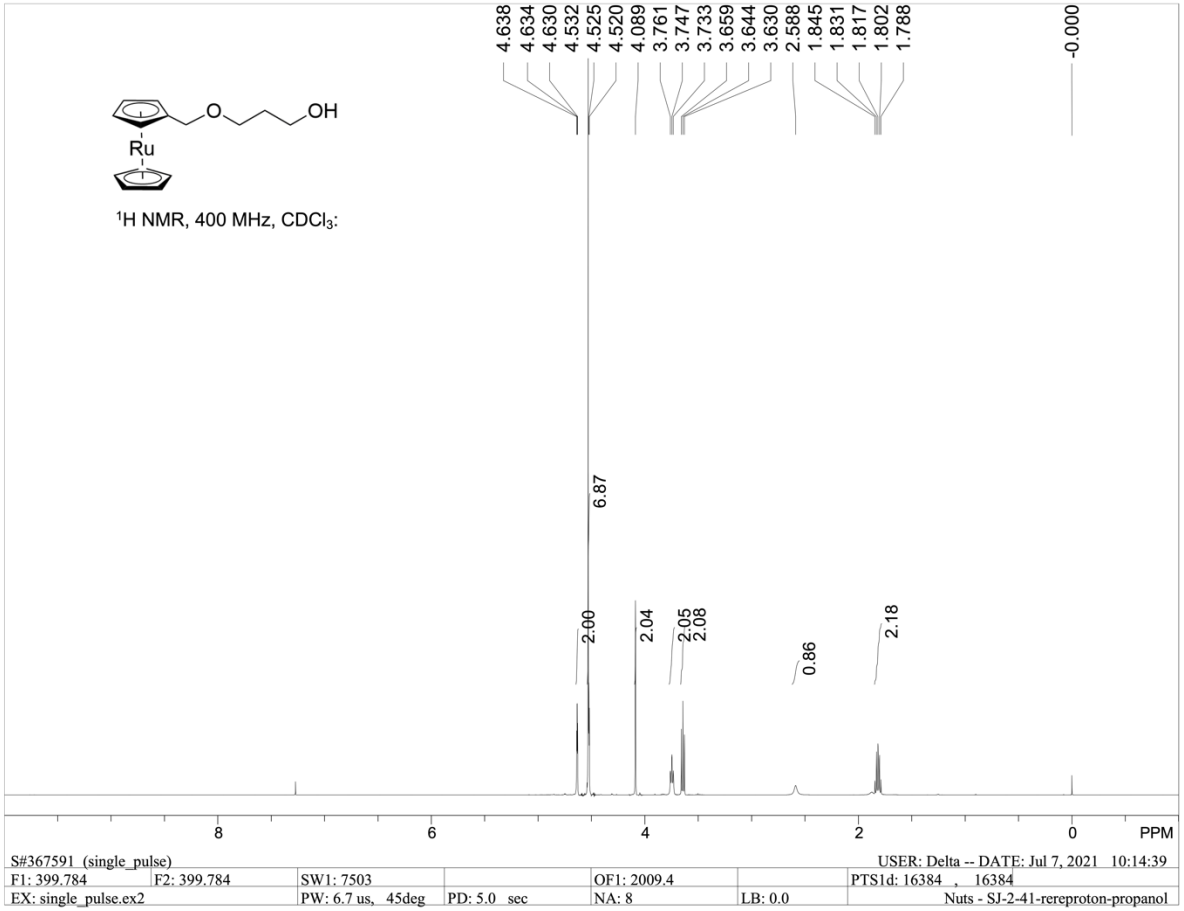

Figure S15. The ^{1}H NMR spectrum ($CDCl_3$) of 3-(Ruthenocenyloxy)propan-1-ol **(3)**.

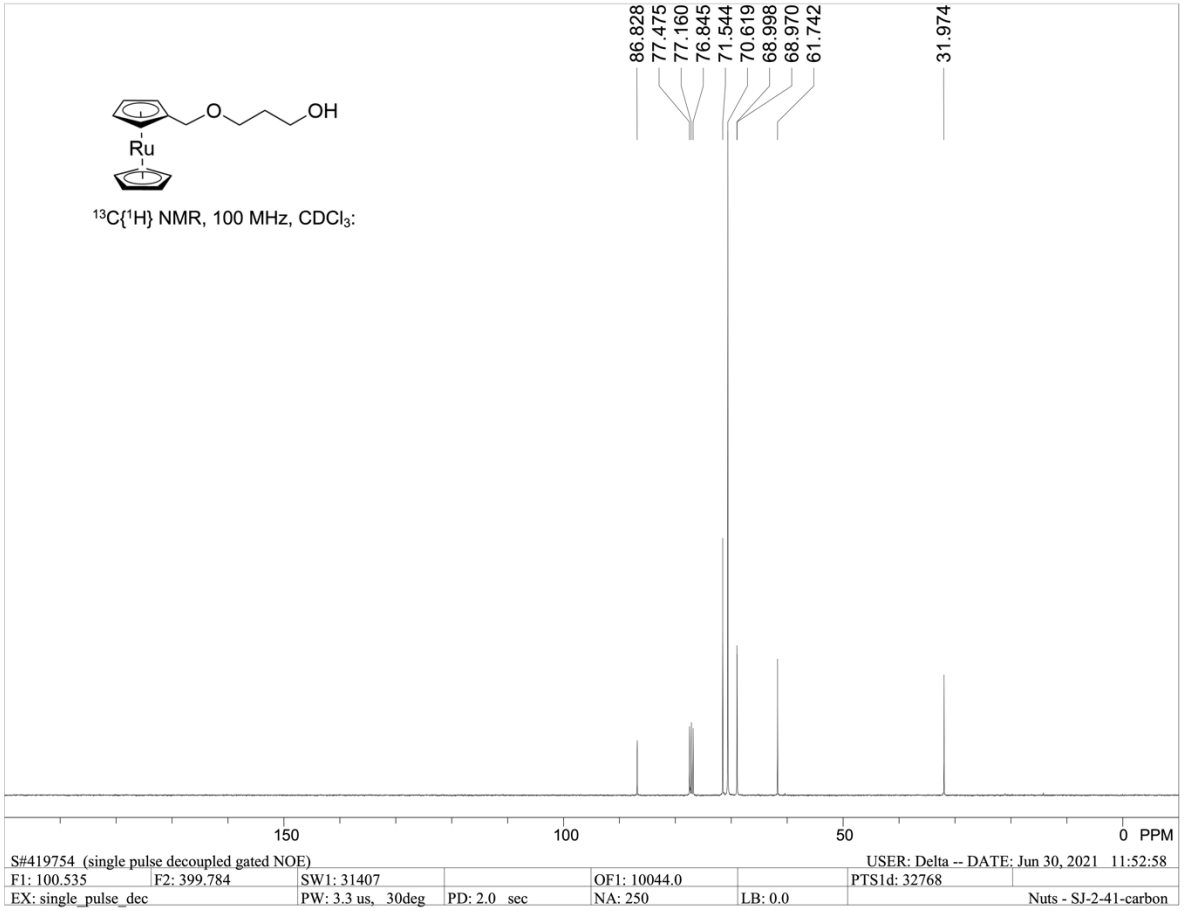

Figure S16. The ^{13}C NMR spectrum ($CDCl_3$) of 3-(Ruthenocenyloxy)propan-1-ol **(3)**.

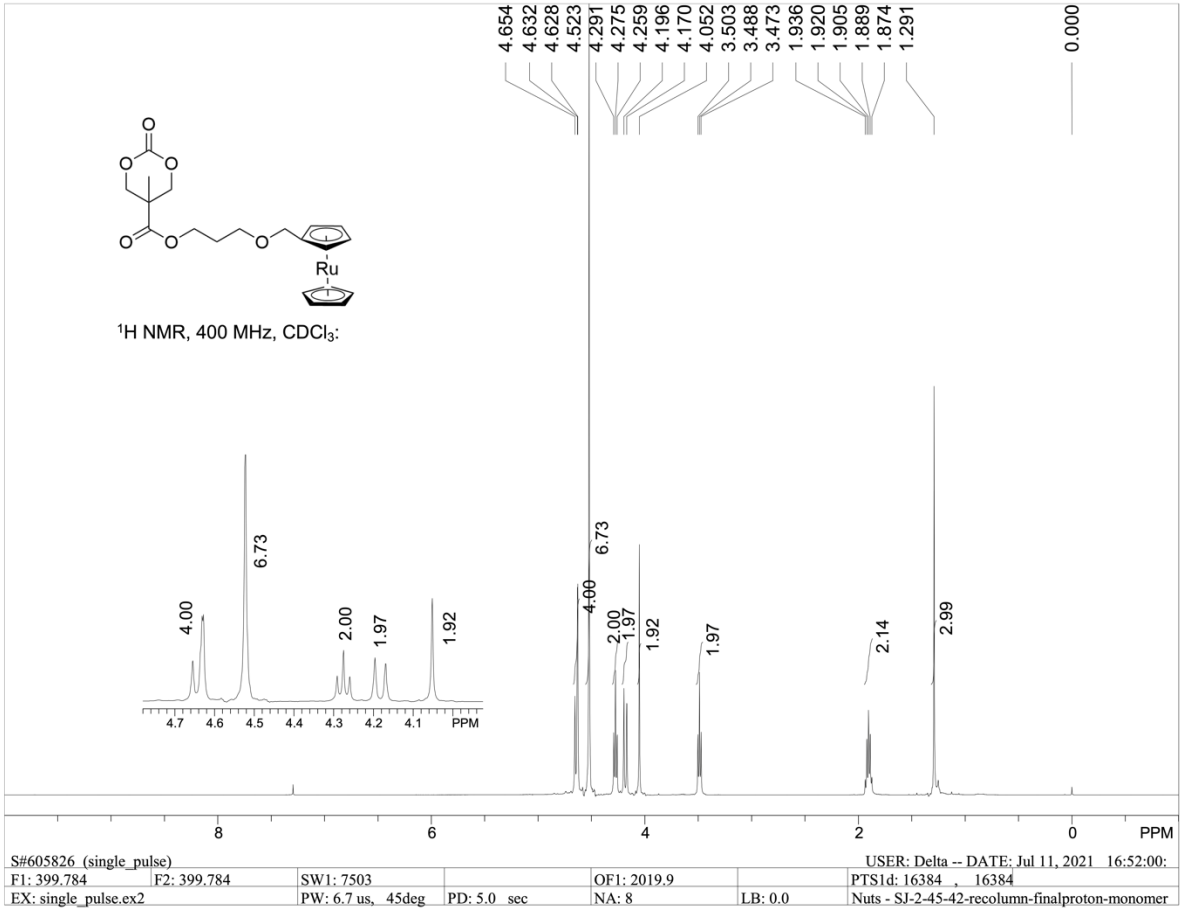

Figure S17. The ^{1}H NMR spectrum ($CDCl_3$) of 3-(Ruthenocenyloxy)propyl 5-methyl-2-oxo-1,3-dioxane-5-carboxylate **(4)**.

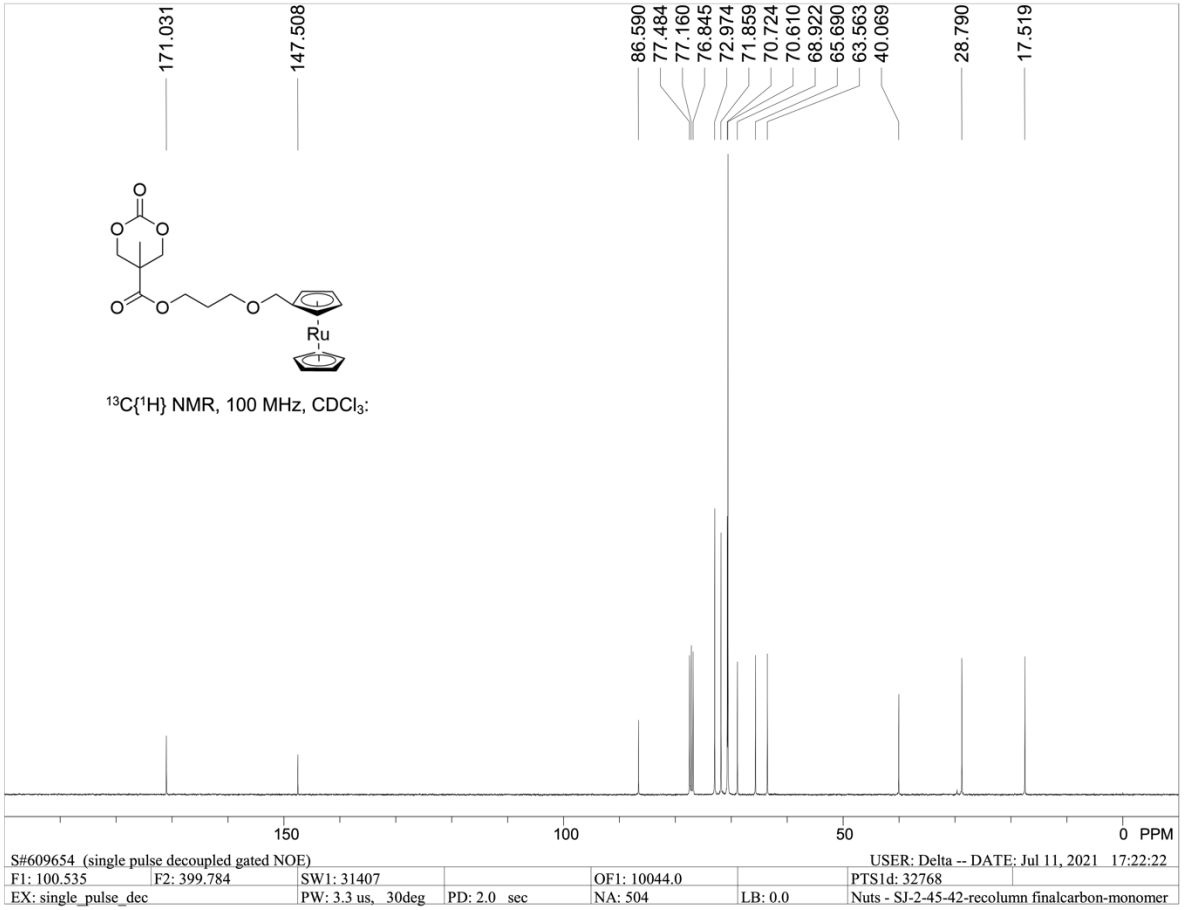

Figure S18. The ^{13}C NMR spectrum ($CDCl_3$) of 3-(Ruthenocenyloxy)propyl 5-methyl-2-oxo-1,3-dioxane-5-carboxylate **(4)**.

III. X-Ray Structure of Ferrocene Monomer 2

Experimental. Yellow crystals suitable for X-ray diffraction were obtained by layering pentane on top of a concentrated solution of **2** in dichloromethane. Single crystals were coated with a trace of Fomblin oil and were mounted on the goniometer head of a Bruker Quest diffractometer with a fixed chi angle, a Mo Kα wavelength (λ = 0.71073 Å) sealed tube fine focus X-ray tube, single crystal curved graphite incident beam monochromator, and a Photon II area detector. The instrument is equipped with an Oxford Cryosystems low temperature device and examination and data collection were performed at 150 K. Data were collected, reflections were indexed and processed, and the files scaled and corrected for absorption using APEX3 [1] and SADABS [2]. The space group was assigned using XPREP within the SHELXTL suite of programs [3,4] and solved by direct methods using ShelXS [4] and refined by full matrix least squares against F^2 with all reflections using Shelxl2018 [5] using the graphical interface Shelxle [6]. H atoms were positioned geometrically and constrained to ride on their parent atoms. C-H bond distances were constrained to 0.95 Å for cyclopentadienyl C-H moieties, and to 0.99 and 0.98 Å for aliphatic CH_2 and CH_3 moieties, respectively. Methyl H atoms were allowed to rotate but not to tip to best fit the experimental electron density. U_{iso}(H) values were set to a multiple of U_{eq}(C) with 1.5 for CH_3 and 1.2 for C-H and CH_2 units, respectively.

The structure emulates an orthorhombic C-centered lattice with double the volume of the actual primitive monoclinic cell and is twinned by the apparent orthorhombic symmetry. Application of the transformation matrix 1 0 1, 0 -1 0, 0 0 -1 (180° rotation around the c-axis) resulted in a twin ratio of 0.5371(7) to 0.4629(7). The structure also exhibits minor disorder across a pseudo-mirror plane perpendicular to the b-axis. Disorder is minor, smaller than 8%, but most minor atom positions were well resolved in difference density maps. Refinement of the minor moiety required strong geometry and thermal parameter restraints approximating a rigid body refinement. Major and minor disordered moieties were each restrained to have similar geometries (SAME restraint, esd 0.001 Å). U^{ij} components of ADPs for disordered atoms related by the pseudo-mirror plane were pairwise restrained to be similar (SIMU restraint, esd 0.008 $Å^2$; for atom pairs O2A and O2C, and O2B and O2D an esd of 0.004 $Å^2$ was used). For the iron atoms Fe1B and Fe1D the ADPs were constrained to be exactly identical (EADP command). A rigid bond restraint (RIGU) was used for the minor moieties. Subject to these conditions the occupancy ratio refined to 0.9226(16) to 0.0774(16) for moieties A and C, and to 0.9763(10) to 0.0237(10) for moieties B and D.

Omission of disorder resulted in high residual electron peaks for the alternative iron atom positions (4.69 and 4.42 electrons) and substantially increased R-values (R1 = 5.75 instead of 4.17%). Complete crystallographic data, in CIF format, have been deposited with the Cambridge Crystallographic Data Centre. CCDC 2157240 contain the supplementary crystallographic data for this paper. These data can be obtained free of charge from The Cambridge Crystallographic Data Centre via www.ccdc.cam.ac.uk/data_request/cif.

References

[1] Bruker (2019). Apex3 v2019.11-0, SAINT V8.40B, Bruker AXS Inc.: Madison (WI), USA.
[2] Krause, L., Herbst-Irmer, R., Sheldrick, G.M. & Stalke, D. (2015). J. Appl. Cryst. 48, 3-10.
[3] SHELXTL suite of programs, Version 6.14, 2000-2003, Bruker Advanced X-ray Solutions, Bruker AXS Inc., Madison, Wisconsin: USA
[4] Sheldrick, G.M. A short history of SHELX. Acta Crystallogr A. 2008, 64(1), 112–122.

[5] a) Sheldrick, G.M. University of Göttingen, Germany, 2018. b) Sheldrick, G.M. Crystal structure refinement with SHELXL. Acta Crystallogr Sect C Struct Chem. 2015, 71(1), 3–8.
[6] Hübschle, C.B., Sheldrick, G.M. & Dittrich, B. ShelXle: a Qt graphical user interface for SHELXL. J. Appl. Crystallogr. 2011, 44(6), 1281–1284.

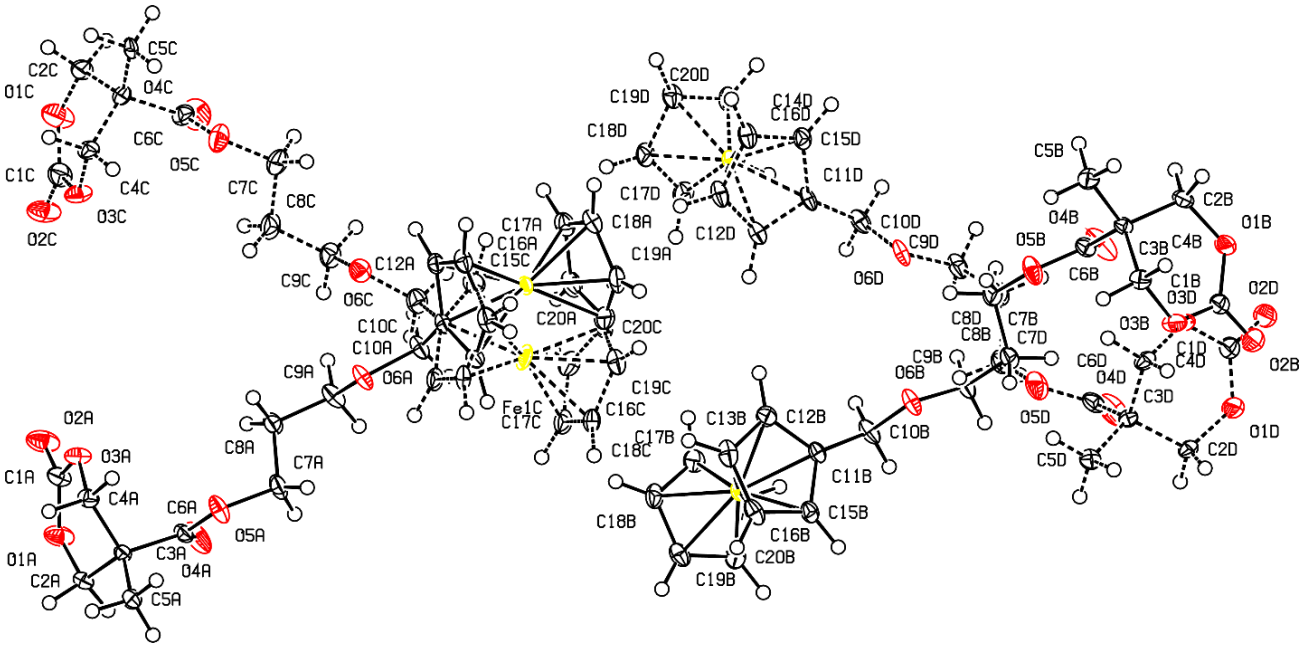

Figure S19. A view of the structure of ferrocene monomer **2**, showing the atom-labelling scheme. Displacement ellipsoids are drawn at the 50% probability level.

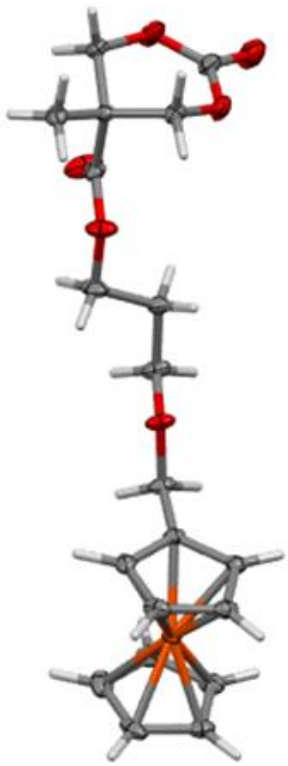

Figure S20. An expansion of one of the major moieties of ferrocene monomer **2**.

Table S2. Experimental details

	KO_152_0m
Crystal data	
Chemical formula	$C_{20}H_{24}FeO_6$
M_r	416.24
Crystal system, space group	Monoclinic, *P*2/*c*
Temperature (K)	150
a, *b*, *c* (Å)	34.6729 (18), 5.8345 (3), 19.159 (1)
β (°)	106.030 (2)
V (Å^3)	3725.1 (3)
Z	8
F(000)	1744
D_x (Mg m^{-3})	1.484
Radiation type	Mo *K*α
No. of reflections for cell measurement	9893
θ range (°) for cell measurement	2.4–36.4
μ (mm^{-1})	0.84
Crystal shape	Plate
Colour	Yellow
Crystal size (mm)	0.41 × 0.39 × 0.05
Data collection	
Diffractometer	Bruker AXS D8 Quest diffractometer with PhotonII charge-integrating pixel array detector (CPAD)
Radiation source	fine focus sealed tube X-ray source
Monochromator	Triumph curved graphite crystal
Detector resolution (pixels mm^{-1})	7.4074
Scan method	ω and phi scans
Absorption correction	Multi-scan, *SADABS* 2016/2: Krause, L., Herbst-Irmer, R., Sheldrick G.M. & Stalke D., J. Appl. Cryst. 48 (2015) 3-10
T_{min}, T_{max}	0.155, 0.223
No. of measured, independent and observed [$I > 2\sigma(I)$] reflections	66968, 16862, 16007
R_{int}	0.039
θ values (°)	θ_{max} = 37.1, θ_{min} = 1.8
$(\sin\theta/\lambda)_{max}$ (Å^{-1})	0.849
Range of *h*, *k*, *l*	*h* = -58→42, *k* = -8→9, *l* = -30→32

Refinement	
Refinement on	F^2
$R[F^2 > 2\sigma(F^2)]$, $wR(F^2)$, S	0.042, 0.094, 1.13
No. of reflections	16862
No. of parameters	972
No. of restraints	1169
H-atom treatment	H-atom parameters constrained
Weighting scheme	$w = 1/[\sigma^2(F_o^2) + (0.0295P)^2 + 2.0271P]$ where $P = (F_o^2 + 2F_c^2)/3$
$(\Delta/\sigma)_{max}$	0.001
$\Delta\rho_{max}$, $\Delta\rho_{min}$ (e Å^{-3})	0.68, -0.55

Table S3. Selected geometric parameters (Å, º)

Fe1A–C11A	2.0348 (17)	Fe1C–C11C	2.0348 (18)
Fe1A–C15A	2.0349 (18)	Fe1C–C15C	2.035 (2)
Fe1A–C12A	2.0362 (17)	Fe1C–C12C	2.0362 (19)
Fe1A–C13A	2.0399 (18)	Fe1C–C13C	2.040 (2)
Fe1A–C16A	2.0431 (19)	Fe1C–C18C	2.043 (2)
Fe1A–C18A	2.0431 (19)	Fe1C–C16C	2.043 (2)
Fe1A–C17A	2.0432 (19)	Fe1C–C17C	2.043 (2)
Fe1A–C20A	2.047 (2)	Fe1C–C20C	2.047 (2)
Fe1A–C19A	2.0489 (18)	Fe1C–C19C	2.0489 (19)
Fe1A–C14A	2.049 (2)	Fe1C–C14C	2.049 (2)
O1A–C1A	1.324 (3)	O1C–C1C	1.324 (3)
O1A–C2A	1.454 (3)	O1C–C2C	1.454 (3)
O2A–C1A	1.201 (3)	O2C–C1C	1.201 (3)
O3A–C1A	1.344 (3)	O3C–C1C	1.344 (3)
O3A–C4A	1.454 (2)	O3C–C4C	1.454 (3)
O4A–C6A	1.200 (2)	O4C–C6C	1.200 (3)
O5A–C6A	1.337 (2)	O5C–C6C	1.338 (2)
O5A–C7A	1.464 (2)	O5C–C7C	1.464 (3)
O6A–C9A	1.426 (2)	O6C–C9C	1.426 (3)
O6A–C10A	1.440 (2)	O6C–C10C	1.440 (2)
C2A–C3A	1.521 (3)	C2C–C3C	1.521 (3)
C2A–H2AA	0.9900	C2C–H2CA	0.9900
C2A–H2AB	0.9900	C2C–H2CB	0.9900
C3A–C4A	1.512 (2)	C3C–C4C	1.512 (3)
C3A–C6A	1.525 (2)	C3C–C6C	1.525 (2)
C3A–C5A	1.534 (3)	C3C–C5C	1.534 (3)
C4A–H4AA	0.9900	C4C–H4CA	0.9900
C4A–H4AB	0.9900	C4C–H4CB	0.9900
C5A–H5AA	0.9800	C5C–H5CA	0.9800
C5A–H5AB	0.9800	C5C–H5CB	0.9800
C5A–H5AC	0.9800	C5C–H5CC	0.9800
C7A–C8A	1.503 (3)	C7C–C8C	1.503 (3)
C7A–H7AA	0.9900	C7C–H7CA	0.9900
C7A–H7AB	0.9900	C7C–H7CB	0.9900
C8A–C9A	1.508 (3)	C8C–C9C	1.508 (3)
C8A–H8AA	0.9900	C8C–H8CA	0.9900

C8A–H8AB	0.9900	C8C–H8CB	0.9900
C9A–H9AA	0.9900	C9C–H9CA	0.9900
C9A–H9AB	0.9900	C9C–H9CB	0.9900
C10A–C11A	1.491 (3)	C10C–C11C	1.492 (3)
C10A–H10A	0.9900	C10C–H10E	0.9900
C10A–H10B	0.9900	C10C–H10F	0.9900
C11A–C12A	1.426 (3)	C11C–C12C	1.426 (3)
C11A–C15A	1.431 (3)	C11C–C15C	1.431 (3)
C12A–C13A	1.431 (3)	C12C–C13C	1.431 (3)
C12A–H12A	1.0000	C12C–H12C	1.0000
C13A–C14A	1.429 (3)	C13C–C14C	1.429 (3)
C13A–H13A	1.0000	C13C–H13C	1.0000
C14A–C15A	1.432 (3)	C14C–C15C	1.432 (3)
C14A–H14A	1.0000	C14C–H14C	1.0000
C15A–H15A	1.0000	C15C–H15C	1.0000
C16A–C17A	1.413 (3)	C16C–C17C	1.413 (3)
C16A–C20A	1.422 (4)	C16C–C20C	1.422 (4)
C16A–H16A	1.0000	C16C–H16C	1.0000
C17A–C18A	1.423 (3)	C17C–C18C	1.423 (3)
C17A–H17A	1.0000	C17C–H17C	1.0000
C18A–C19A	1.419 (3)	C18C–C19C	1.419 (3)
C18A–H18A	1.0000	C18C–H18C	1.0000
C19A–C20A	1.431 (4)	C19C–C20C	1.431 (4)
C19A–H19A	1.0000	C19C–H19C	1.0000
C20A–H20A	1.0000	C20C–H20C	1.0000
Fe1B–C11B	2.0374 (16)	Fe1D–C11D	2.0349 (18)
Fe1B–C19B	2.0397 (17)	Fe1D–C15D	2.035 (2)
Fe1B–C15B	2.0411 (17)	Fe1D–C12D	2.0362 (19)
Fe1B–C18B	2.0464 (17)	Fe1D–C13D	2.040 (2)
Fe1B–C12B	2.0472 (18)	Fe1D–C18D	2.043 (2)
Fe1B–C20B	2.0489 (18)	Fe1D–C16D	2.043 (2)
Fe1B–C14B	2.0526 (18)	Fe1D–C17D	2.043 (2)
Fe1B–C17B	2.054 (2)	Fe1D–C20D	2.047 (2)
Fe1B–C13B	2.054 (2)	Fe1D–C19D	2.049 (2)
Fe1B–C16B	2.0554 (18)	Fe1D–C14D	2.049 (2)
O1B–C1B	1.327 (2)	O1D–C1D	1.324 (3)
O1B–C2B	1.454 (2)	O1D–C2D	1.454 (3)

O2B–C1B	1.197 (2)	O2D–C1D	1.201 (3)
O3B–C1B	1.350 (2)	O3D–C1D	1.344 (3)
O3B–C4B	1.443 (2)	O3D–C4D	1.454 (3)
O4B–C6B	1.202 (2)	O4D–C6D	1.200 (3)
O5B–C6B	1.338 (2)	O5D–C6D	1.338 (2)
O5B–C7B	1.455 (2)	O5D–C7D	1.464 (3)
O6B–C9B	1.424 (2)	O6D–C9D	1.426 (3)
O6B–C10B	1.435 (2)	O6D–C10D	1.440 (2)
C2B–C3B	1.516 (2)	C2D–C3D	1.521 (3)
C2B–H2BA	0.9900	C2D–H2DA	0.9900
C2B–H2BB	0.9900	C2D–H2DB	0.9900
C3B–C4B	1.521 (2)	C3D–C4D	1.512 (3)
C3B–C6B	1.527 (2)	C3D–C6D	1.525 (2)
C3B–C5B	1.533 (2)	C3D–C5D	1.534 (3)
C4B–H4BA	0.9900	C4D–H4DA	0.9900
C4B–H4BB	0.9900	C4D–H4DB	0.9900
C5B–H5BA	0.9800	C5D–H5DA	0.9800
C5B–H5BB	0.9800	C5D–H5DB	0.9800
C5B–H5BC	0.9800	C5D–H5DC	0.9800
C7B–C8B	1.493 (3)	C7D–C8D	1.503 (3)
C7B–H7BA	0.9900	C7D–H7DA	0.9900
C7B–H7BB	0.9900	C7D–H7DB	0.9900
C8B–C9B	1.527 (3)	C8D–C9D	1.508 (3)
C8B–H8BA	0.9900	C8D–H8DA	0.9900
C8B–H8BB	0.9900	C8D–H8DB	0.9900
C9B–H9BA	0.9900	C9D–H9DA	0.9900
C9B–H9BB	0.9900	C9D–H9DB	0.9900
C10B–C11B	1.486 (3)	C10D–C11D	1.491 (3)
C10B–H10C	0.9900	C10D–H10G	0.9900
C10B–H10D	0.9900	C10D–H10H	0.9900
C11B–C12B	1.429 (3)	C11D–C12D	1.426 (3)
C11B–C15B	1.437 (3)	C11D–C15D	1.431 (3)
C12B–C13B	1.435 (3)	C12D–C13D	1.431 (3)
C12B–H12B	1.0000	C12D–H12D	1.0000
C13B–C14B	1.420 (3)	C13D–C14D	1.429 (3)
C13B–H13B	1.0000	C13D–H13D	1.0000
C14B–C15B	1.429 (3)	C14D–C15D	1.432 (3)

C14B–H14B	1.0000	C14D–H14D	1.0000
C15B–H15B	1.0000	C15D–H15D	1.0000
C16B–C20B	1.420 (3)	C16D–C17D	1.413 (3)
C16B–C17B	1.432 (3)	C16D–C20D	1.422 (4)
C16B–H16B	1.0000	C16D–H16D	1.0000
C17B–C18B	1.426 (3)	C17D–C18D	1.423 (3)
C17B–H17B	1.0000	C17D–H17D	1.0000
C18B–C19B	1.417 (3)	C18D–C19D	1.419 (3)
C18B–H18B	1.0000	C18D–H18D	1.0000
C19B–C20B	1.431 (3)	C19D–C20D	1.431 (4)
C19B–H19B	1.0000	C19D–H19D	1.0000
C20B–H20B	1.0000	C20D–H20D	1.0000
C11A–Fe1A–C15A	41.18 (8)	C11C–Fe1C–C15C	41.18 (9)
C11A–Fe1A–C12A	41.02 (8)	C11C–Fe1C–C12C	41.02 (8)
C15A–Fe1A–C12A	69.03 (8)	C15C–Fe1C–C12C	69.03 (9)
C11A–Fe1A–C13A	69.23 (8)	C11C–Fe1C–C13C	69.24 (9)
C15A–Fe1A–C13A	68.97 (8)	C15C–Fe1C–C13C	68.98 (9)
C12A–Fe1A–C13A	41.12 (7)	C12C–Fe1C–C13C	41.12 (8)
C11A–Fe1A–C16A	106.54 (8)	C11C–Fe1C–C18C	158.35 (12)
C15A–Fe1A–C16A	122.47 (9)	C15C–Fe1C–C18C	159.27 (11)
C12A–Fe1A–C16A	122.09 (9)	C12C–Fe1C–C18C	122.43 (11)
C13A–Fe1A–C16A	158.61 (9)	C13C–Fe1C–C18C	107.30 (10)
C11A–Fe1A–C18A	158.36 (8)	C11C–Fe1C–C16C	106.52 (10)
C15A–Fe1A–C18A	159.27 (8)	C15C–Fe1C–C16C	122.47 (11)
C12A–Fe1A–C18A	122.42 (8)	C12C–Fe1C–C16C	122.07 (11)
C13A–Fe1A–C18A	107.29 (8)	C13C–Fe1C–C16C	158.59 (12)
C16A–Fe1A–C18A	68.49 (8)	C18C–Fe1C–C16C	68.48 (10)
C11A–Fe1A–C17A	121.93 (8)	C11C–Fe1C–C17C	121.92 (11)
C15A–Fe1A–C17A	158.42 (9)	C15C–Fe1C–C17C	158.42 (12)
C12A–Fe1A–C17A	106.91 (8)	C12C–Fe1C–C17C	106.90 (10)
C13A–Fe1A–C17A	122.76 (9)	C13C–Fe1C–C17C	122.75 (11)
C16A–Fe1A–C17A	40.45 (9)	C18C–Fe1C–C17C	40.75 (9)
C18A–Fe1A–C17A	40.75 (8)	C16C–Fe1C–C17C	40.45 (9)
C11A–Fe1A–C20A	122.55 (10)	C11C–Fe1C–C20C	122.53 (12)
C15A–Fe1A–C20A	107.54 (10)	C15C–Fe1C–C20C	107.54 (12)
C12A–Fe1A–C20A	158.62 (10)	C12C–Fe1C–C20C	158.59 (12)

C13A–Fe1A–C20A	159.14 (10)	C13C–Fe1C–C20C	159.16 (13)
C16A–Fe1A–C20A	40.68 (10)	C18C–Fe1C–C20C	68.27 (11)
C18A–Fe1A–C20A	68.28 (10)	C16C–Fe1C–C20C	40.67 (11)
C17A–Fe1A–C20A	68.09 (10)	C17C–Fe1C–C20C	68.09 (11)
C11A–Fe1A–C19A	159.24 (9)	C11C–Fe1C–C19C	159.23 (12)
C15A–Fe1A–C19A	123.00 (8)	C15C–Fe1C–C19C	123.00 (11)
C12A–Fe1A–C19A	158.64 (9)	C12C–Fe1C–C19C	158.66 (12)
C13A–Fe1A–C19A	122.51 (9)	C13C–Fe1C–C19C	122.54 (11)
C16A–Fe1A–C19A	68.82 (9)	C18C–Fe1C–C19C	40.57 (9)
C18A–Fe1A–C19A	40.57 (9)	C16C–Fe1C–C19C	68.81 (10)
C17A–Fe1A–C19A	68.48 (8)	C17C–Fe1C–C19C	68.48 (9)
C20A–Fe1A–C19A	40.90 (11)	C20C–Fe1C–C19C	40.90 (11)
C11A–Fe1A–C14A	69.34 (8)	C11C–Fe1C–C14C	69.34 (9)
C15A–Fe1A–C14A	41.06 (9)	C15C–Fe1C–C14C	41.06 (10)
C12A–Fe1A–C14A	69.09 (8)	C12C–Fe1C–C14C	69.10 (9)
C13A–Fe1A–C14A	40.90 (9)	C13C–Fe1C–C14C	40.90 (10)
C16A–Fe1A–C14A	159.03 (10)	C18C–Fe1C–C14C	122.88 (11)
C18A–Fe1A–C14A	122.87 (9)	C16C–Fe1C–C14C	159.04 (13)
C17A–Fe1A–C14A	159.12 (10)	C17C–Fe1C–C14C	159.12 (12)
C20A–Fe1A–C14A	123.05 (10)	C20C–Fe1C–C14C	123.06 (13)
C19A–Fe1A–C14A	107.37 (8)	C19C–Fe1C–C14C	107.39 (10)
C1A–O1A–C2A	123.57 (16)	C1C–O1C–C2C	123.5 (2)
C1A–O3A–C4A	120.02 (17)	C1C–O3C–C4C	120.0 (3)
C6A–O5A–C7A	116.10 (16)	C6C–O5C–C7C	116.1 (2)
C9A–O6A–C10A	111.62 (14)	C9C–O6C–C10C	111.6 (2)
O2A–C1A–O1A	120.9 (2)	O2C–C1C–O1C	120.9 (3)
O2A–C1A–O3A	119.57 (19)	O2C–C1C–O3C	119.6 (2)
O1A–C1A–O3A	119.55 (19)	O1C–C1C–O3C	119.6 (2)
O1A–C2A–C3A	113.38 (14)	O1C–C2C–C3C	113.4 (2)
O1A–C2A–H2AA	108.9	O1C–C2C–H2CA	108.9
C3A–C2A–H2AA	108.9	C3C–C2C–H2CA	108.9
O1A–C2A–H2AB	108.9	O1C–C2C–H2CB	108.9
C3A–C2A–H2AB	108.9	C3C–C2C–H2CB	108.9
H2AA–C2A–H2AB	107.7	H2CA–C2C–H2CB	107.7
C4A–C3A–C2A	105.95 (15)	C4C–C3C–C2C	105.97 (19)
C4A–C3A–C6A	109.77 (14)	C4C–C3C–C6C	109.77 (19)
C2A–C3A–C6A	110.02 (15)	C2C–C3C–C6C	110.0 (2)

C4A–C3A–C5A	110.07 (15)	C4C–C3C–C5C	110.1 (2)
C2A–C3A–C5A	110.20 (15)	C2C–C3C–C5C	110.2 (2)
C6A–C3A–C5A	110.72 (15)	C6C–C3C–C5C	110.7 (2)
O3A–C4A–C3A	109.80 (15)	O3C–C4C–C3C	109.8 (2)
O3A–C4A–H4AA	109.7	O3C–C4C–H4CA	109.7
C3A–C4A–H4AA	109.7	C3C–C4C–H4CA	109.7
O3A–C4A–H4AB	109.7	O3C–C4C–H4CB	109.7
C3A–C4A–H4AB	109.7	C3C–C4C–H4CB	109.7
H4AA–C4A–H4AB	108.2	H4CA–C4C–H4CB	108.2
C3A–C5A–H5AA	109.5	C3C–C5C–H5CA	109.5
C3A–C5A–H5AB	109.5	C3C–C5C–H5CB	109.5
H5AA–C5A–H5AB	109.5	H5CA–C5C–H5CB	109.5
C3A–C5A–H5AC	109.5	C3C–C5C–H5CC	109.5
H5AA–C5A–H5AC	109.5	H5CA–C5C–H5CC	109.5
H5AB–C5A–H5AC	109.5	H5CB–C5C–H5CC	109.5
O4A–C6A–O5A	124.28 (17)	O4C–C6C–O5C	124.2 (2)
O4A–C6A–C3A	124.60 (17)	O4C–C6C–C3C	124.5 (2)
O5A–C6A–C3A	111.12 (15)	O5C–C6C–C3C	111.1 (2)
O5A–C7A–C8A	110.52 (17)	O5C–C7C–C8C	110.5 (2)
O5A–C7A–H7AA	109.5	O5C–C7C–H7CA	109.5
C8A–C7A–H7AA	109.5	C8C–C7C–H7CA	109.5
O5A–C7A–H7AB	109.5	O5C–C7C–H7CB	109.5
C8A–C7A–H7AB	109.5	C8C–C7C–H7CB	109.5
H7AA–C7A–H7AB	108.1	H7CA–C7C–H7CB	108.1
C7A–C8A–C9A	112.89 (18)	C7C–C8C–C9C	112.9 (2)
C7A–C8A–H8AA	109.0	C7C–C8C–H8CA	109.0
C9A–C8A–H8AA	109.0	C9C–C8C–H8CA	109.0
C7A–C8A–H8AB	109.0	C7C–C8C–H8CB	109.0
C9A–C8A–H8AB	109.0	C9C–C8C–H8CB	109.0
H8AA–C8A–H8AB	107.8	H8CA–C8C–H8CB	107.8
O6A–C9A–C8A	108.15 (16)	O6C–C9C–C8C	108.1 (2)
O6A–C9A–H9AA	110.1	O6C–C9C–H9CA	110.1
C8A–C9A–H9AA	110.1	C8C–C9C–H9CA	110.1
O6A–C9A–H9AB	110.1	O6C–C9C–H9CB	110.1
C8A–C9A–H9AB	110.1	C8C–C9C–H9CB	110.1
H9AA–C9A–H9AB	108.4	H9CA–C9C–H9CB	108.4
O6A–C10A–C11A	107.72 (14)	O6C–C10C–C11C	107.7 (2)

O6A–C10A–H10A	110.2	O6C–C10C–H10E	110.2
C11A–C10A–H10A	110.2	C11C–C10C–H10E	110.2
O6A–C10A–H10B	110.2	O6C–C10C–H10F	110.2
C11A–C10A–H10B	110.2	C11C–C10C–H10F	110.2
H10A–C10A–H10B	108.5	H10E–C10C–H10F	108.5
C12A–C11A–C15A	107.64 (16)	C12C–C11C–C15C	107.65 (18)
C12A–C11A–C10A	126.92 (18)	C12C–C11C–C10C	126.9 (2)
C15A–C11A–C10A	125.39 (19)	C15C–C11C–C10C	125.4 (2)
C12A–C11A–Fe1A	69.54 (10)	C12C–C11C–Fe1C	69.54 (11)
C15A–C11A–Fe1A	69.41 (10)	C15C–C11C–Fe1C	69.41 (11)
C10A–C11A–Fe1A	128.41 (13)	C10C–C11C–Fe1C	128.28 (19)
C11A–C12A–C13A	108.20 (17)	C11C–C12C–C13C	108.20 (19)
C11A–C12A–Fe1A	69.44 (10)	C11C–C12C–Fe1C	69.44 (10)
C13A–C12A–Fe1A	69.58 (10)	C13C–C12C–Fe1C	69.57 (11)
C11A–C12A–H12A	125.9	C11C–C12C–H12C	125.9
C13A–C12A–H12A	125.9	C13C–C12C–H12C	125.9
Fe1A–C12A–H12A	125.9	Fe1C–C12C–H12C	125.9
C14A–C13A–C12A	108.21 (17)	C14C–C13C–C12C	108.21 (19)
C14A–C13A–Fe1A	69.91 (11)	C14C–C13C–Fe1C	69.91 (12)
C12A–C13A–Fe1A	69.31 (10)	C12C–C13C–Fe1C	69.31 (11)
C14A–C13A–H13A	125.9	C14C–C13C–H13C	125.9
C12A–C13A–H13A	125.9	C12C–C13C–H13C	125.9
Fe1A–C13A–H13A	125.9	Fe1C–C13C–H13C	125.9
C13A–C14A–C15A	107.49 (17)	C13C–C14C–C15C	107.50 (19)
C13A–C14A–Fe1A	69.19 (11)	C13C–C14C–Fe1C	69.19 (12)
C15A–C14A–Fe1A	68.93 (11)	C15C–C14C–Fe1C	68.93 (12)
C13A–C14A–H14A	126.2	C13C–C14C–H14C	126.2
C15A–C14A–H14A	126.2	C15C–C14C–H14C	126.2
Fe1A–C14A–H14A	126.2	Fe1C–C14C–H14C	126.2
C11A–C15A–C14A	108.45 (18)	C11C–C15C–C14C	108.4 (2)
C11A–C15A–Fe1A	69.40 (10)	C11C–C15C–Fe1C	69.40 (11)
C14A–C15A–Fe1A	70.02 (11)	C14C–C15C–Fe1C	70.01 (12)
C11A–C15A–H15A	125.8	C11C–C15C–H15C	125.8
C14A–C15A–H15A	125.8	C14C–C15C–H15C	125.8
Fe1A–C15A–H15A	125.8	Fe1C–C15C–H15C	125.8
C17A–C16A–C20A	107.8 (2)	C17C–C16C–C20C	107.8 (2)
C17A–C16A–Fe1A	69.78 (11)	C17C–C16C–Fe1C	69.78 (12)

C20A–C16A–Fe1A	69.82 (13)	C20C–C16C–Fe1C	69.82 (13)
C17A–C16A–H16A	126.1	C17C–C16C–H16C	126.1
C20A–C16A–H16A	126.1	C20C–C16C–H16C	126.1
Fe1A–C16A–H16A	126.1	Fe1C–C16C–H16C	126.1
C16A–C17A–C18A	108.37 (19)	C16C–C17C–C18C	108.4 (2)
C16A–C17A–Fe1A	69.77 (11)	C16C–C17C–Fe1C	69.77 (12)
C18A–C17A–Fe1A	69.62 (11)	C18C–C17C–Fe1C	69.62 (12)
C16A–C17A–H17A	125.8	C16C–C17C–H17C	125.8
C18A–C17A–H17A	125.8	C18C–C17C–H17C	125.8
Fe1A–C17A–H17A	125.8	Fe1C–C17C–H17C	125.8
C19A–C18A–C17A	108.24 (19)	C19C–C18C–C17C	108.2 (2)
C19A–C18A–Fe1A	69.93 (11)	C19C–C18C–Fe1C	69.93 (12)
C17A–C18A–Fe1A	69.63 (11)	C17C–C18C–Fe1C	69.63 (11)
C19A–C18A–H18A	125.9	C19C–C18C–H18C	125.9
C17A–C18A–H18A	125.9	C17C–C18C–H18C	125.9
Fe1A–C18A–H18A	125.9	Fe1C–C18C–H18C	125.9
C18A–C19A–C20A	107.3 (2)	C18C–C19C–C20C	107.3 (2)
C18A–C19A–Fe1A	69.50 (10)	C18C–C19C–Fe1C	69.49 (11)
C20A–C19A–Fe1A	69.49 (12)	C20C–C19C–Fe1C	69.50 (12)
C18A–C19A–H19A	126.3	C18C–C19C–H19C	126.3
C20A–C19A–H19A	126.3	C20C–C19C–H19C	126.3
Fe1A–C19A–H19A	126.3	Fe1C–C19C–H19C	126.3
C16A–C20A–C19A	108.3 (2)	C16C–C20C–C19C	108.3 (2)
C16A–C20A–Fe1A	69.50 (12)	C16C–C20C–Fe1C	69.51 (13)
C19A–C20A–Fe1A	69.61 (12)	C19C–C20C–Fe1C	69.60 (13)
C16A–C20A–H20A	125.9	C16C–C20C–H20C	125.9
C19A–C20A–H20A	125.9	C19C–C20C–H20C	125.9
Fe1A–C20A–H20A	125.9	Fe1C–C20C–H20C	125.9
C11B–Fe1B–C19B	159.91 (8)	C11D–Fe1D–C15D	41.18 (9)
C11B–Fe1B–C15B	41.25 (7)	C11D–Fe1D–C12D	41.02 (8)
C19B–Fe1B–C15B	122.71 (8)	C15D–Fe1D–C12D	69.03 (9)
C11B–Fe1B–C18B	158.17 (8)	C11D–Fe1D–C13D	69.23 (9)
C19B–Fe1B–C18B	40.59 (8)	C15D–Fe1D–C13D	68.98 (9)
C15B–Fe1B–C18B	159.24 (8)	C12D–Fe1D–C13D	41.12 (8)
C11B–Fe1B–C12B	40.95 (7)	C11D–Fe1D–C18D	158.35 (11)
C19B–Fe1B–C12B	157.49 (8)	C15D–Fe1D–C18D	159.28 (11)
C15B–Fe1B–C12B	69.14 (8)	C12D–Fe1D–C18D	122.43 (11)

C18B–Fe1B–C12B	122.12 (8)	C13D–Fe1D–C18D	107.30 (10)
C11B–Fe1B–C20B	123.42 (7)	C11D–Fe1D–C16D	106.53 (10)
C19B–Fe1B–C20B	40.97 (8)	C15D–Fe1D–C16D	122.46 (11)
C15B–Fe1B–C20B	106.86 (8)	C12D–Fe1D–C16D	122.08 (11)
C18B–Fe1B–C20B	68.48 (8)	C13D–Fe1D–C16D	158.61 (12)
C12B–Fe1B–C20B	160.23 (8)	C18D–Fe1D–C16D	68.49 (10)
C11B–Fe1B–C14B	68.99 (7)	C11D–Fe1D–C17D	121.92 (11)
C19B–Fe1B–C14B	106.56 (8)	C15D–Fe1D–C17D	158.41 (12)
C15B–Fe1B–C14B	40.87 (7)	C12D–Fe1D–C17D	106.91 (10)
C18B–Fe1B–C14B	122.98 (8)	C13D–Fe1D–C17D	122.76 (11)
C12B–Fe1B–C14B	68.88 (8)	C18D–Fe1D–C17D	40.75 (9)
C20B–Fe1B–C14B	121.56 (9)	C16D–Fe1D–C17D	40.45 (9)
C11B–Fe1B–C17B	122.32 (8)	C11D–Fe1D–C20D	122.54 (12)
C19B–Fe1B–C17B	68.58 (8)	C15D–Fe1D–C20D	107.54 (12)
C15B–Fe1B–C17B	158.30 (8)	C12D–Fe1D–C20D	158.61 (12)
C18B–Fe1B–C17B	40.71 (8)	C13D–Fe1D–C20D	159.15 (13)
C12B–Fe1B–C17B	107.65 (8)	C18D–Fe1D–C20D	68.28 (11)
C20B–Fe1B–C17B	68.51 (8)	C16D–Fe1D–C20D	40.68 (11)
C14B–Fe1B–C17B	159.75 (8)	C17D–Fe1D–C20D	68.09 (11)
C11B–Fe1B–C13B	68.70 (8)	C11D–Fe1D–C19D	159.24 (12)
C19B–Fe1B–C13B	121.41 (8)	C15D–Fe1D–C19D	123.00 (11)
C15B–Fe1B–C13B	68.51 (8)	C12D–Fe1D–C19D	158.65 (12)
C18B–Fe1B–C13B	107.52 (8)	C13D–Fe1D–C19D	122.53 (11)
C12B–Fe1B–C13B	40.97 (8)	C18D–Fe1D–C19D	40.57 (9)
C20B–Fe1B–C13B	157.26 (9)	C16D–Fe1D–C19D	68.81 (10)
C14B–Fe1B–C13B	40.45 (9)	C17D–Fe1D–C19D	68.48 (9)
C17B–Fe1B–C13B	124.00 (9)	C20D–Fe1D–C19D	40.90 (11)
C11B–Fe1B–C16B	107.71 (7)	C11D–Fe1D–C14D	69.34 (9)
C19B–Fe1B–C16B	68.51 (8)	C15D–Fe1D–C14D	41.06 (10)
C15B–Fe1B–C16B	122.05 (8)	C12D–Fe1D–C14D	69.10 (9)
C18B–Fe1B–C16B	68.40 (8)	C13D–Fe1D–C14D	40.90 (10)
C12B–Fe1B–C16B	124.06 (8)	C18D–Fe1D–C14D	122.88 (11)
C20B–Fe1B–C16B	40.48 (8)	C16D–Fe1D–C14D	159.03 (13)
C14B–Fe1B–C16B	157.59 (9)	C17D–Fe1D–C14D	159.13 (12)
C17B–Fe1B–C16B	40.78 (8)	C20D–Fe1D–C14D	123.05 (13)
C13B–Fe1B–C16B	160.83 (9)	C19D–Fe1D–C14D	107.38 (10)
C1B–O1B–C2B	124.25 (15)	C1D–O1D–C2D	123.6 (2)

C1B–O3B–C4B	119.94 (15)	C1D–O3D–C4D	120.0 (2)
C6B–O5B–C7B	116.98 (16)	C6D–O5D–C7D	116.1 (2)
C9B–O6B–C10B	111.22 (14)	C9D–O6D–C10D	111.6 (2)
O2B–C1B–O1B	120.81 (19)	O2D–C1D–O1D	120.8 (3)
O2B–C1B–O3B	120.34 (19)	O2D–C1D–O3D	119.5 (3)
O1B–C1B–O3B	118.83 (16)	O1D–C1D–O3D	119.5 (2)
O1B–C2B–C3B	112.70 (14)	O1D–C2D–C3D	113.4 (2)
O1B–C2B–H2BA	109.1	O1D–C2D–H2DA	108.9
C3B–C2B–H2BA	109.1	C3D–C2D–H2DA	108.9
O1B–C2B–H2BB	109.1	O1D–C2D–H2DB	108.9
C3B–C2B–H2BB	109.1	C3D–C2D–H2DB	108.9
H2BA–C2B–H2BB	107.8	H2DA–C2D–H2DB	107.7
C2B–C3B–C4B	105.63 (14)	C4D–C3D–C2D	105.98 (19)
C2B–C3B–C6B	110.52 (15)	C4D–C3D–C6D	109.78 (19)
C4B–C3B–C6B	110.02 (14)	C2D–C3D–C6D	110.0 (2)
C2B–C3B–C5B	109.94 (14)	C4D–C3D–C5D	110.1 (2)
C4B–C3B–C5B	109.55 (15)	C2D–C3D–C5D	110.2 (2)
C6B–C3B–C5B	111.04 (14)	C6D–C3D–C5D	110.7 (2)
O3B–C4B–C3B	109.67 (14)	O3D–C4D–C3D	109.8 (2)
O3B–C4B–H4BA	109.7	O3D–C4D–H4DA	109.7
C3B–C4B–H4BA	109.7	C3D–C4D–H4DA	109.7
O3B–C4B–H4BB	109.7	O3D–C4D–H4DB	109.7
C3B–C4B–H4BB	109.7	C3D–C4D–H4DB	109.7
H4BA–C4B–H4BB	108.2	H4DA–C4D–H4DB	108.2
C3B–C5B–H5BA	109.5	C3D–C5D–H5DA	109.5
C3B–C5B–H5BB	109.5	C3D–C5D–H5DB	109.5
H5BA–C5B–H5BB	109.5	H5DA–C5D–H5DB	109.5
C3B–C5B–H5BC	109.5	C3D–C5D–H5DC	109.5
H5BA–C5B–H5BC	109.5	H5DA–C5D–H5DC	109.5
H5BB–C5B–H5BC	109.5	H5DB–C5D–H5DC	109.5
O4B–C6B–O5B	123.94 (17)	O4D–C6D–O5D	124.2 (3)
O4B–C6B–C3B	124.63 (16)	O4D–C6D–C3D	124.5 (3)
O5B–C6B–C3B	111.42 (15)	O5D–C6D–C3D	111.0 (2)
O5B–C7B–C8B	110.52 (16)	O5D–C7D–C8D	110.5 (2)
O5B–C7B–H7BA	109.5	O5D–C7D–H7DA	109.5
C8B–C7B–H7BA	109.5	C8D–C7D–H7DA	109.5
O5B–C7B–H7BB	109.5	O5D–C7D–H7DB	109.5

C8B–C7B–H7BB	109.5	C8D–C7D–H7DB	109.5
H7BA–C7B–H7BB	108.1	H7DA–C7D–H7DB	108.1
C7B–C8B–C9B	112.56 (17)	C7D–C8D–C9D	112.9 (2)
C7B–C8B–H8BA	109.1	C7D–C8D–H8DA	109.0
C9B–C8B–H8BA	109.1	C9D–C8D–H8DA	109.0
C7B–C8B–H8BB	109.1	C7D–C8D–H8DB	109.0
C9B–C8B–H8BB	109.1	C9D–C8D–H8DB	109.0
H8BA–C8B–H8BB	107.8	H8DA–C8D–H8DB	107.8
O6B–C9B–C8B	107.97 (16)	O6D–C9D–C8D	108.1 (2)
O6B–C9B–H9BA	110.1	O6D–C9D–H9DA	110.1
C8B–C9B–H9BA	110.1	C8D–C9D–H9DA	110.1
O6B–C9B–H9BB	110.1	O6D–C9D–H9DB	110.1
C8B–C9B–H9BB	110.1	C8D–C9D–H9DB	110.1
H9BA–C9B–H9BB	108.4	H9DA–C9D–H9DB	108.4
O6B–C10B–C11B	107.65 (14)	O6D–C10D–C11D	107.7 (2)
O6B–C10B–H10C	110.2	O6D–C10D–H10G	110.2
C11B–C10B–H10C	110.2	C11D–C10D–H10G	110.2
O6B–C10B–H10D	110.2	O6D–C10D–H10H	110.2
C11B–C10B–H10D	110.2	C11D–C10D–H10H	110.2
H10C–C10B–H10D	108.5	H10G–C10D–H10H	108.5
C12B–C11B–C15B	108.10 (16)	C12D–C11D–C15D	107.65 (18)
C12B–C11B–C10B	125.84 (18)	C12D–C11D–C10D	126.9 (2)
C15B–C11B–C10B	126.04 (17)	C15D–C11D–C10D	125.4 (2)
C12B–C11B–Fe1B	69.89 (10)	C12D–C11D–Fe1D	69.54 (11)
C15B–C11B–Fe1B	69.51 (9)	C15D–C11D–Fe1D	69.41 (11)
C10B–C11B–Fe1B	127.58 (13)	C10D–C11D–Fe1D	128.4 (2)
C11B–C12B–C13B	107.43 (17)	C11D–C12D–C13D	108.20 (19)
C11B–C12B–Fe1B	69.15 (10)	C11D–C12D–Fe1D	69.44 (10)
C13B–C12B–Fe1B	69.78 (11)	C13D–C12D–Fe1D	69.57 (11)
C11B–C12B–H12B	126.3	C11D–C12D–H12D	125.9
C13B–C12B–H12B	126.3	C13D–C12D–H12D	125.9
Fe1B–C12B–H12B	126.3	Fe1D–C12D–H12D	125.9
C14B–C13B–C12B	108.60 (17)	C14D–C13D–C12D	108.2 (2)
C14B–C13B–Fe1B	69.71 (11)	C14D–C13D–Fe1D	69.91 (12)
C12B–C13B–Fe1B	69.25 (11)	C12D–C13D–Fe1D	69.31 (11)
C14B–C13B–H13B	125.7	C14D–C13D–H13D	125.9
C12B–C13B–H13B	125.7	C12D–C13D–H13D	125.9

Fe1B–C13B–H13B	125.7	Fe1D–C13D–H13D	125.9
C13B–C14B–C15B	108.02 (16)	C13D–C14D–C15D	107.49 (19)
C13B–C14B–Fe1B	69.84 (11)	C13D–C14D–Fe1D	69.19 (12)
C15B–C14B–Fe1B	69.13 (10)	C15D–C14D–Fe1D	68.93 (12)
C13B–C14B–H14B	126.0	C13D–C14D–H14D	126.2
C15B–C14B–H14B	126.0	C15D–C14D–H14D	126.2
Fe1B–C14B–H14B	126.0	Fe1D–C14D–H14D	126.2
C14B–C15B–C11B	107.85 (16)	C11D–C15D–C14D	108.4 (2)
C14B–C15B–Fe1B	70.00 (10)	C11D–C15D–Fe1D	69.41 (11)
C11B–C15B–Fe1B	69.24 (9)	C14D–C15D–Fe1D	70.01 (12)
C14B–C15B–H15B	126.1	C11D–C15D–H15D	125.8
C11B–C15B–H15B	126.1	C14D–C15D–H15D	125.8
Fe1B–C15B–H15B	126.1	Fe1D–C15D–H15D	125.8
C20B–C16B–C17B	108.17 (17)	C17D–C16D–C20D	107.8 (2)
C20B–C16B–Fe1B	69.52 (10)	C17D–C16D–Fe1D	69.78 (12)
C17B–C16B–Fe1B	69.56 (11)	C20D–C16D–Fe1D	69.82 (13)
C20B–C16B–H16B	125.9	C17D–C16D–H16D	126.1
C17B–C16B–H16B	125.9	C20D–C16D–H16D	126.1
Fe1B–C16B–H16B	125.9	Fe1D–C16D–H16D	126.1
C18B–C17B–C16B	107.54 (17)	C16D–C17D–C18D	108.4 (2)
C18B–C17B–Fe1B	69.36 (11)	C16D–C17D–Fe1D	69.77 (12)
C16B–C17B–Fe1B	69.66 (11)	C18D–C17D–Fe1D	69.62 (12)
C18B–C17B–H17B	126.2	C16D–C17D–H17D	125.8
C16B–C17B–H17B	126.2	C18D–C17D–H17D	125.8
Fe1B–C17B–H17B	126.2	Fe1D–C17D–H17D	125.8
C19B–C18B–C17B	108.39 (17)	C19D–C18D–C17D	108.2 (2)
C19B–C18B–Fe1B	69.45 (10)	C19D–C18D–Fe1D	69.93 (12)
C17B–C18B–Fe1B	69.93 (10)	C17D–C18D–Fe1D	69.63 (11)
C19B–C18B–H18B	125.8	C19D–C18D–H18D	125.9
C17B–C18B–H18B	125.8	C17D–C18D–H18D	125.9
Fe1B–C18B–H18B	125.8	Fe1D–C18D–H18D	125.9
C18B–C19B–C20B	107.98 (17)	C18D–C19D–C20D	107.3 (2)
C18B–C19B–Fe1B	69.96 (10)	C18D–C19D–Fe1D	69.49 (11)
C20B–C19B–Fe1B	69.86 (10)	C20D–C19D–Fe1D	69.50 (12)
C18B–C19B–H19B	126.0	C18D–C19D–H19D	126.3
C20B–C19B–H19B	126.0	C20D–C19D–H19D	126.3
Fe1B–C19B–H19B	126.0	Fe1D–C19D–H19D	126.3

C16B–C20B–C19B	107.91 (17)	C16D–C20D–C19D	108.3 (2)
C16B–C20B–Fe1B	70.00 (11)	C16D–C20D–Fe1D	69.50 (13)
C19B–C20B–Fe1B	69.17 (10)	C19D–C20D–Fe1D	69.60 (13)
C16B–C20B–H20B	126.0	C16D–C20D–H20D	125.9
C19B–C20B–H20B	126.0	C19D–C20D–H20D	125.9
Fe1B–C20B–H20B	126.0	Fe1D–C20D–H20D	125.9
C2A–O1A–C1A–O2A	174.1 (2)	C2C–O1C–C1C–O2C	-173.8 (19)
C2A–O1A–C1A–O3A	-5.7 (3)	C2C–O1C–C1C–O3C	8 (3)
C4A–O3A–C1A–O2A	170.2 (2)	C4C–O3C–C1C–O2C	-170 (2)
C4A–O3A–C1A–O1A	-10.1 (3)	C4C–O3C–C1C–O1C	8 (3)
C1A–O1A–C2A–C3A	-14.3 (3)	C1C–O1C–C2C–C3C	12 (2)
O1A–C2A–C3A–C4A	45.2 (2)	O1C–C2C–C3C–C4C	-44.8 (8)
O1A–C2A–C3A–C6A	-73.4 (2)	O1C–C2C–C3C–C6C	73.8 (8)
O1A–C2A–C3A–C5A	164.24 (17)	O1C–C2C–C3C–C5C	-163.8 (8)
C1A–O3A–C4A–C3A	44.1 (3)	C1C–O3C–C4C–C3C	-43.4 (10)
C2A–C3A–C4A–O3A	-58.75 (19)	C2C–C3C–C4C–O3C	58.9 (4)
C6A–C3A–C4A–O3A	60.0 (2)	C6C–C3C–C4C–O3C	-59.9 (4)
C5A–C3A–C4A–O3A	-177.88 (15)	C5C–C3C–C4C–O3C	178.0 (4)
C7A–O5A–C6A–O4A	0.6 (3)	C7C–O5C–C6C–O4C	2 (2)
C7A–O5A–C6A–C3A	-178.33 (16)	C7C–O5C–C6C–C3C	176.2 (6)
C4A–C3A–C6A–O4A	-114.7 (2)	C4C–C3C–C6C–O4C	111.3 (17)
C2A–C3A–C6A–O4A	1.5 (3)	C2C–C3C–C6C–O4C	-5.0 (17)
C5A–C3A–C6A–O4A	123.5 (2)	C5C–C3C–C6C–O4C	-127.0 (17)
C4A–C3A–C6A–O5A	64.2 (2)	C4C–C3C–C6C–O5C	-63.4 (10)
C2A–C3A–C6A–O5A	-179.60 (16)	C2C–C3C–C6C–O5C	-179.7 (10)
C5A–C3A–C6A–O5A	-57.5 (2)	C5C–C3C–C6C–O5C	58.3 (10)
C6A–O5A–C7A–C8A	84.3 (2)	C6C–O5C–C7C–C8C	-83.3 (12)
O5A–C7A–C8A–C9A	174.94 (17)	O5C–C7C–C8C–C9C	-174.1 (5)
C10A–O6A–C9A–C8A	-176.65 (17)	C10C–O6C–C9C–C8C	177.9 (10)
C7A–C8A–C9A–O6A	-77.4 (2)	C7C–C8C–C9C–O6C	74.3 (11)
C9A–O6A–C10A–C11A	173.50 (18)	C9C–O6C–C10C–C11C	-173.8 (11)
O6A–C10A–C11A–C12A	-95.9 (2)	O6C–C10C–C11C–C12C	96.0 (10)
O6A–C10A–C11A–C15A	81.2 (2)	O6C–C10C–C11C–C15C	-81.3 (10)
O6A–C10A–C11A–Fe1A	171.93 (14)	O6C–C10C–C11C–Fe1C	-171.9 (10)
C15A–C11A–C12A–C13A	0.21 (19)	C15C–C11C–C12C–C13C	-0.2 (2)
C10A–C11A–C12A–C13A	177.73 (16)	C10C–C11C–C12C–C13C	-177.9 (3)

Fe1A–C11A–C12A–C13A	-58.96 (12)	Fe1C–C11C–C12C–C13C	58.96 (14)
C15A–C11A–C12A–Fe1A	59.17 (12)	C15C–C11C–C12C–Fe1C	-59.17 (13)
C10A–C11A–C12A–Fe1A	-123.31 (18)	C10C–C11C–C12C–Fe1C	123.1 (3)
C11A–C12A–C13A–C14A	-0.4 (2)	C11C–C12C–C13C–C14C	0.4 (2)
Fe1A–C12A–C13A–C14A	-59.28 (13)	Fe1C–C12C–C13C–C14C	59.28 (14)
C11A–C12A–C13A–Fe1A	58.87 (12)	C11C–C12C–C13C–Fe1C	-58.87 (13)
C12A–C13A–C14A–C15A	0.4 (2)	C12C–C13C–C14C–C15C	-0.4 (2)
Fe1A–C13A–C14A–C15A	-58.46 (13)	Fe1C–C13C–C14C–C15C	58.46 (15)
C12A–C13A–C14A–Fe1A	58.91 (12)	C12C–C13C–C14C–Fe1C	-58.91 (14)
C12A–C11A–C15A–C14A	0.1 (2)	C12C–C11C–C15C–C14C	-0.1 (2)
C10A–C11A–C15A–C14A	-177.50 (16)	C10C–C11C–C15C–C14C	177.7 (2)
Fe1A–C11A–C15A–C14A	59.32 (13)	Fe1C–C11C–C15C–C14C	-59.31 (15)
C12A–C11A–C15A–Fe1A	-59.26 (12)	C12C–C11C–C15C–Fe1C	59.25 (13)
C10A–C11A–C15A–Fe1A	123.18 (17)	C10C–C11C–C15C–Fe1C	-123.0 (2)
C13A–C14A–C15A–C11A	-0.3 (2)	C13C–C14C–C15C–C11C	0.3 (2)
Fe1A–C14A–C15A–C11A	-58.94 (13)	Fe1C–C14C–C15C–C11C	58.94 (14)
C13A–C14A–C15A–Fe1A	58.63 (13)	C13C–C14C–C15C–Fe1C	-58.63 (15)
C20A–C16A–C17A–C18A	-0.6 (2)	C20C–C16C–C17C–C18C	0.6 (2)
Fe1A–C16A–C17A–C18A	59.10 (13)	Fe1C–C16C–C17C–C18C	-59.10 (15)
C20A–C16A–C17A–Fe1A	-59.73 (14)	C20C–C16C–C17C–Fe1C	59.72 (16)
C16A–C17A–C18A–C19A	0.3 (2)	C16C–C17C–C18C–C19C	-0.3 (2)
Fe1A–C17A–C18A–C19A	59.48 (13)	Fe1C–C17C–C18C–C19C	-59.49 (15)
C16A–C17A–C18A–Fe1A	-59.19 (13)	C16C–C17C–C18C–Fe1C	59.20 (15)
C17A–C18A–C19A–C20A	0.2 (2)	C17C–C18C–C19C–C20C	-0.2 (2)
Fe1A–C18A–C19A–C20A	59.45 (14)	Fe1C–C18C–C19C–C20C	-59.45 (15)
C17A–C18A–C19A–Fe1A	-59.29 (13)	C17C–C18C–C19C–Fe1C	59.30 (15)
C17A–C16A–C20A–C19A	0.7 (2)	C17C–C16C–C20C–C19C	-0.7 (3)
Fe1A–C16A–C20A–C19A	-58.97 (15)	Fe1C–C16C–C20C–C19C	58.98 (16)
C17A–C16A–C20A–Fe1A	59.70 (14)	C17C–C16C–C20C–Fe1C	-59.69 (15)
C18A–C19A–C20A–C16A	-0.5 (2)	C18C–C19C–C20C–C16C	0.5 (3)
Fe1A–C19A–C20A–C16A	58.91 (14)	Fe1C–C19C–C20C–C16C	-58.92 (16)
C18A–C19A–C20A–Fe1A	-59.45 (14)	C18C–C19C–C20C–Fe1C	59.45 (15)
C2B–O1B–C1B–O2B	172.5 (2)	C2D–O1D–C1D–O2D	-174 (2)
C2B–O1B–C1B–O3B	-6.0 (3)	C2D–O1D–C1D–O3D	2 (3)
C4B–O3B–C1B–O2B	171.36 (19)	C4D–O3D–C1D–O2D	-171 (2)
C4B–O3B–C1B–O1B	-10.1 (3)	C4D–O3D–C1D–O1D	13 (3)
C1B–O1B–C2B–C3B	-14.7 (3)	C1D–O1D–C2D–C3D	17 (2)

O1B–C2B–C3B–C4B	46.0 (2)	O1D–C2D–C3D–C4D	-45.6 (8)
O1B–C2B–C3B–C6B	-73.0 (2)	O1D–C2D–C3D–C6D	73.1 (8)
O1B–C2B–C3B–C5B	164.09 (16)	O1D–C2D–C3D–C5D	-164.6 (8)
C1B–O3B–C4B–C3B	44.8 (2)	C1D–O3D–C4D–C3D	-44.9 (10)
C2B–C3B–C4B–O3B	-60.17 (18)	C2D–C3D–C4D–O3D	58.4 (4)
C6B–C3B–C4B–O3B	59.13 (19)	C6D–C3D–C4D–O3D	-60.4 (5)
C5B–C3B–C4B–O3B	-178.54 (14)	C5D–C3D–C4D–O3D	177.5 (4)
C7B–O5B–C6B–O4B	0.5 (3)	C7D–O5D–C6D–O4D	-14 (3)
C7B–O5B–C6B–C3B	-178.56 (15)	C7D–O5D–C6D–C3D	171.8 (10)
C2B–C3B–C6B–O4B	1.5 (3)	C4D–C3D–C6D–O4D	111 (3)
C4B–C3B–C6B–O4B	-114.8 (2)	C2D–C3D–C6D–O4D	-5 (3)
C5B–C3B–C6B–O4B	123.8 (2)	C5D–C3D–C6D–O4D	-127 (3)
C2B–C3B–C6B–O5B	-179.50 (15)	C4D–C3D–C6D–O5D	-74.8 (15)
C4B–C3B–C6B–O5B	64.23 (19)	C2D–C3D–C6D–O5D	168.9 (15)
C5B–C3B–C6B–O5B	-57.2 (2)	C5D–C3D–C6D–O5D	46.9 (15)
C6B–O5B–C7B–C8B	84.2 (2)	C6D–O5D–C7D–C8D	-100.8 (18)
O5B–C7B–C8B–C9B	175.91 (17)	O5D–C7D–C8D–C9D	-173.1 (7)
C10B–O6B–C9B–C8B	-177.39 (17)	C10D–O6D–C9D–C8D	174.6 (15)
C7B–C8B–C9B–O6B	-76.3 (2)	C7D–C8D–C9D–O6D	98.2 (16)
C9B–O6B–C10B–C11B	174.09 (17)	C9D–O6D–C10D–C11D	-169.4 (18)
O6B–C10B–C11B–C12B	83.0 (2)	O6D–C10D–C11D–C12D	-79.7 (15)
O6B–C10B–C11B–C15B	-95.0 (2)	O6D–C10D–C11D–C15D	97.5 (15)
O6B–C10B–C11B–Fe1B	174.21 (13)	O6D–C10D–C11D–Fe1D	-171.8 (15)
C15B–C11B–C12B–C13B	0.3 (2)	C15D–C11D–C12D–C13D	0.2 (2)
C10B–C11B–C12B–C13B	-178.01 (16)	C10D–C11D–C12D–C13D	177.8 (3)
Fe1B–C11B–C12B–C13B	59.52 (13)	Fe1D–C11D–C12D–C13D	-58.96 (14)
C15B–C11B–C12B–Fe1B	-59.22 (12)	C15D–C11D–C12D–Fe1D	59.17 (13)
C10B–C11B–C12B–Fe1B	122.46 (18)	C10D–C11D–C12D–Fe1D	-123.2 (3)
C11B–C12B–C13B–C14B	-0.4 (2)	C11D–C12D–C13D–C14D	-0.4 (2)
Fe1B–C12B–C13B–C14B	58.75 (13)	Fe1D–C12D–C13D–C14D	-59.28 (14)
C11B–C12B–C13B–Fe1B	-59.13 (12)	C11D–C12D–C13D–Fe1D	58.87 (13)
C12B–C13B–C14B–C15B	0.3 (2)	C12D–C13D–C14D–C15D	0.4 (2)
Fe1B–C13B–C14B–C15B	58.77 (12)	Fe1D–C13D–C14D–C15D	-58.46 (15)
C12B–C13B–C14B–Fe1B	-58.47 (13)	C12D–C13D–C14D–Fe1D	58.91 (14)
C13B–C14B–C15B–C11B	-0.1 (2)	C12D–C11D–C15D–C14D	0.1 (2)
Fe1B–C14B–C15B–C11B	59.10 (12)	C10D–C11D–C15D–C14D	-177.6 (3)
C13B–C14B–C15B–Fe1B	-59.21 (13)	Fe1D–C11D–C15D–C14D	59.32 (15)

C12B–C11B–C15B–C14B	-0.12 (19)	C12D–C11D–C15D–Fe1D	-59.25 (13)
C10B–C11B–C15B–C14B	178.19 (16)	C10D–C11D–C15D–Fe1D	123.1 (3)
Fe1B–C11B–C15B–C14B	-59.58 (12)	C13D–C14D–C15D–C11D	-0.3 (2)
C12B–C11B–C15B–Fe1B	59.46 (12)	Fe1D–C14D–C15D–C11D	-58.94 (14)
C10B–C11B–C15B–Fe1B	-122.23 (17)	C13D–C14D–C15D–Fe1D	58.63 (15)
C20B–C16B–C17B–C18B	-0.3 (2)	C20D–C16D–C17D–C18D	-0.6 (2)
Fe1B–C16B–C17B–C18B	-59.24 (13)	Fe1D–C16D–C17D–C18D	59.10 (15)
C20B–C16B–C17B–Fe1B	58.98 (13)	C20D–C16D–C17D–Fe1D	-59.72 (16)
C16B–C17B–C18B–C19B	0.5 (2)	C16D–C17D–C18D–C19D	0.3 (2)
Fe1B–C17B–C18B–C19B	-58.98 (13)	Fe1D–C17D–C18D–C19D	59.48 (15)
C16B–C17B–C18B–Fe1B	59.43 (13)	C16D–C17D–C18D–Fe1D	-59.20 (15)
C17B–C18B–C19B–C20B	-0.5 (2)	C17D–C18D–C19D–C20D	0.2 (2)
Fe1B–C18B–C19B–C20B	-59.75 (12)	Fe1D–C18D–C19D–C20D	59.45 (15)
C17B–C18B–C19B–Fe1B	59.28 (13)	C17D–C18D–C19D–Fe1D	-59.30 (15)
C17B–C16B–C20B–C19B	0.0 (2)	C17D–C16D–C20D–C19D	0.7 (3)
Fe1B–C16B–C20B–C19B	58.98 (12)	Fe1D–C16D–C20D–C19D	-58.98 (16)
C17B–C16B–C20B–Fe1B	-59.01 (13)	C17D–C16D–C20D–Fe1D	59.69 (15)
C18B–C19B–C20B–C16B	0.3 (2)	C18D–C19D–C20D–C16D	-0.5 (3)
Fe1B–C19B–C20B–C16B	-59.50 (13)	Fe1D–C19D–C20D–C16D	58.91 (16)
C18B–C19B–C20B–Fe1B	59.81 (13)	C18D–C19D–C20D–Fe1D	-59.45 (15)

IV. NMR and GPC Spectra of Polymers

A. Monomer Activation

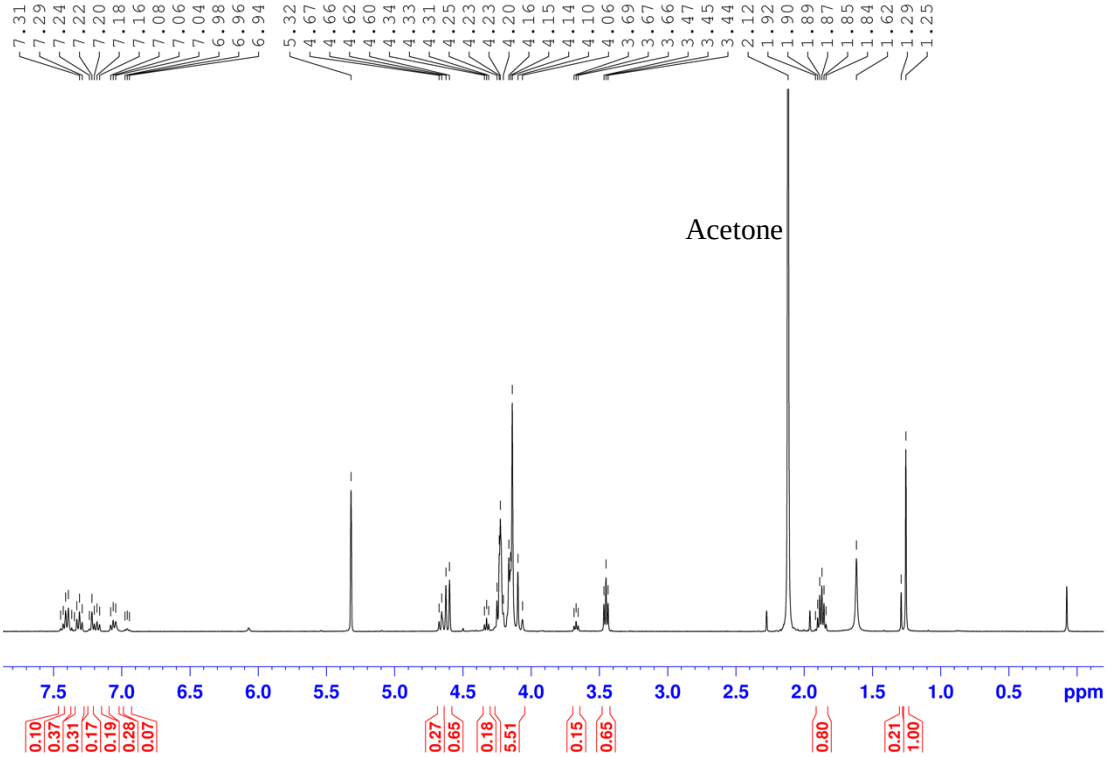

Figure S21. The ^{1}H NMR spectrum (CD_2Cl_2) of monomer activation, obtained by mixing a 1:1 molar ratio of monomer **2** and H-bonding catalyst **DPU**.

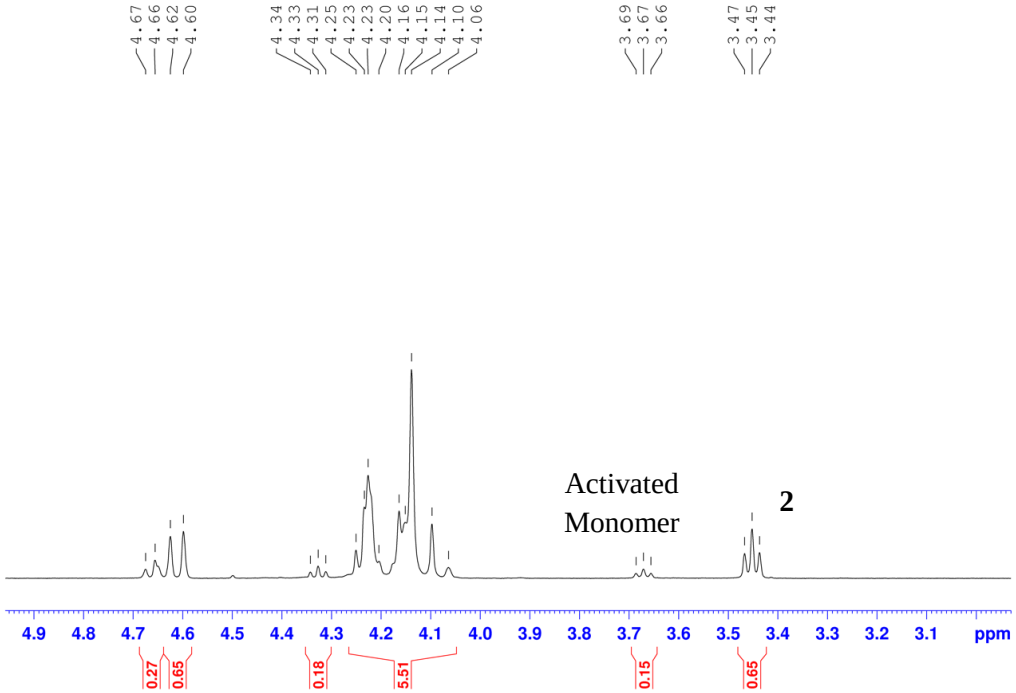

Figure S22. Expansion of the ^{1}H NMR spectrum (CD_2Cl_2) of monomer activation, showing distinct resonances for monomer **2** and the activated monomer **2**.

B. Homopolymers

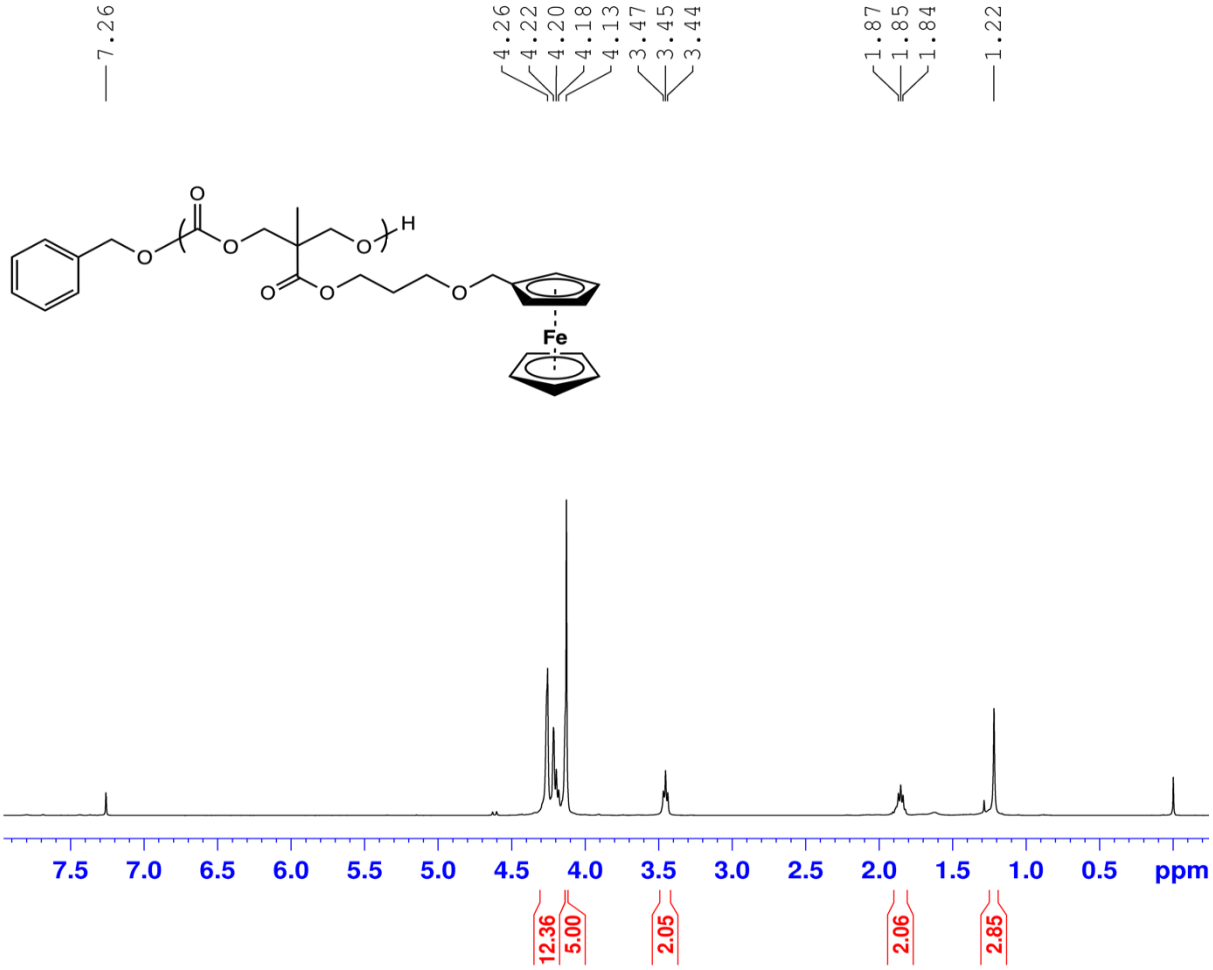

Figure S23. The ^{1}H NMR spectrum ($CDCl_3$) of the polymerization of ferrocene monomer **2** (monomer:initiator =300:1) with TU. Entry 1 in Table 1.

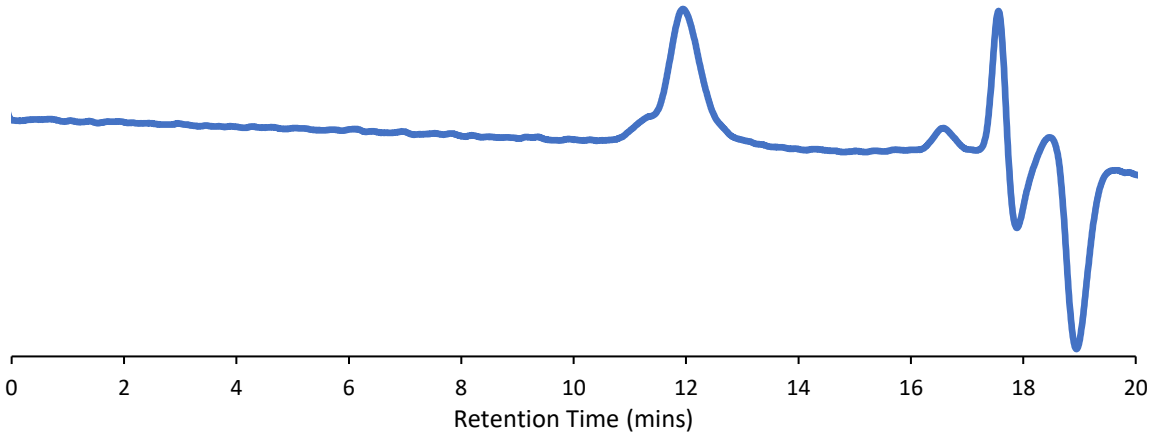

Figure S24. The GPC (THF) of the polymerization of ferrocene monomer **2** with TU. The M_n=85,850 and the $Đ$=1.13

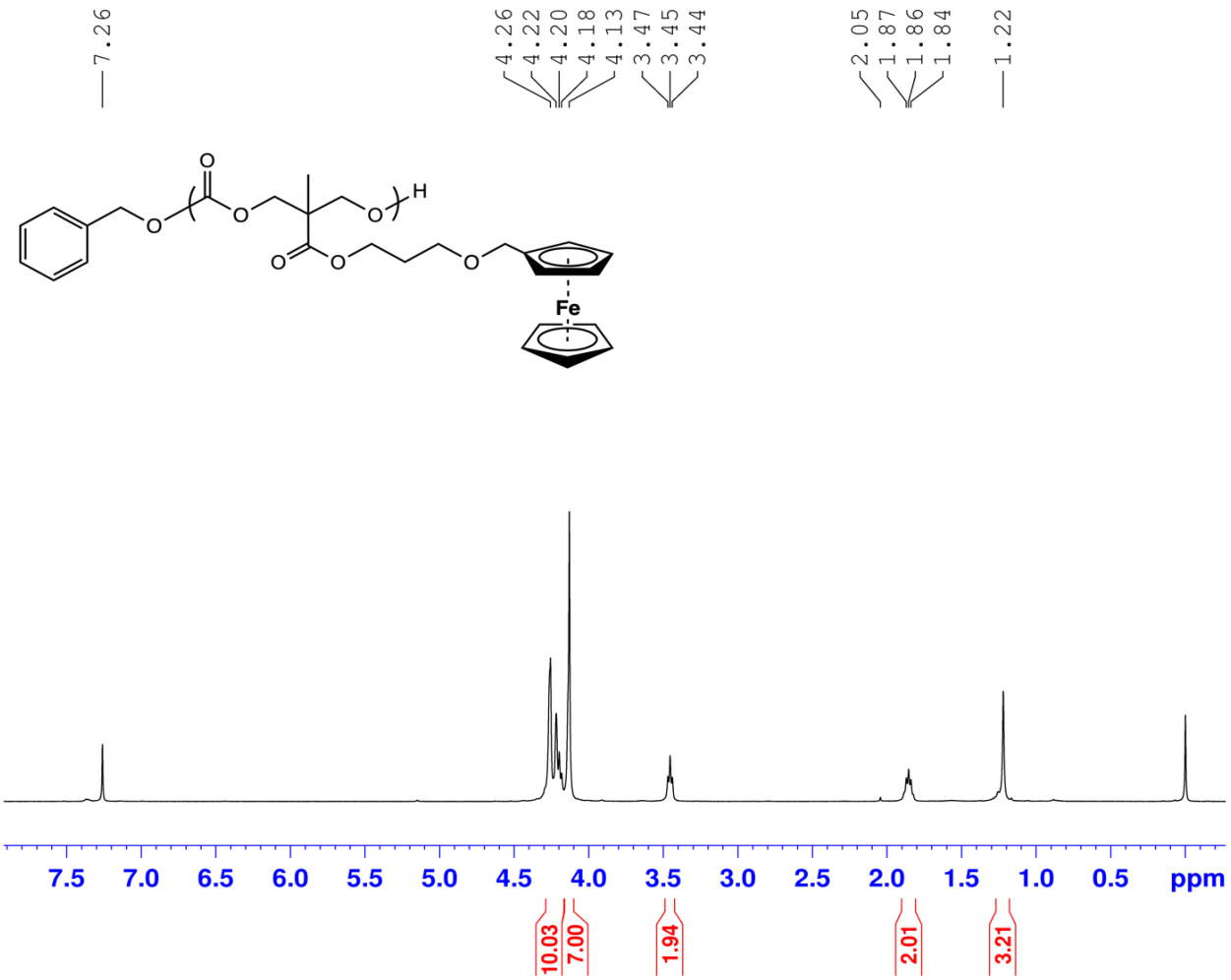

Figure S25. The ^{1}H NMR spectrum ($CDCl_3$) of the polymerization of ferrocene monomer **2** (monomer:initiator =100:1). Entry 2 in Table 1.

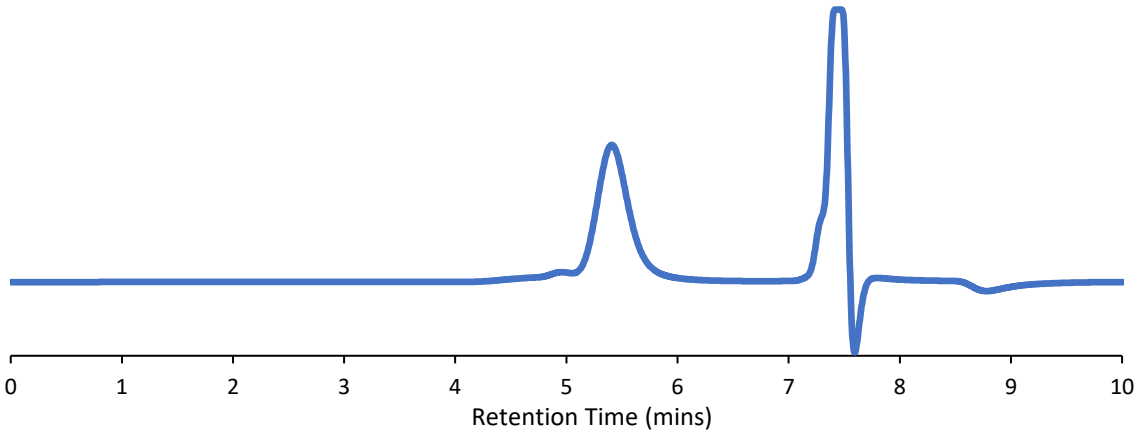

Figure S26. The GPC (THF) of the polymerization of ferrocene monomer **2**. The M_n= 35,249 and the $Đ$=1.18.

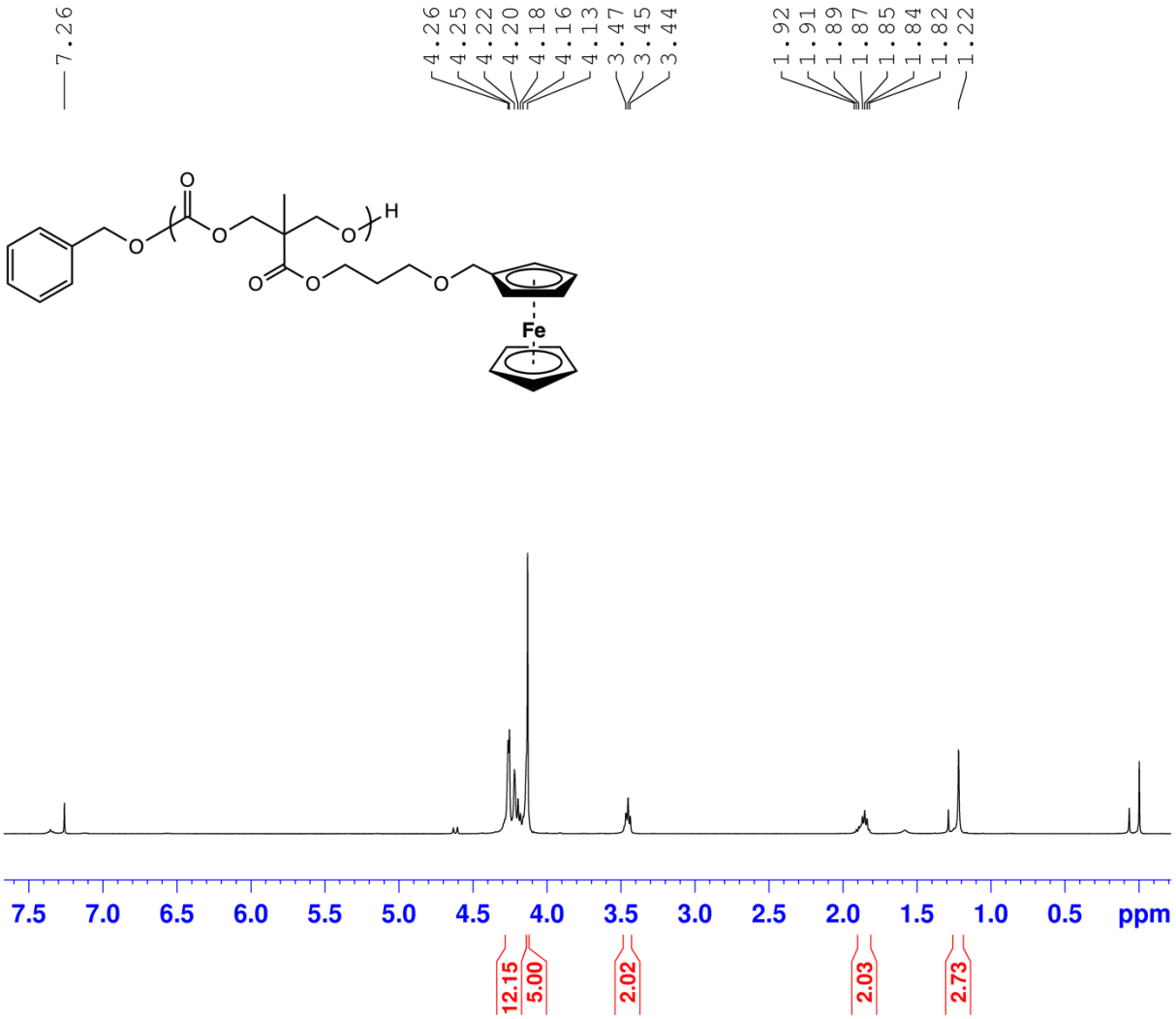

Figure S27. The ^{1}H NMR spectrum ($CDCl_3$) of the polymerization of ferrocene monomer **2** (monomer:initiator =300:1) with DPU. Entry 3 in Table 1.

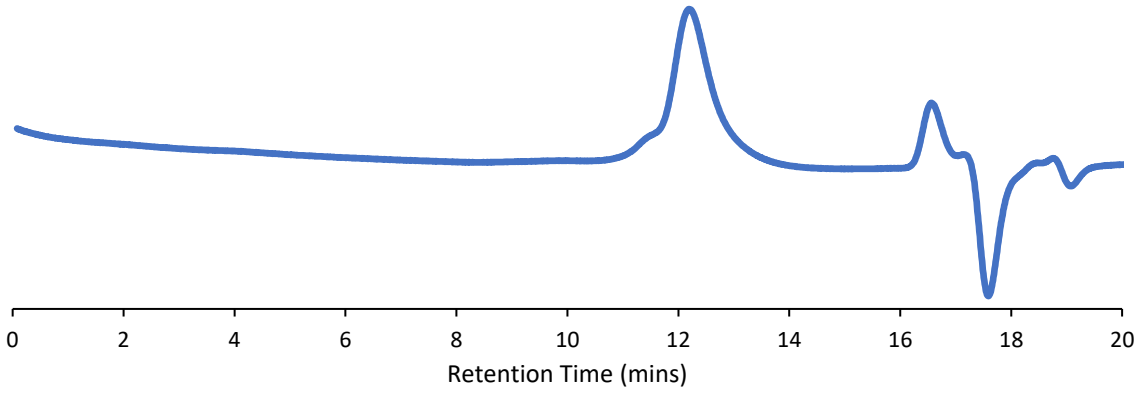

Figure S28. The GPC (THF) of the polymerization of ferrocene monomer **2** with DPU. The M_n= 81,560 and the $Đ$=1.22

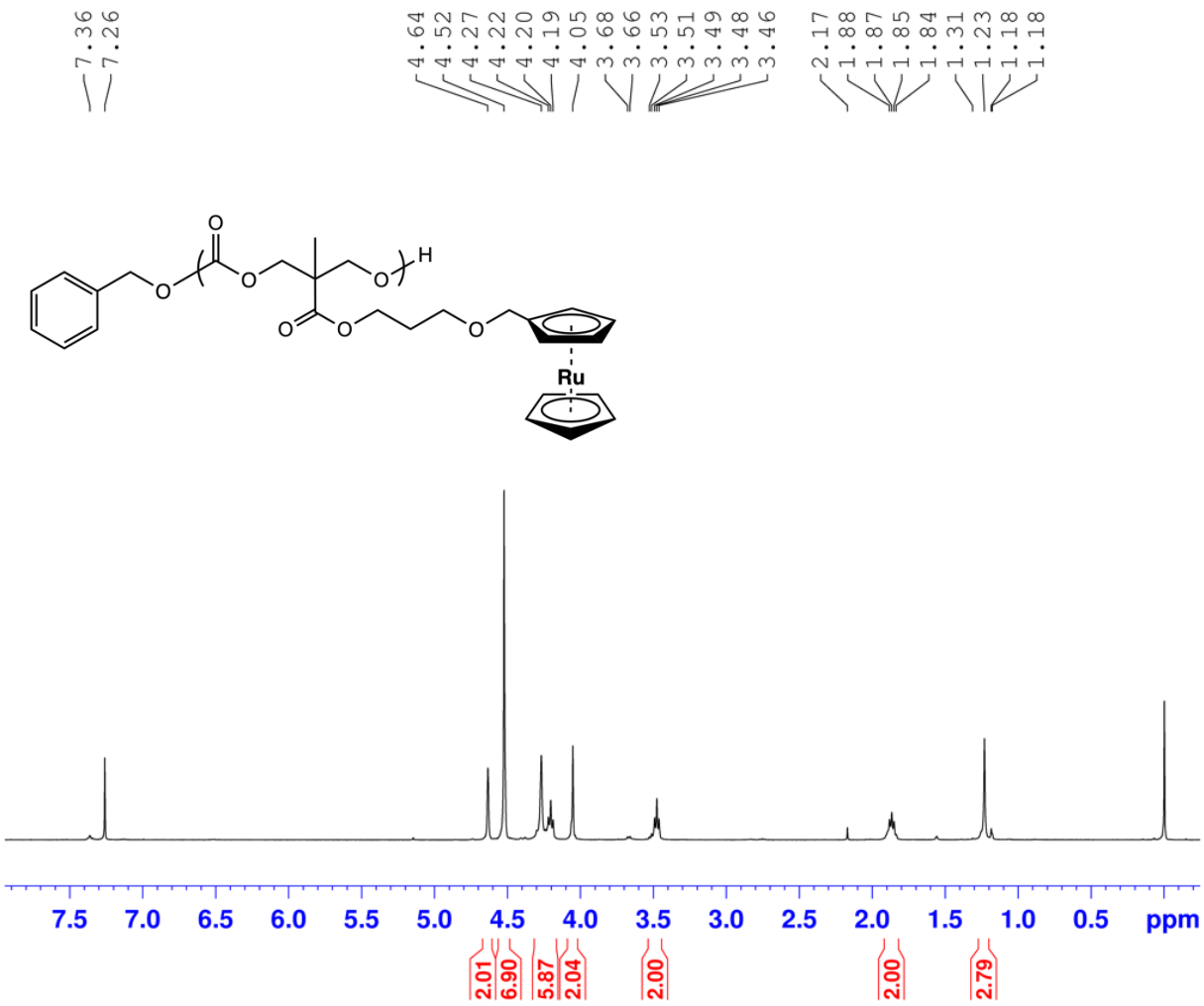

Figure S29. The ^{1}H NMR spectrum ($CDCl_3$) of the polymerization of the ruthenocene monomer **4** (monomer:initiator =90:1). Entry 4 in Table 1.

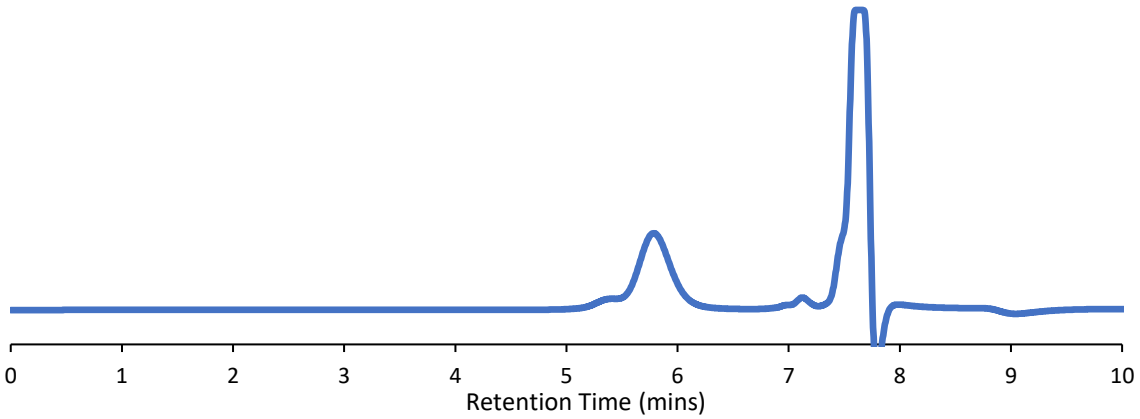

Figure S30. The GPC (THF) of the polymerization of the ruthenocene monomer **4**. The M_n =37,980 and the $Đ$=1.25

C. Diblocks

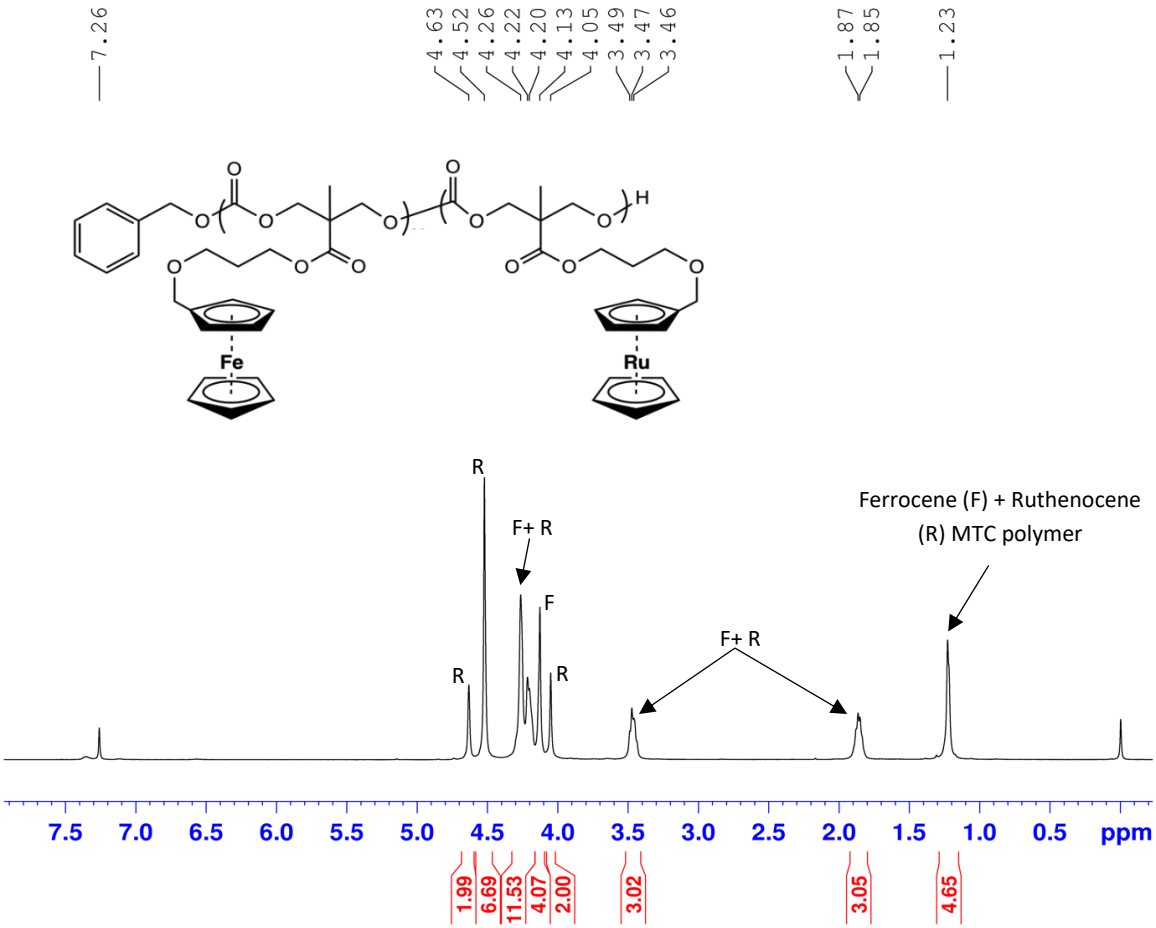

Figure S31. The ^{1}H NMR spectra ($CDCl_3$) of the copolymerization of the ferrocene **2** and ruthenocene **4** monomer (**2**:**4**:initiator = 100:100:1). Entry 5 in Table 2.

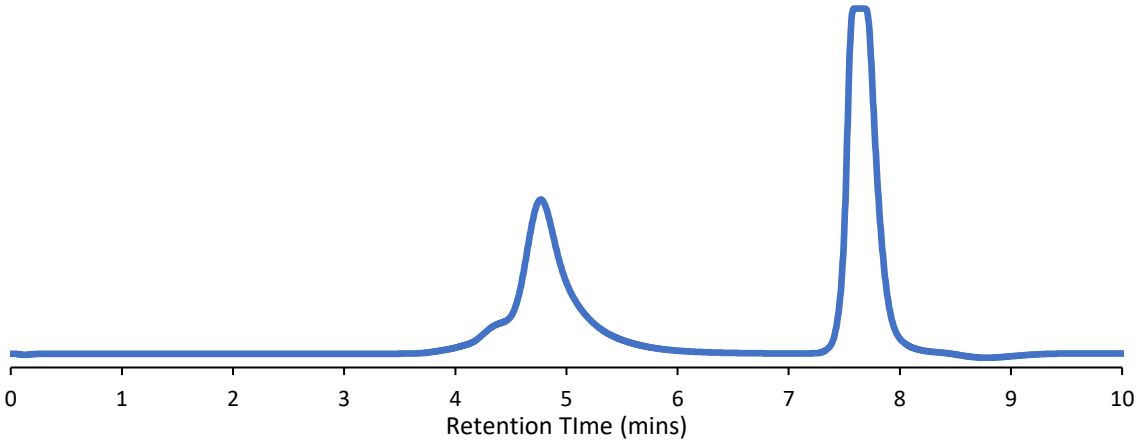

Figure S32. The GPC (THF) of the copolymerization of the ferrocene **2** and ruthenocene **4** monomer. M_n =96,401 and the $Đ$=1.16.

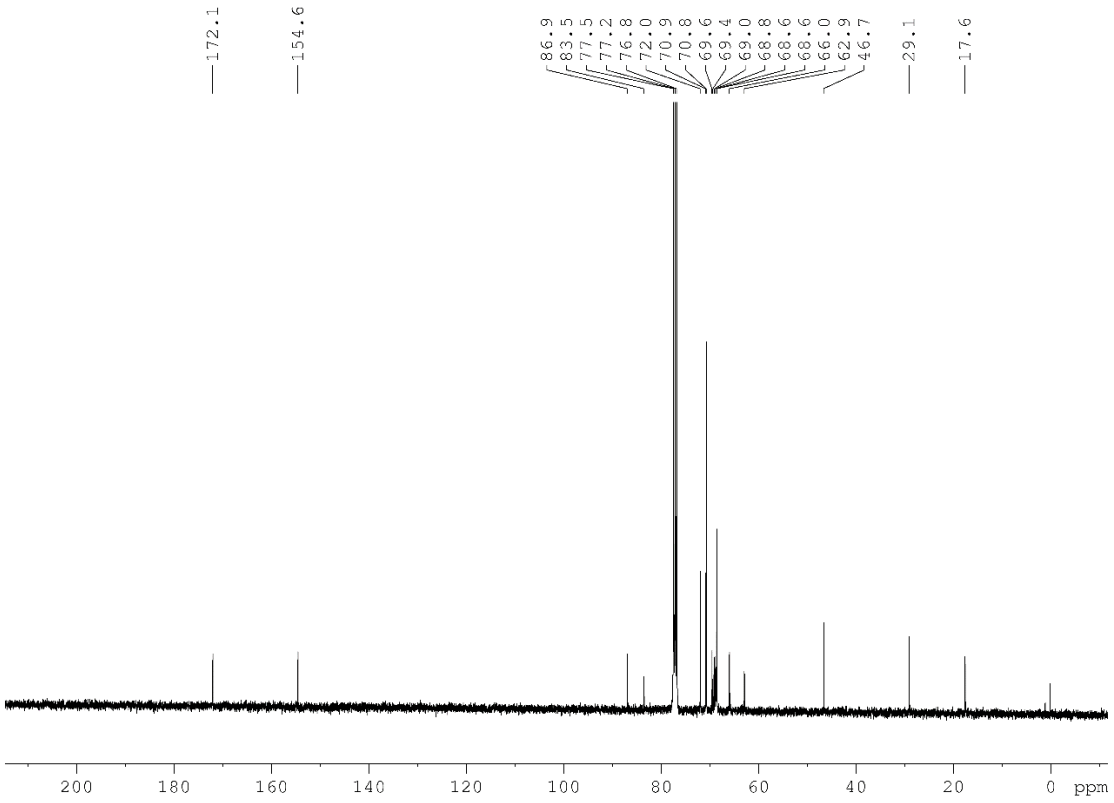

Figure S33. The ^{13}C NMR spectra ($CDCl_3$) of the copolymerization of the ferrocene **2** and ruthenocene **4** monomer (**2**:**4**:initiator = 100:100:1). Entry 5 in Table 2.

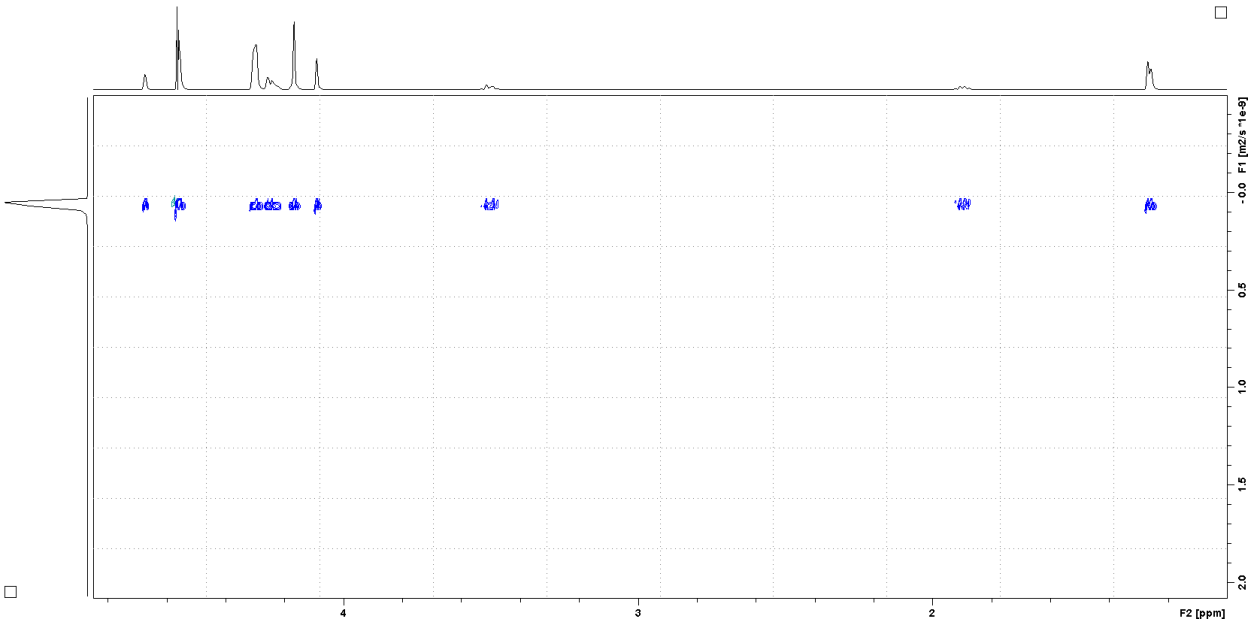

Figure S34. The DOSY NMR spectra ($CDCl_3$) of the copolymerization of the ferrocene **2** and ruthenocene **4** monomer (**2**:**4**:initiator = 100:100:1). Entry 5 in Table 2.

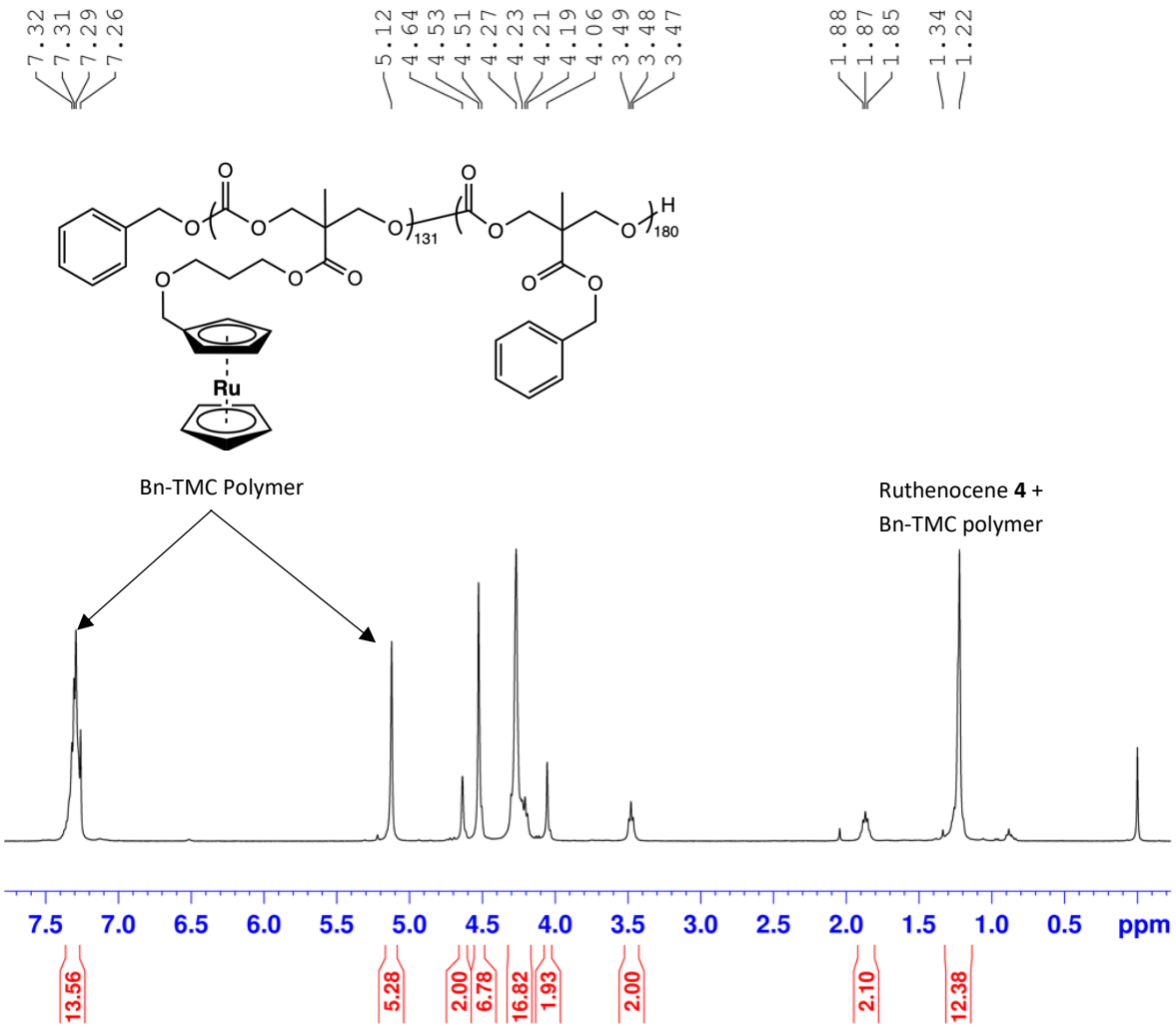

Figure S35. The ^{1}H NMR spectra ($CDCl_3$) of the copolymerization of ruthenocene **4** and **Bn-TMC** monomer (**4**:**Bn-TMC**:initiator = 145:200:1). Entry 6 in Table 2.

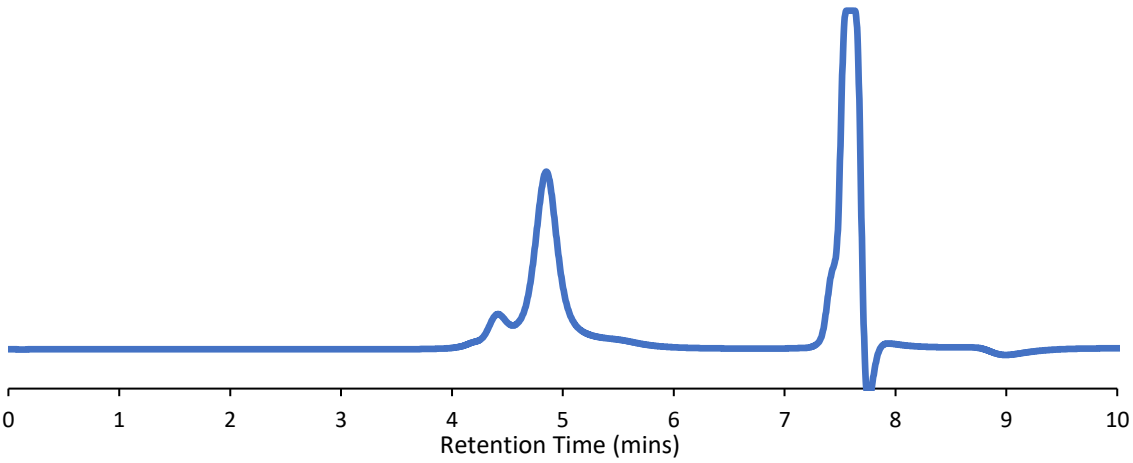

Figure S36. The GPC spectra (THF) of the copolymerization of ruthenocene **4** and **Bn-TMC** monomer. M_n=92,707 and the $Đ$=1.13.

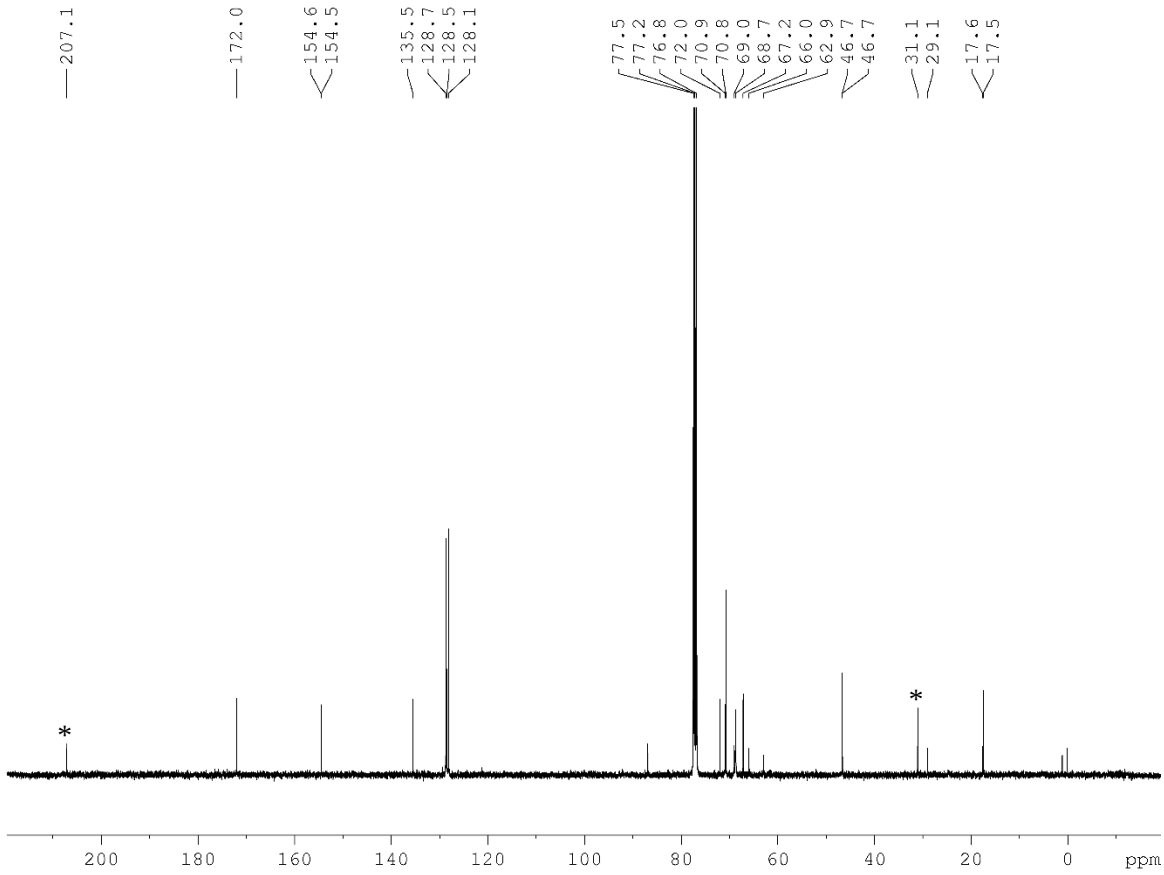

Figure S37. The ^{13}C NMR spectra ($CDCl_3$) of the copolymer of ruthenocene **4** and **Bn-TMC** monomer (**4**: **Bn-TMC**:initiator = 145:200:1). Entry 6 in Table 2. Some acetone (*) is present (207.1, 31.1 ppm).

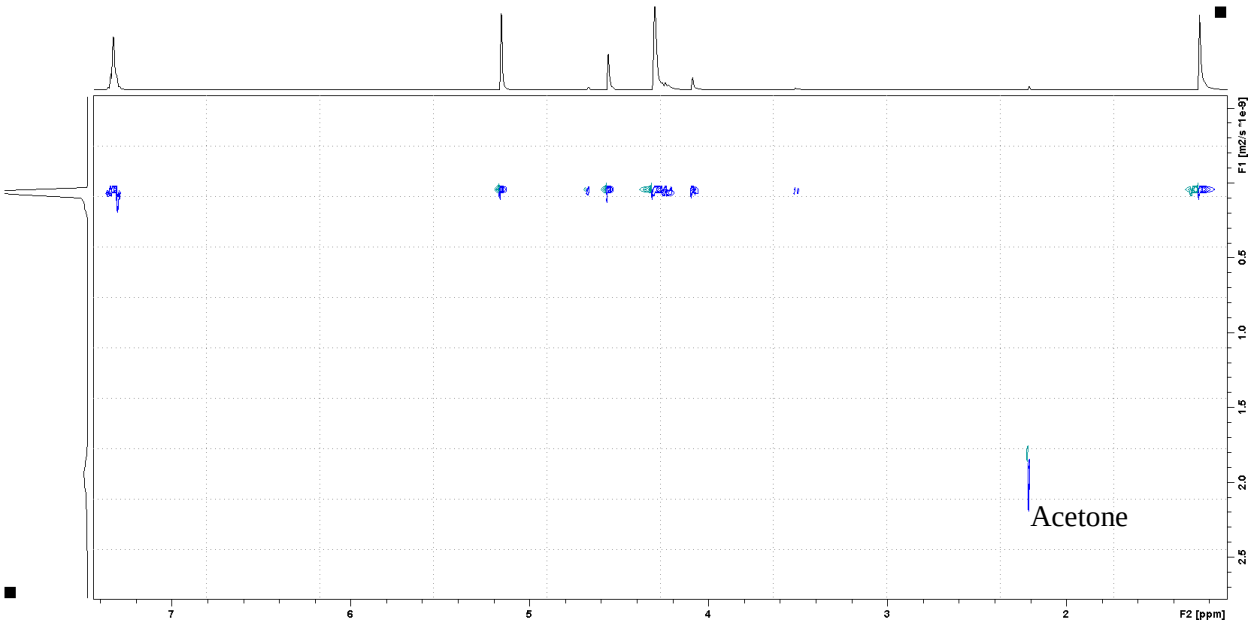

Figure S38. The DOSY NMR spectra ($CDCl_3$) of the copolymer of ruthenocene **4** and **Bn-TMC** monomer (**4**:**Bn-TMC**:initiator = 145:200:1). Entry 6 in Table 2. Some acetone is present (2.1 ppm).

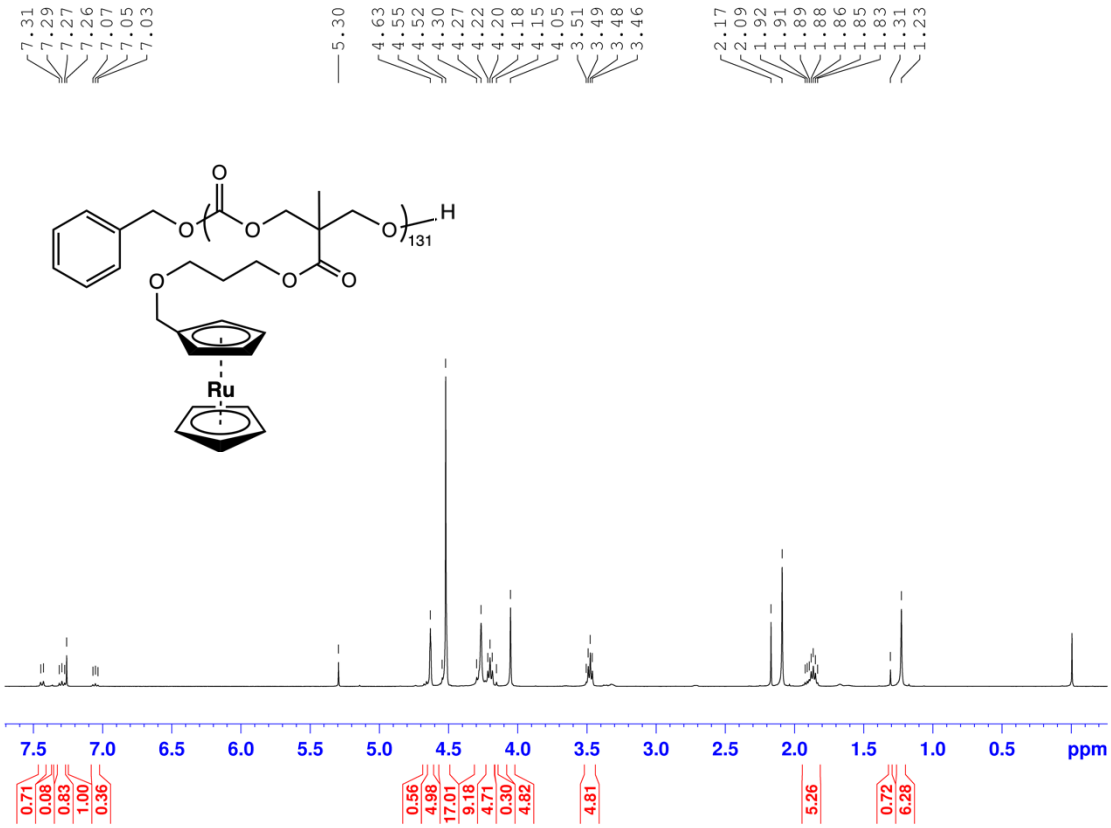

Figure S39. The ^{1}H NMR spectra ($CDCl_3$) of an aliquot of the **4** block, for the copolymerization of ruthenocene monomer **4** and **Bn-TMC** (**4**:initiator = 145:1). % Conversion = 90%. Entry 6 in Table 2.

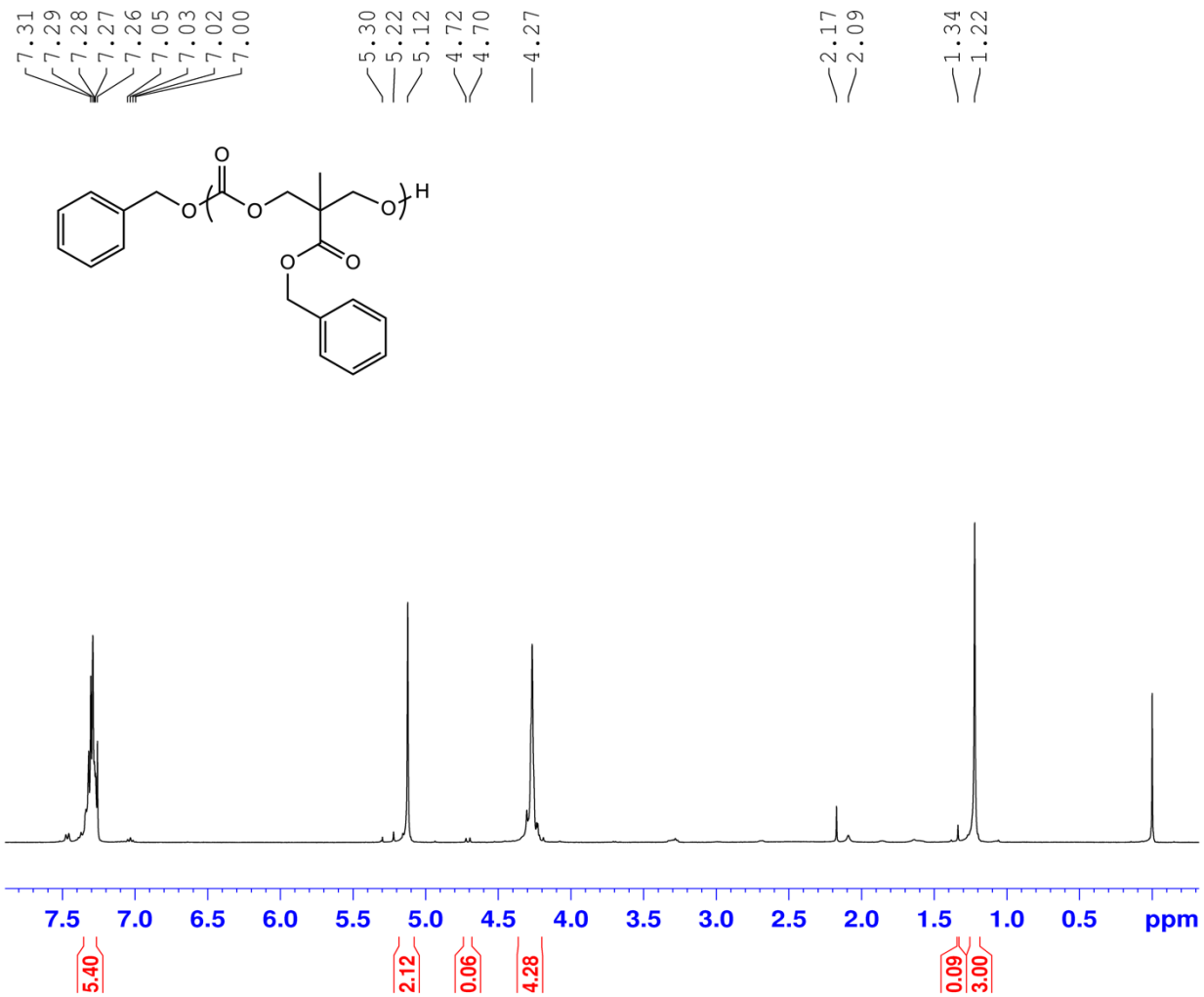

Figure S40. The ^{1}H NMR spectra ($CDCl_3$) of an aliquot of the **Bn-TMC** block, for the copolymerization of **Bn-TMC** and ruthenocene monomer **4** (**Bn-TMC**:initiator = 200:1). % Conversion = 97%. Entry 7 in Table 2.

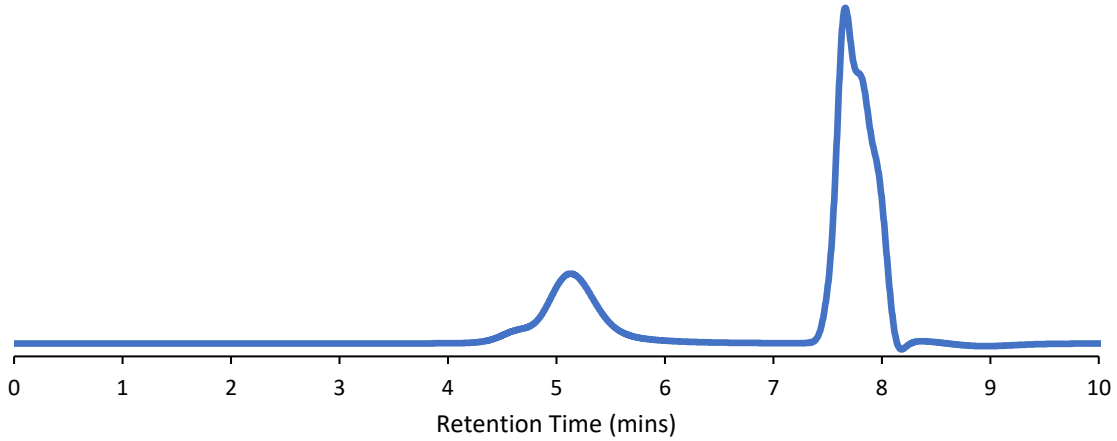

Figure S41. The GPC (THF) of the aliquot of the **Bn-TMC** block. M_n = 48,073 and the $Đ$ = 1.19. Entry 7 in Table 2.

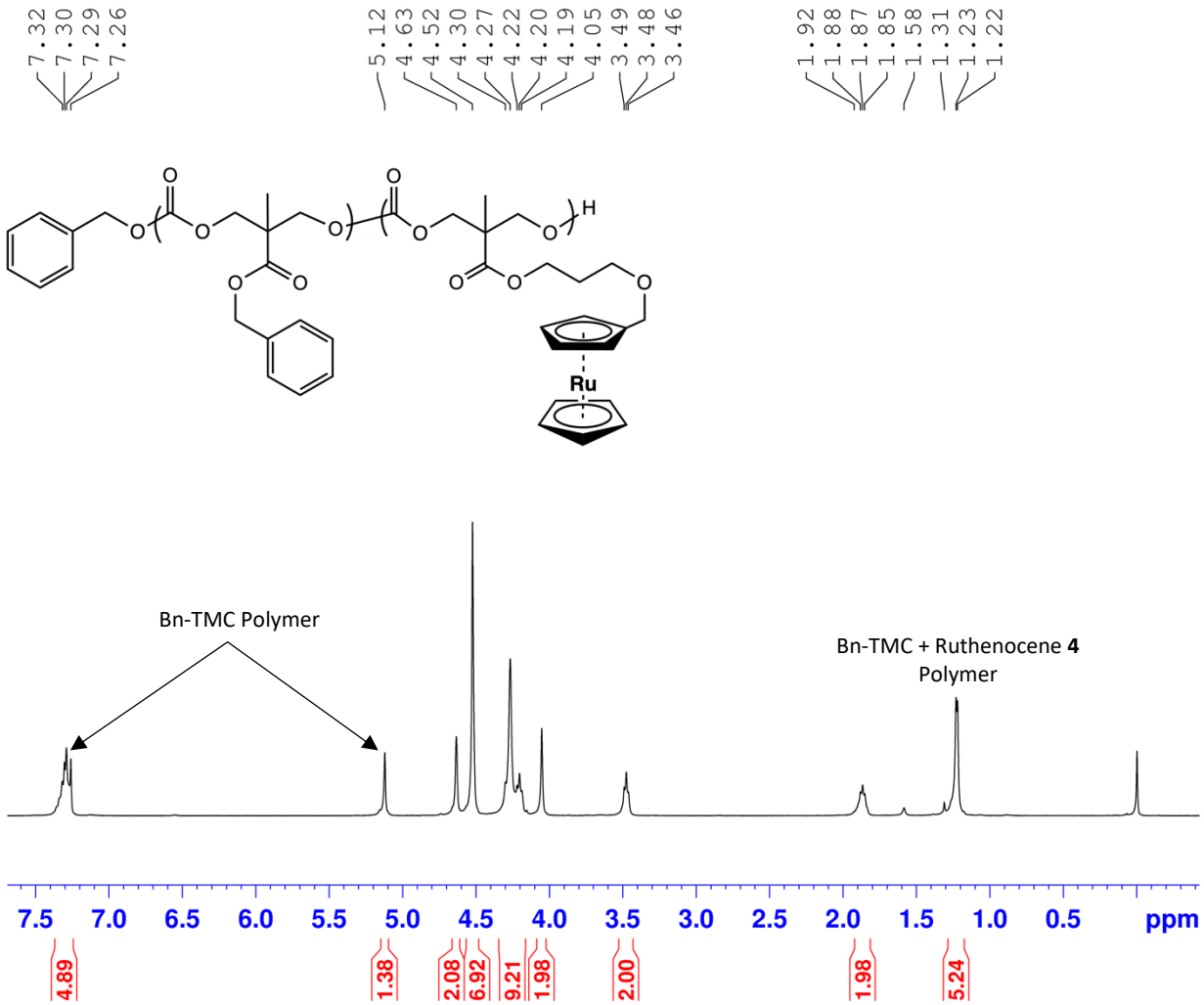

Figure S42. The ^{1}H NMR spectra ($CDCl_3$) of the copolymerization of **Bn-TMC** and ruthenocene monomer **4** (**Bn-TMC**:4:initiator = 200:145:1). Entry 7 in Table 2.

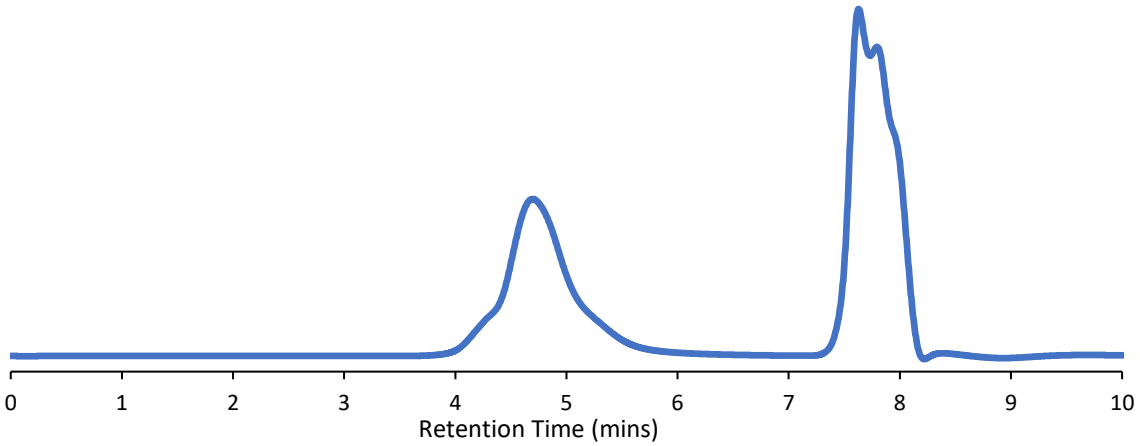

Figure S43. The GPC (THF) of the copolymerization of **Bn-TMC** and ruthenocene monomer **4**. M_n = 115,357 and the $Đ$ = 1.11.

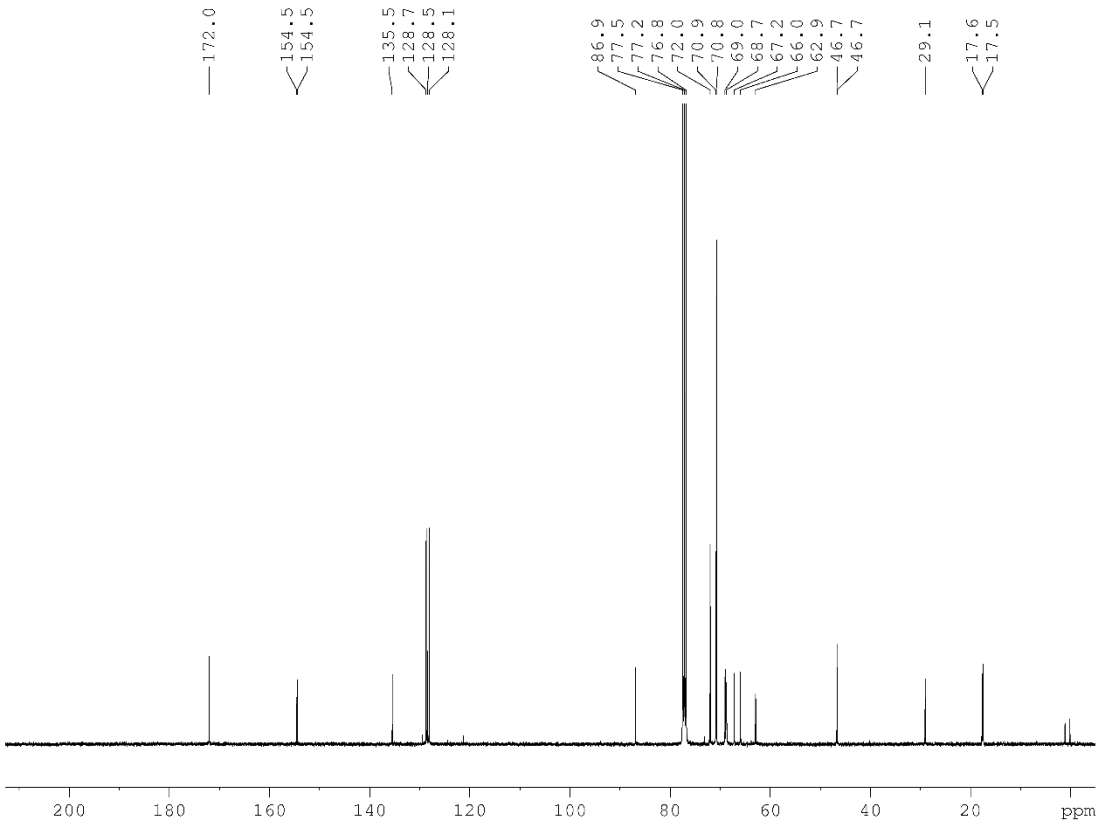

Figure S44. The ^{13}C NMR spectra ($CDCl_3$) of the copolymerization of **Bn-TMC** and ruthenocene monomer **4** (**Bn-TMC**:4:initiator = 200:145:1). Entry 7 in Table 2.

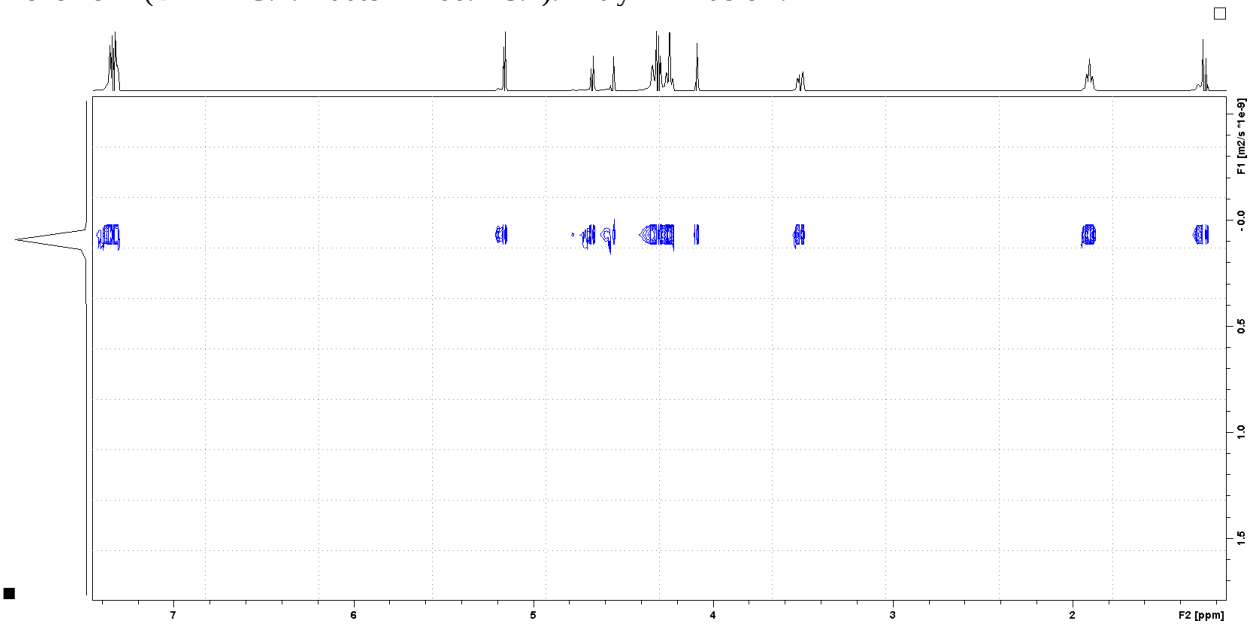

Figure S45. The DOSY NMR spectra ($CDCl_3$) of the copolymerization of **Bn-TMC** and ruthenocene monomer **4** (**Bn-TMC**:4:initiator = 200:145:1). Entry 7 in Table 2.

V. Mechanistic Studies

A. Chain Extension

Figure S46. The ^{1}H NMR spectra ($CDCl_3$) of the chain extension experiment with the ferrocene monomer **2**. a) The initial reaction with a monomer:initiator ratio of 150:1. b) Addition of monomer **2** to reach a total monomer:initiator ratio of 300:1 after stirring 30 additional minutes.

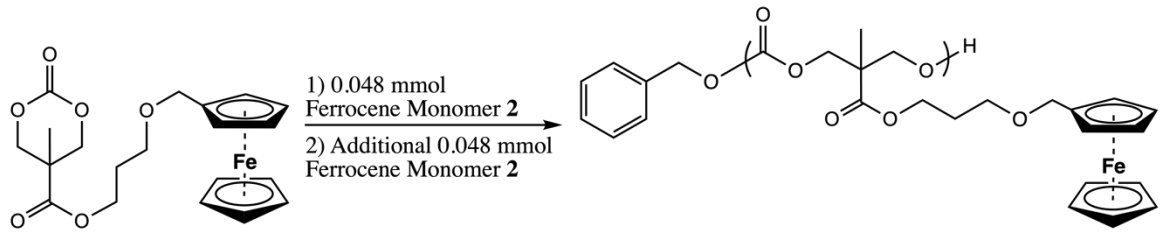

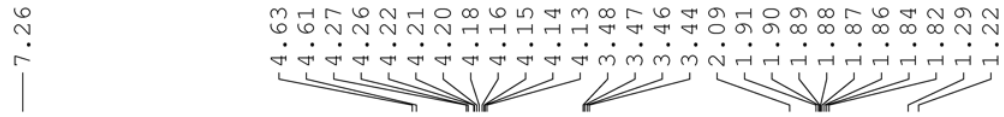

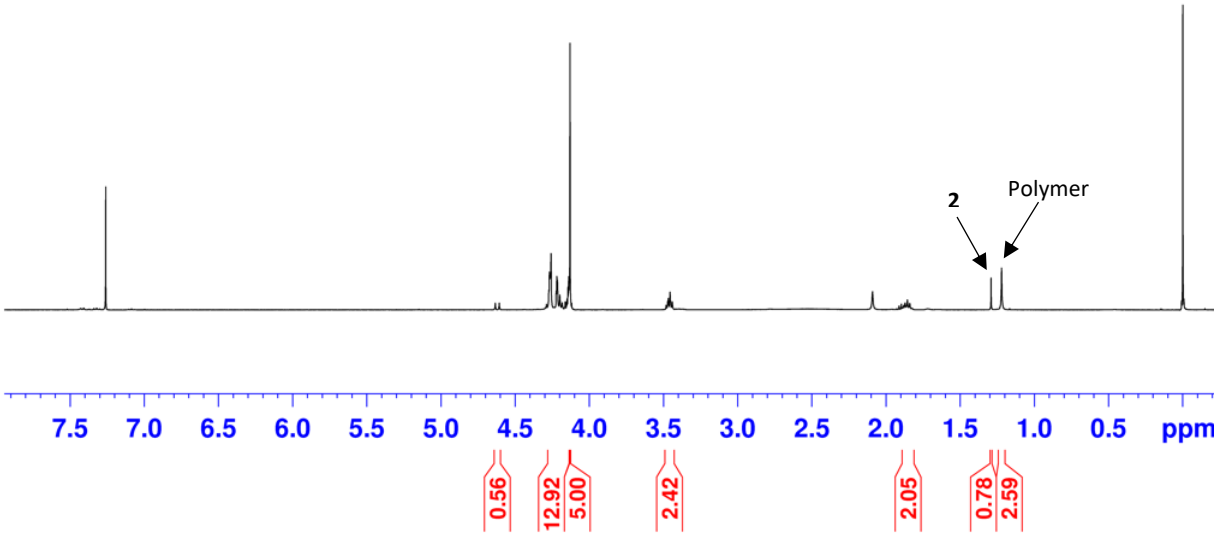

a) Initial polymerization. % Conversion = 76%.

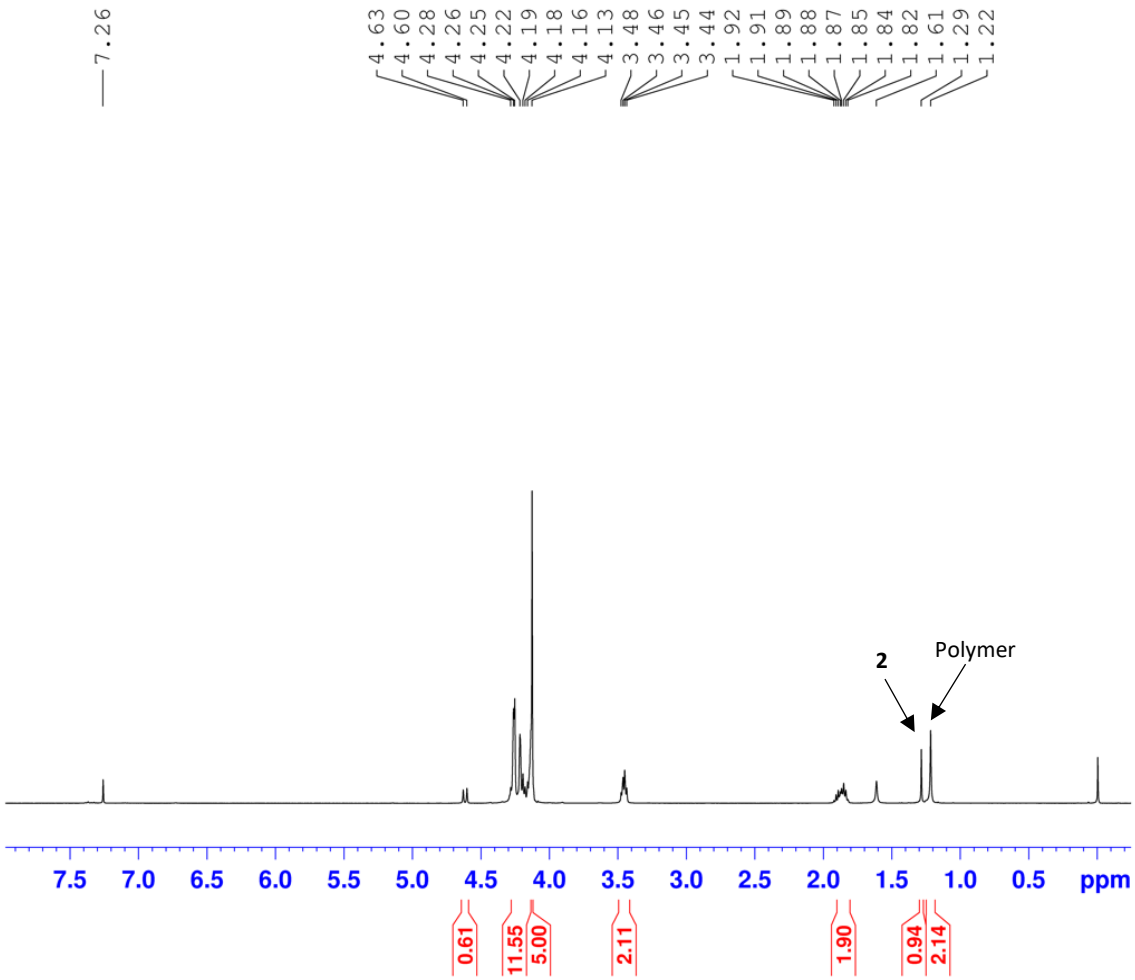

b) Additional monomer. Total % Conversion = 67%.

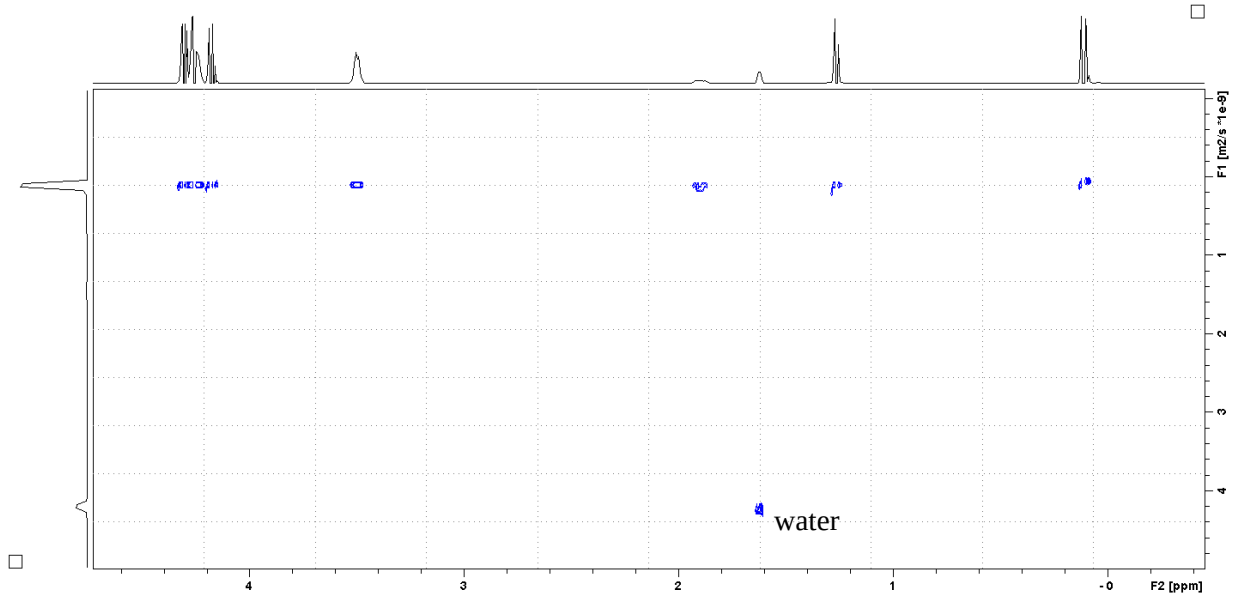

Figure S47. The DOSY NMR spectra ($CDCl_3$) of the completed chain extension experiment. Some water is present in the sample at 1.6 ppm.

Figure S48. The GPC (THF) of the chain extension experiment with the ferrocene monomer **2**. a) The initial reaction with a monomer:initiator ratio of 150:1. b) Addition of monomer **2** to reach a total monomer:initiator ratio of 300:1 after stirring 30 additional minutes.

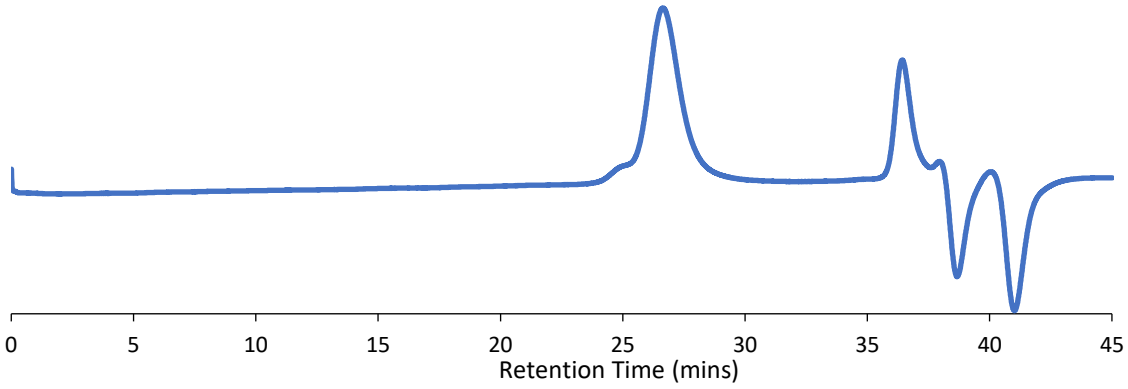

a) Initial polymerization reaction. GPC-LS M_n= 50,983 and the $Đ$= 1.07.

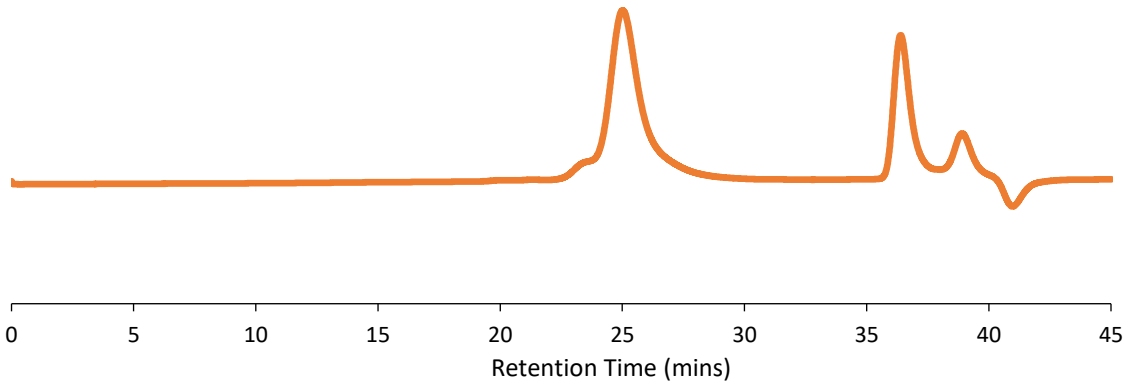

b) Additional monomer. GPC-LS M_n= 106,972 and the $Đ$=1.08.

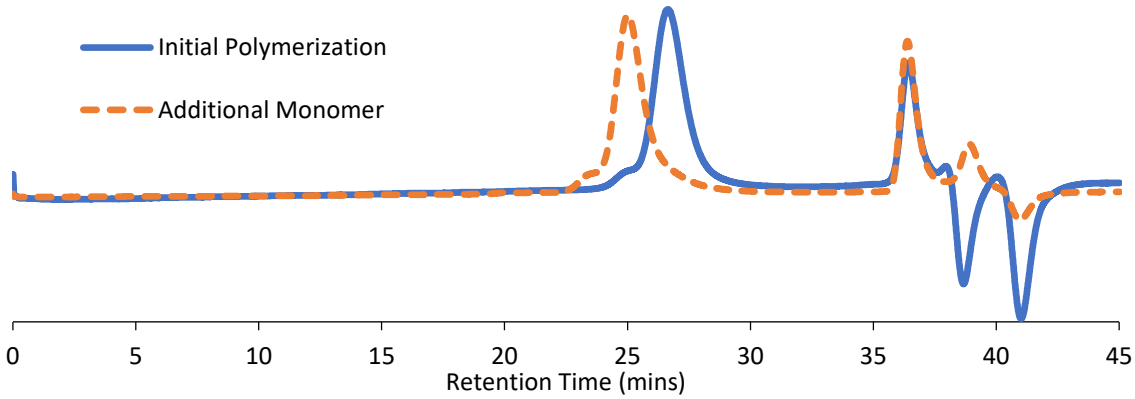

c) Overlay of the initial polymerization and after chain extension with additional monomer **2**.

B. Conversion and Molecular Weight Versus Time

Figure S49. The ^{1}H NMR spectra ($CDCl_3$) and GPC (THF) of aliquots of a homopolymerization of ferrocene monomer **2** (monomer:initiator ratio of 300:1). The M_n's are calculated by GPC-RI using polystyrene standards, which gives lower-than-expected measurements for molecular weight. The presence of unreacted **2** in the aliquots complicated M_n calculation with GPC-LS.

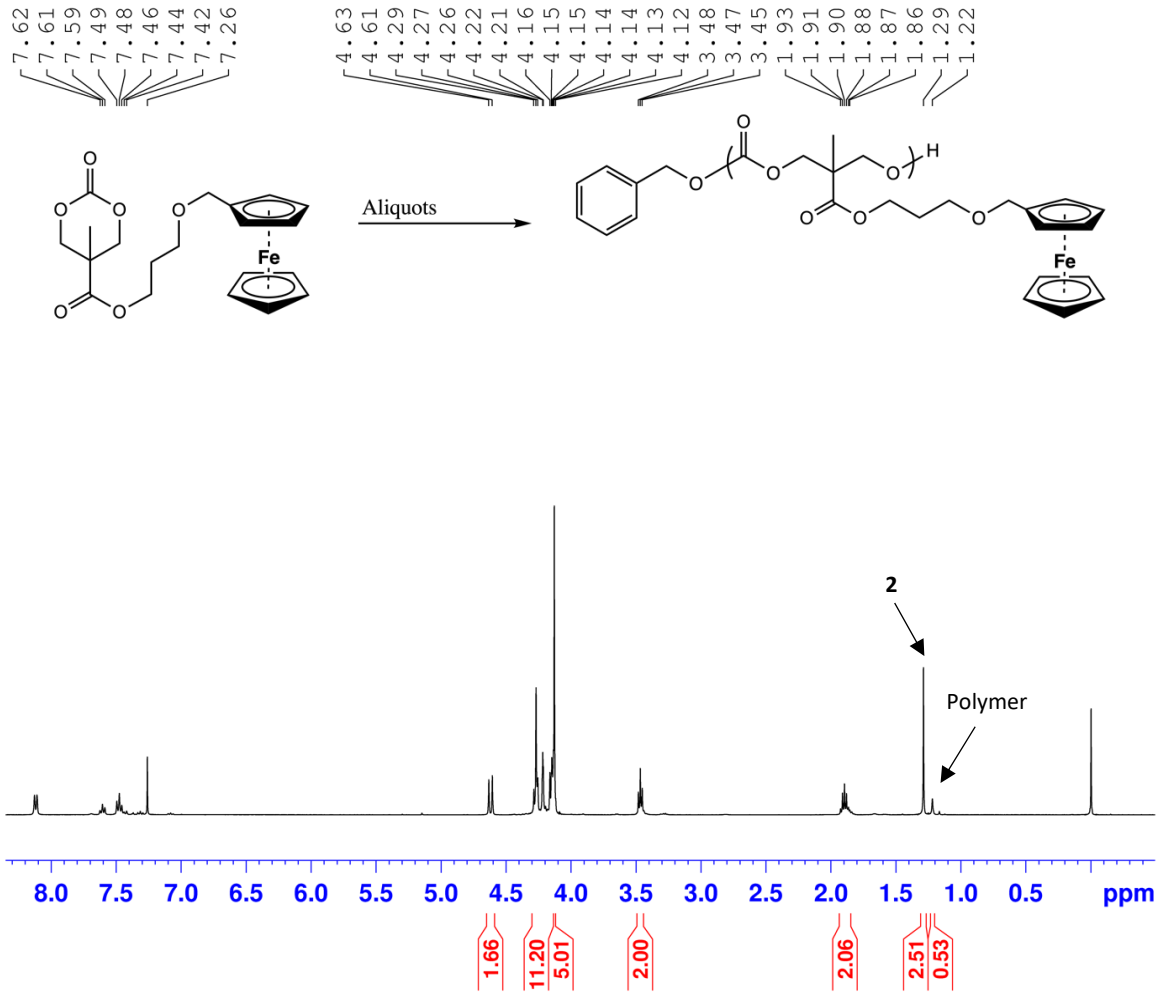

a) ^{1}H NMR spectrum ($CDCl_3$) of aliquot after 2 mins. % Conversion=17.5%.

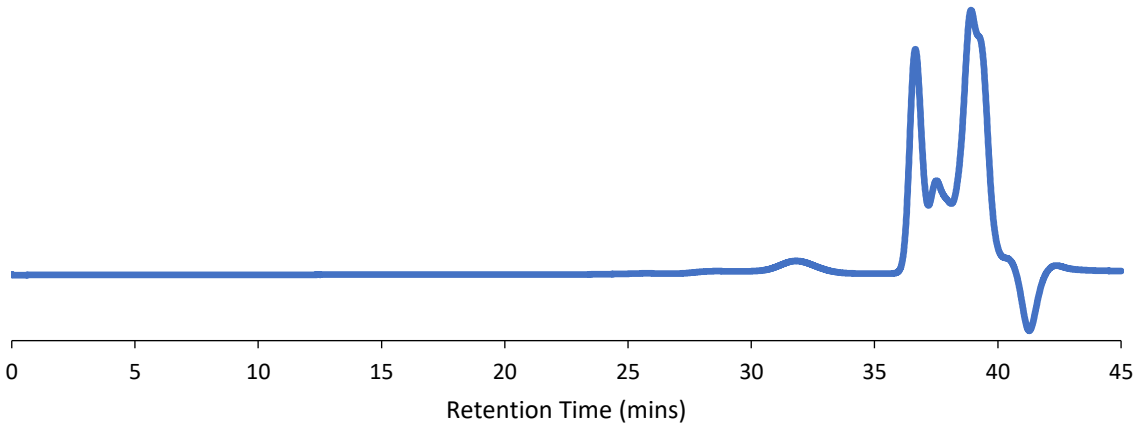

b) GPC-RI of aliquot after 2 mins. M_n=3,613, $Đ$=1.39.

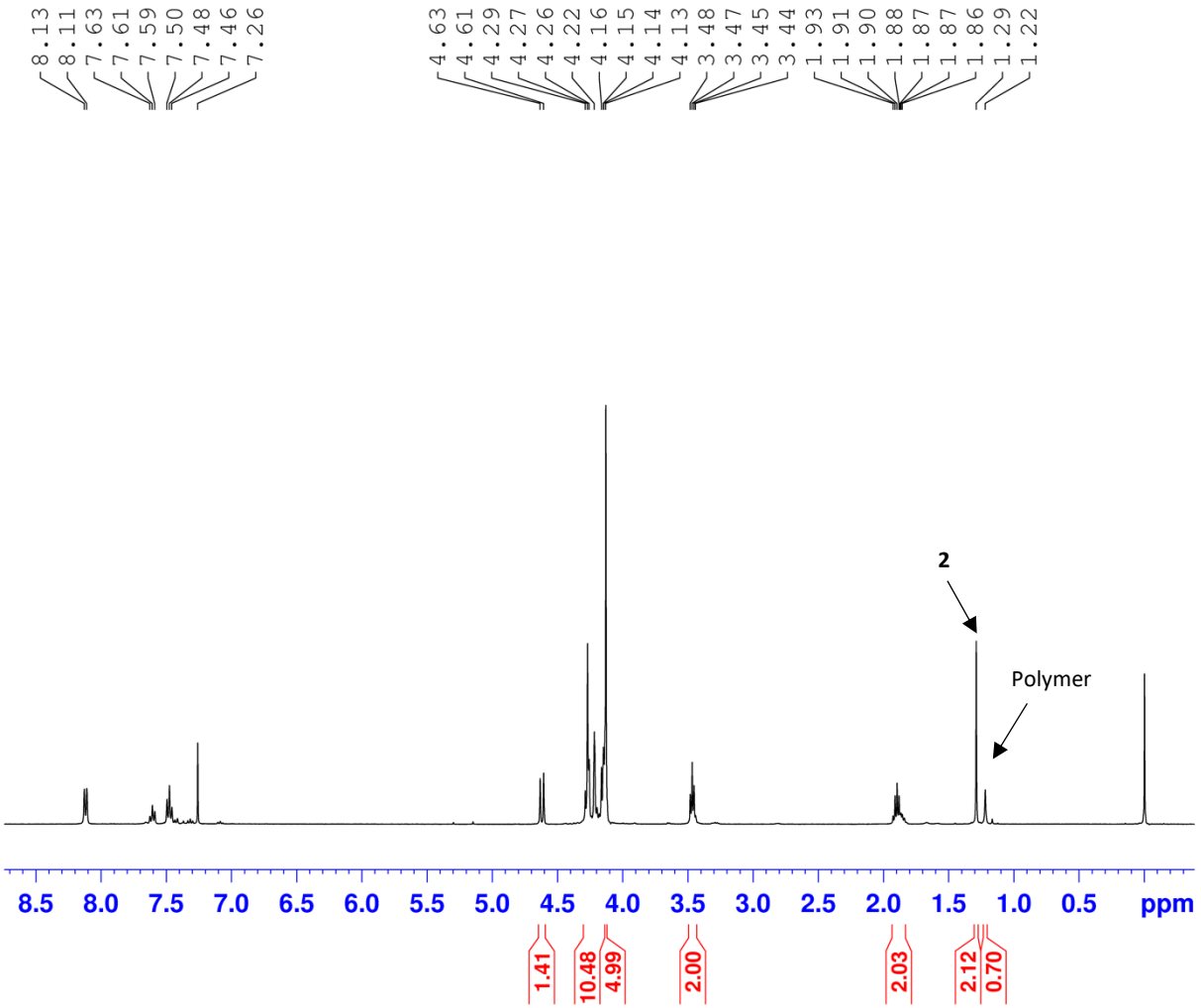

c) ^{1}H NMR spectrum ($CDCl_3$) of aliquot after 4 mins. % Conversion=25%.

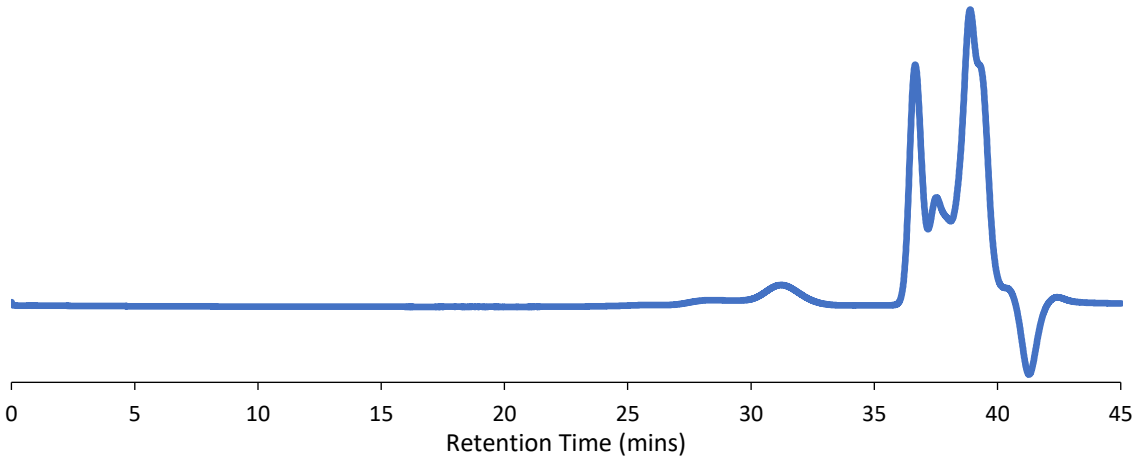

d) GPC-RI of aliquot after 4 mins. M_n=4,758, $Đ$=1.31.

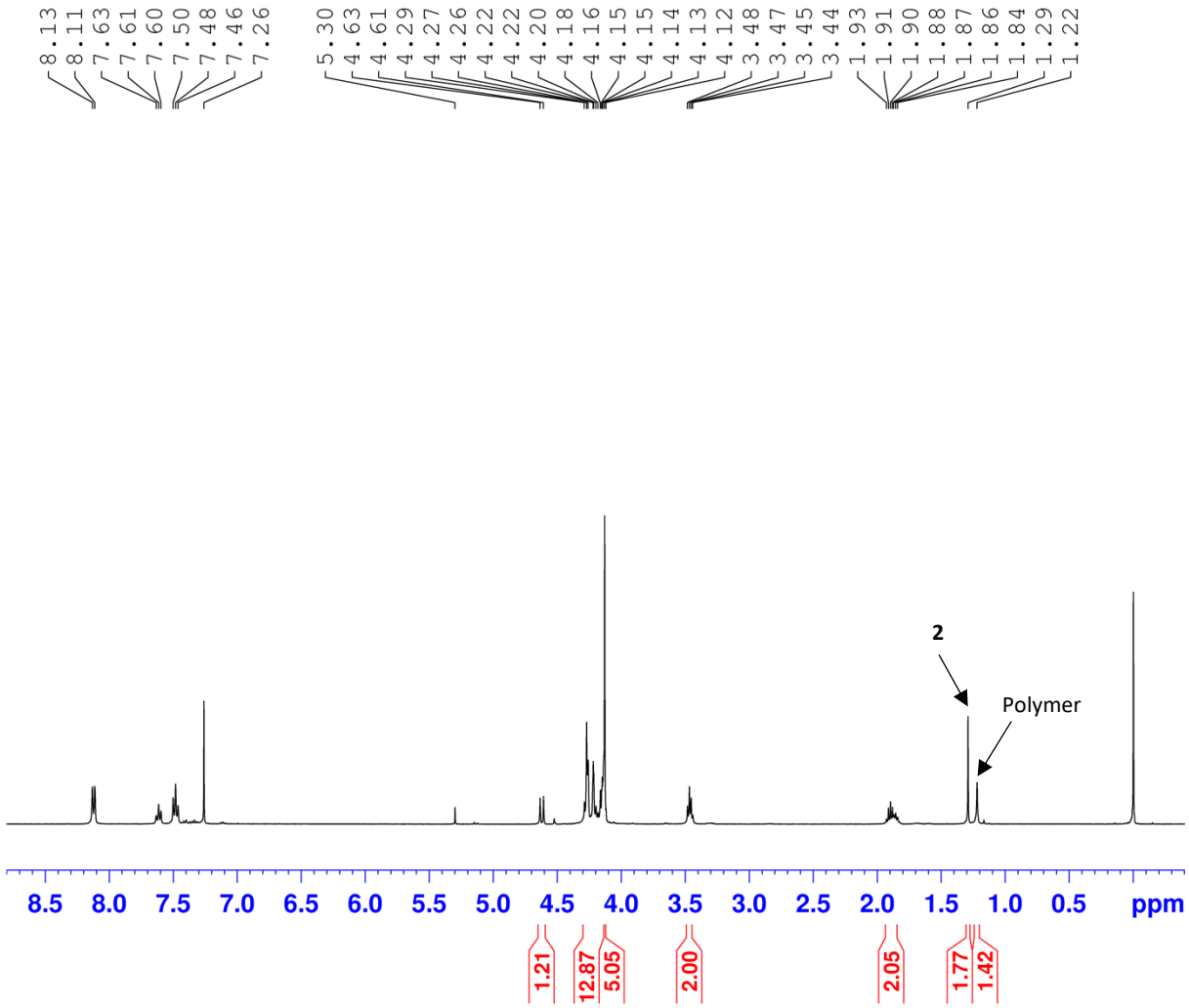

e) ^{1}H NMR spectrum ($CDCl_3$) of aliquot after 6 mins. % Conversion= 45%.

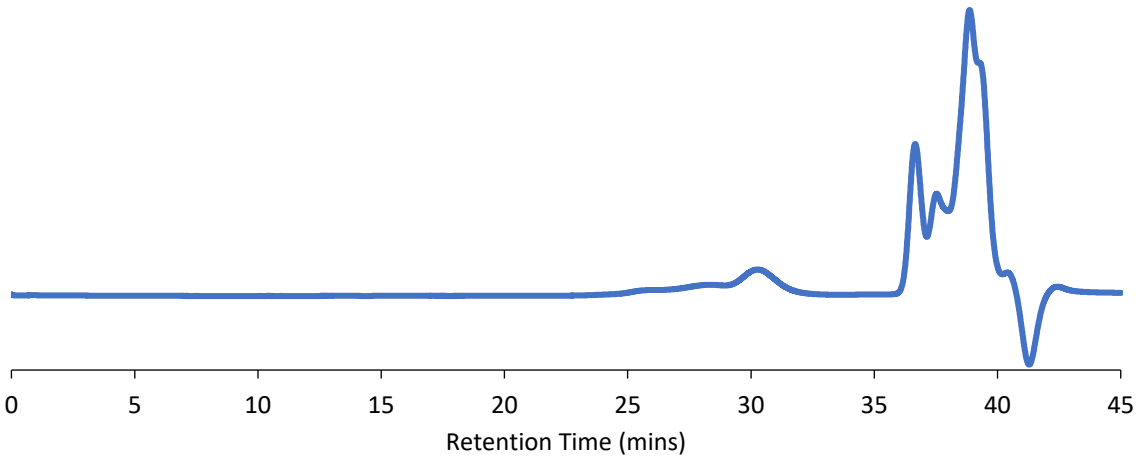

f) GPC-RI of aliquot after 6 mins. M_n=8,137, $Đ$=1.57.

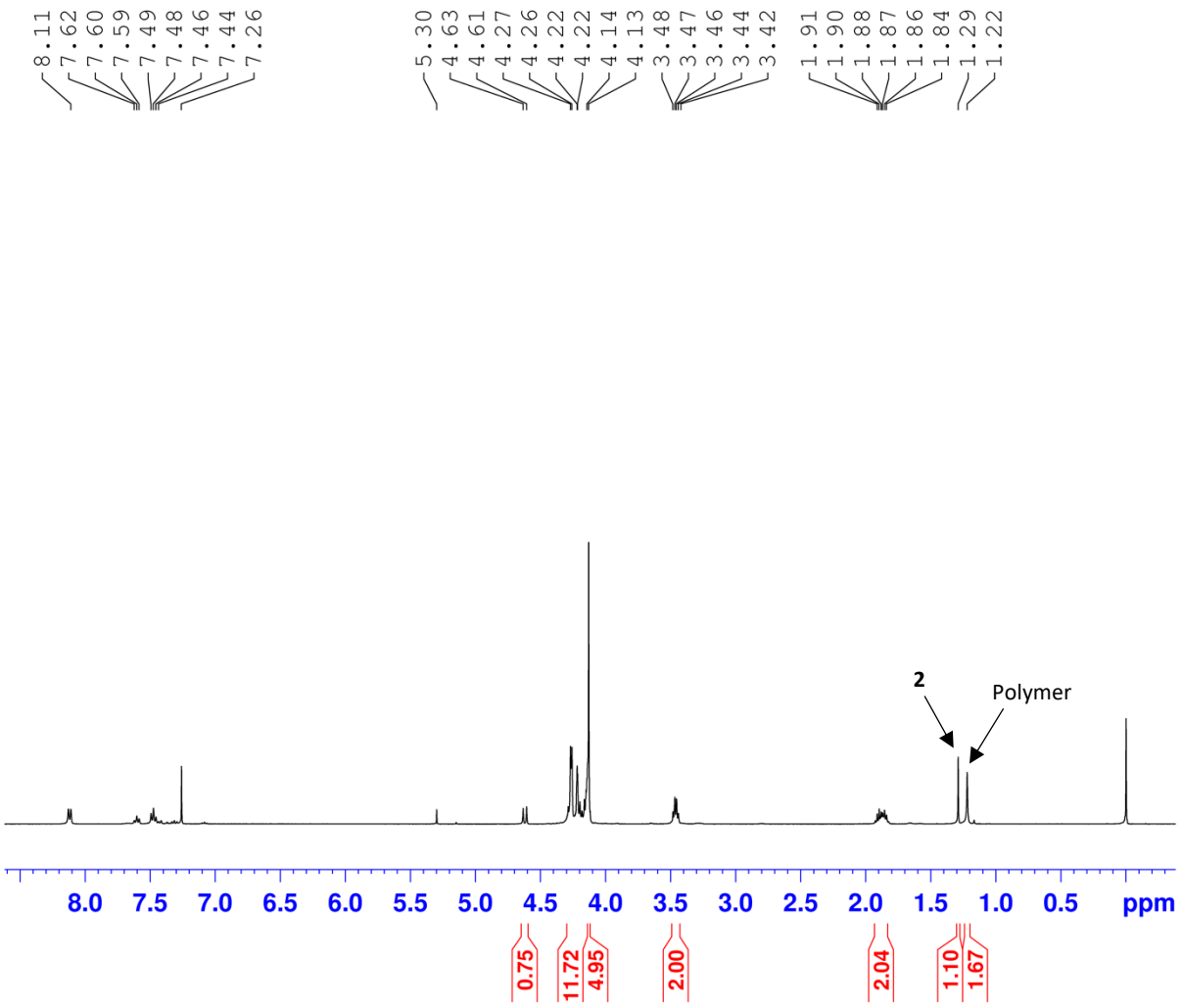

g) ^{1}H NMR spectrum ($CDCl_3$) of aliquot after 8 mins. % Conversion= 60%.

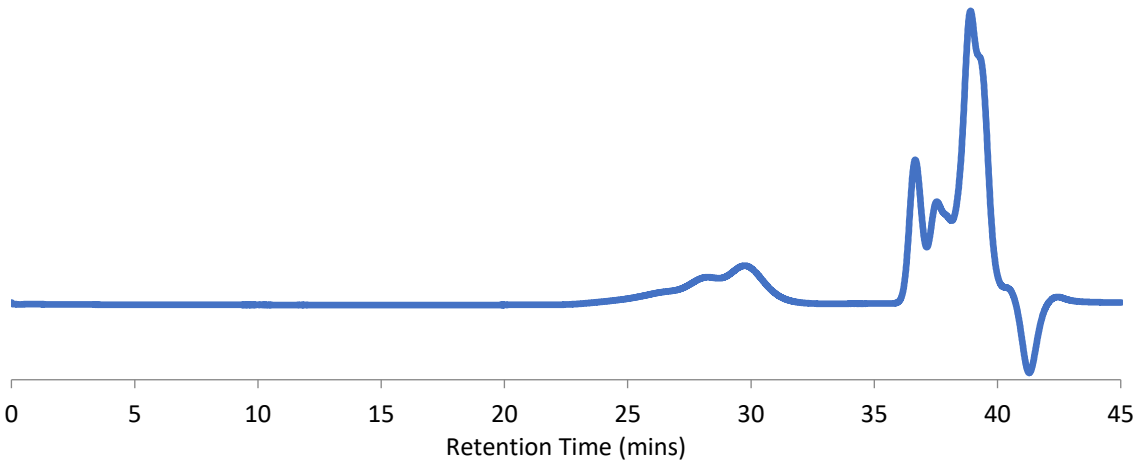

h) GPC-RI of aliquot after 8 mins. M_n=10,208, $Đ$=1.48.

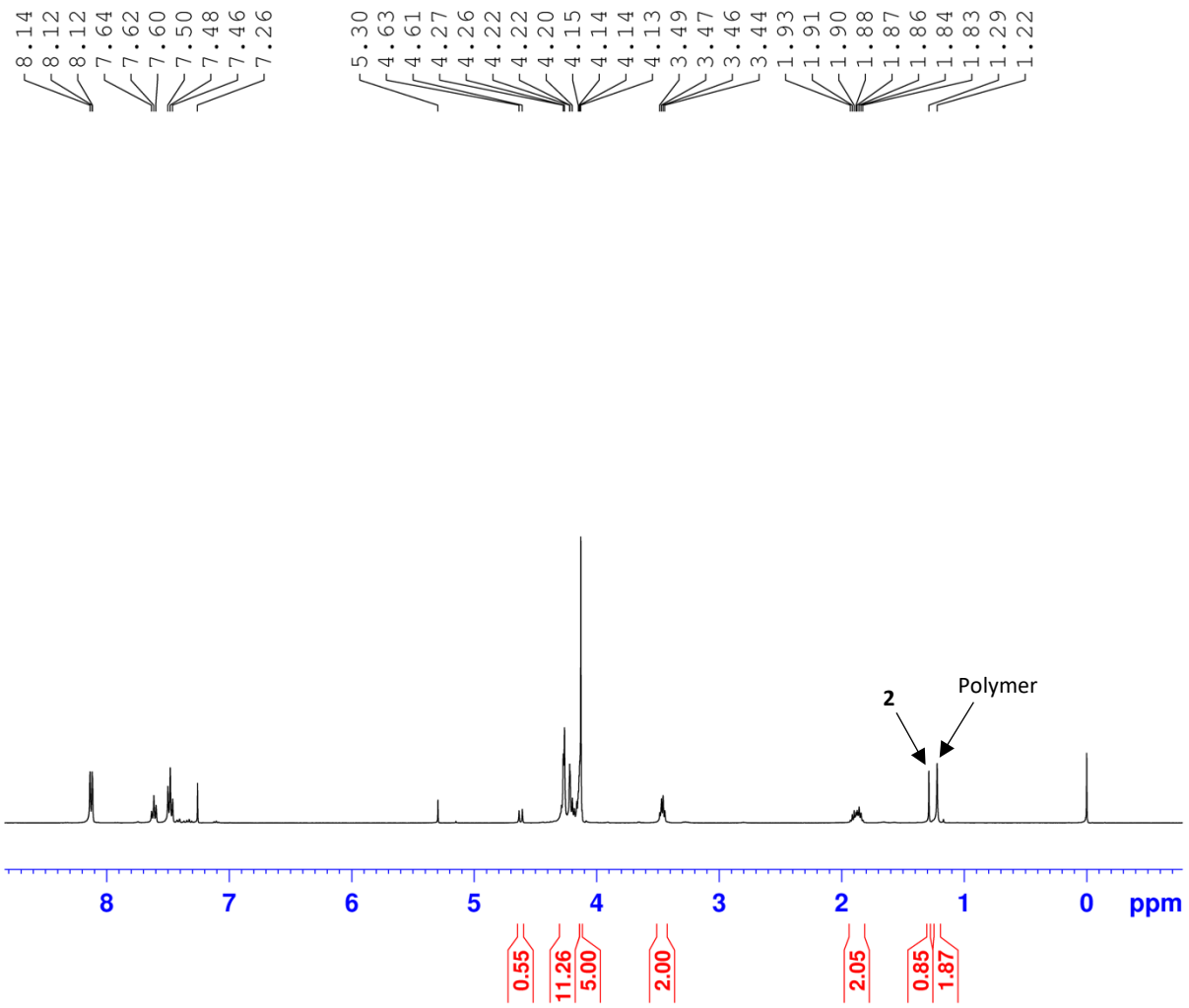

i) ^{1}H NMR spectrum ($CDCl_3$) of aliquot after 10 mins. % Conversion= 69%.

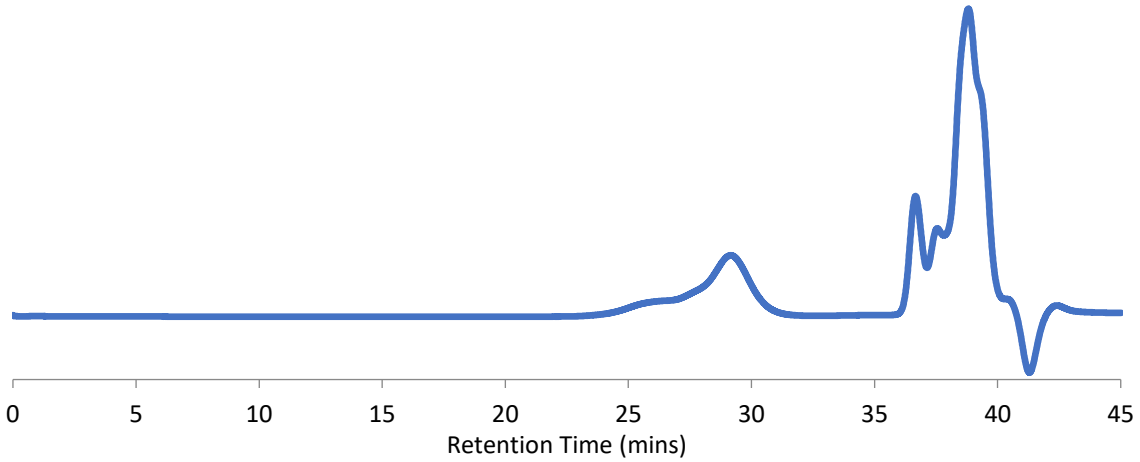

j) GPC-RI of aliquot after 10 mins. M_n=11,347, $Đ$=1.33.

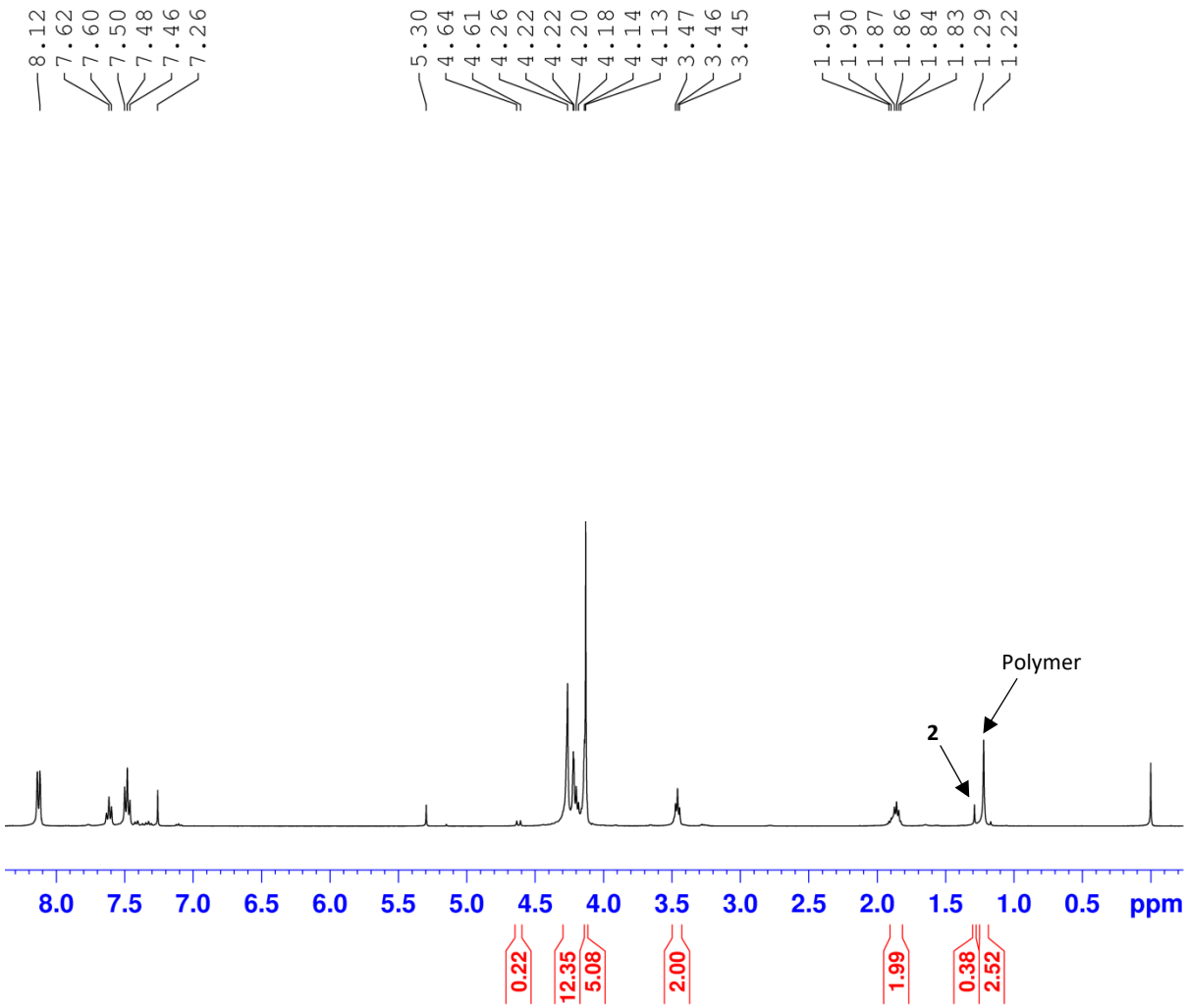

k) ^{1}H NMR spectrum ($CDCl_3$) of aliquot after 15 mins. % Conversion= 87%.

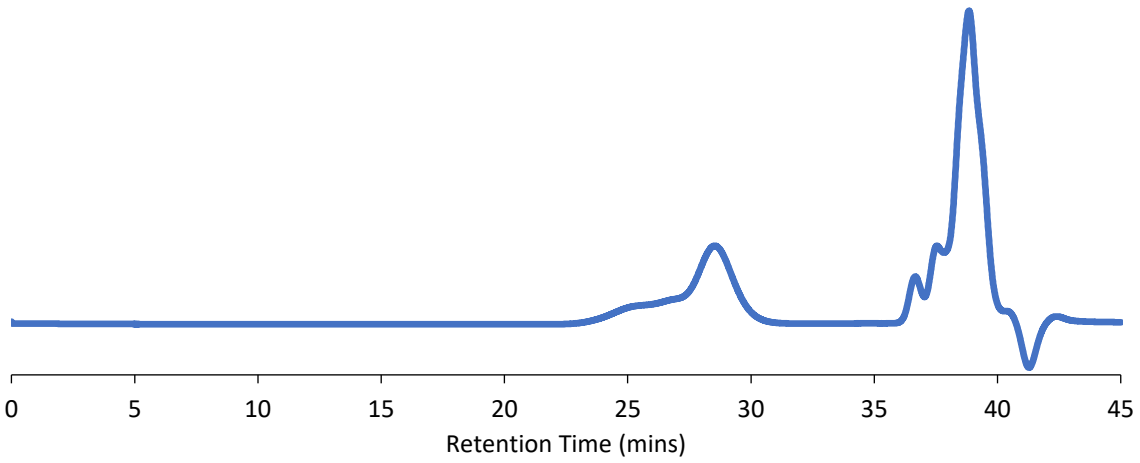

l) GPC-RI of aliquot after 15 mins. M_n=14,215, $Đ$=1.36.

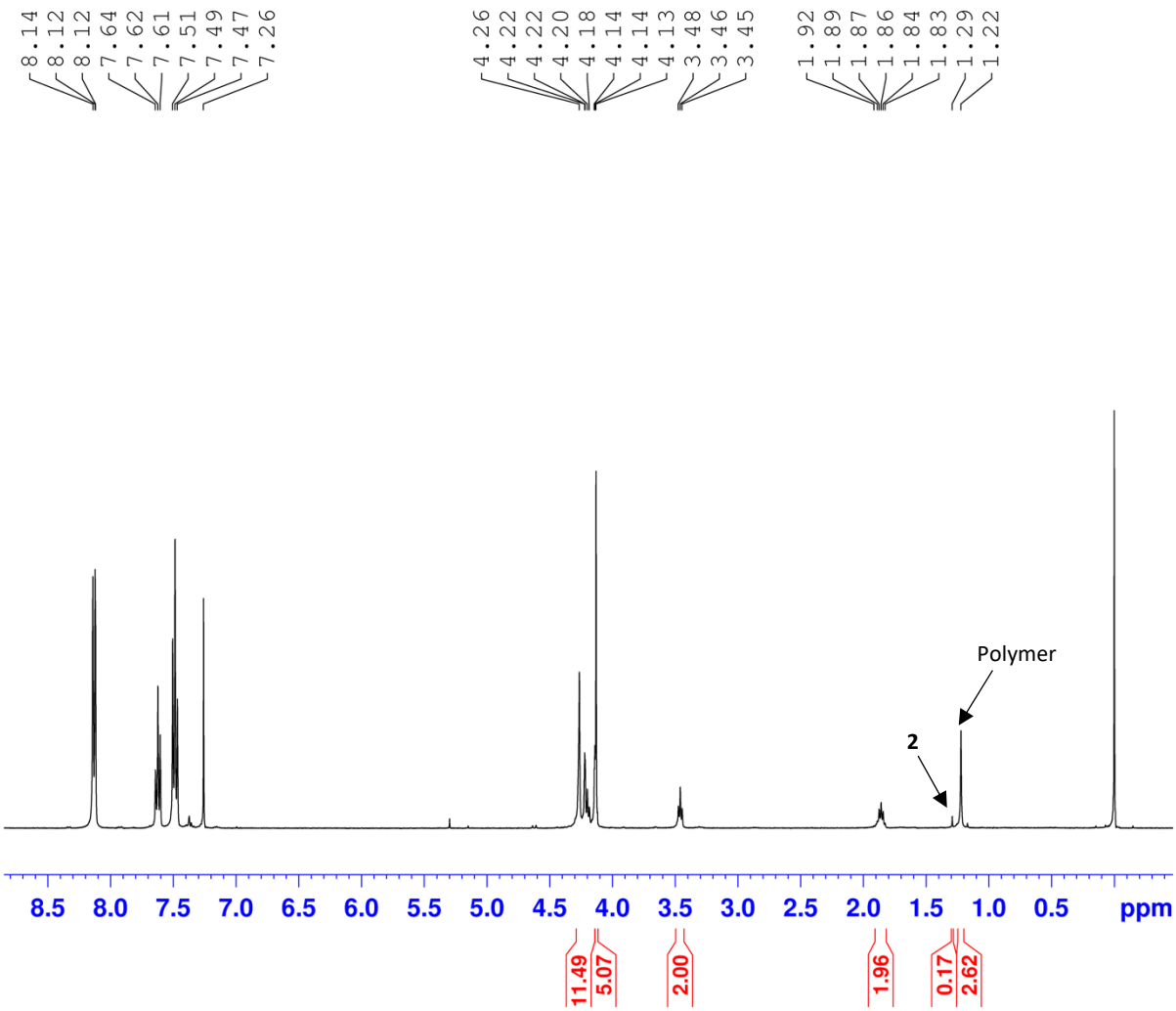

m) ^{1}H NMR spectrum ($CDCl_3$) of aliquot after 20 mins. % Conversion= 94%.

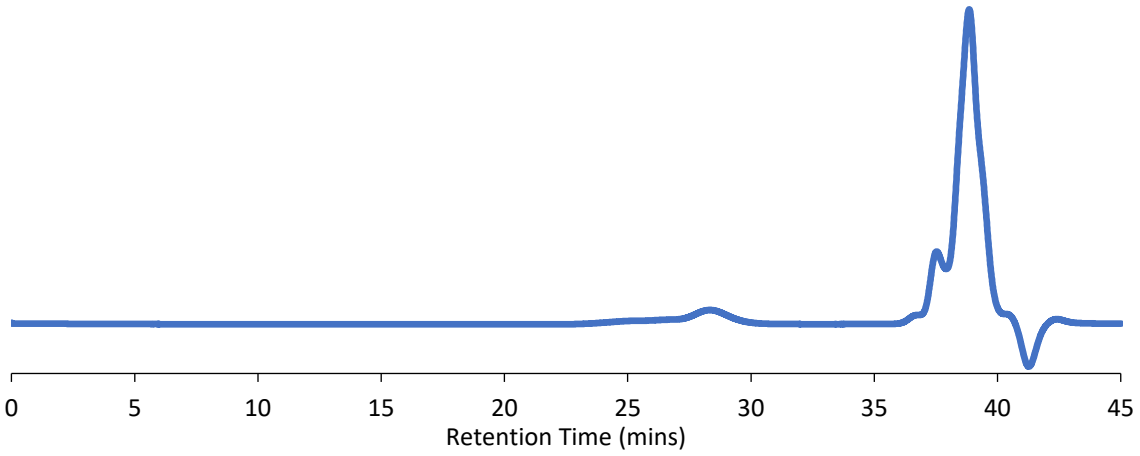

n) GPC-RI of aliquot after 20 mins. M_n=15,240, $Đ$=1.36.

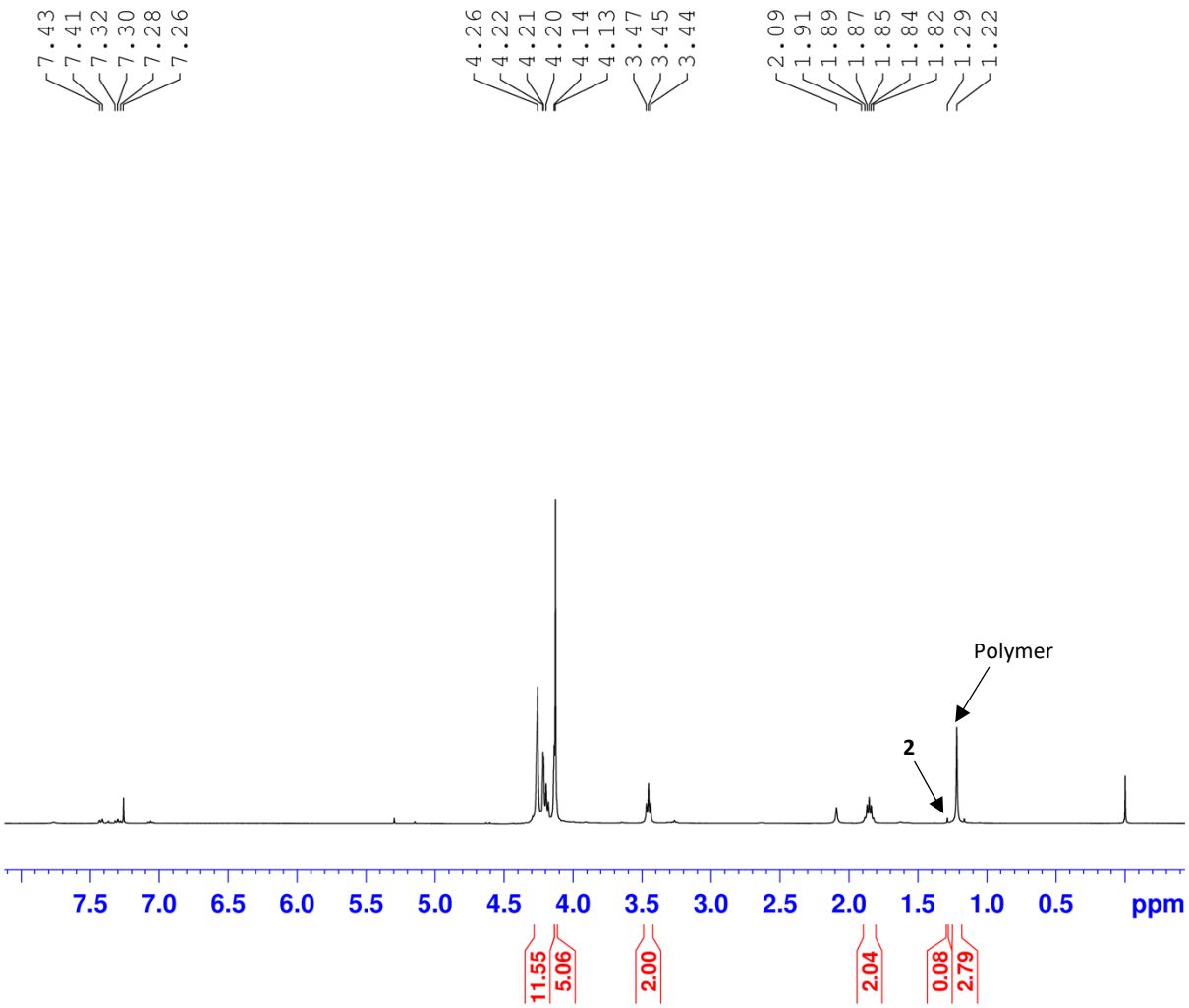

o) ^{1}H NMR spectrum ($CDCl_3$) of aliquot after 30 mins. % Conversion= 97%.

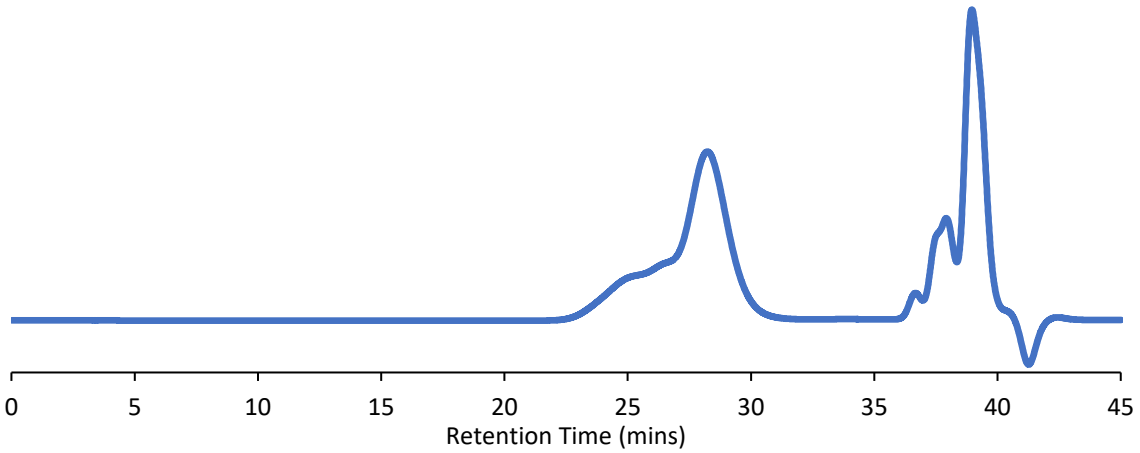

p) GPC-RI of aliquot after 30 mins. M_n=15,657, $Đ$=1.40.

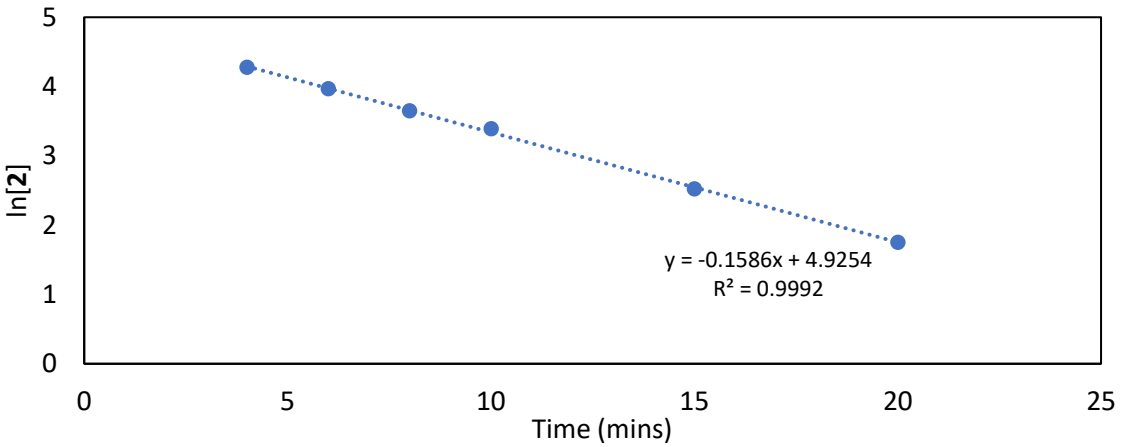

Figure S50. First-order plot of ferrocene monomer **2**. The ln[**2**] plotted as a function of time gave a linear plot. The first order dependence on monomer concentration is characteristic of a living polymerization.